INFLUENCE OF THE QUASI-BIENNIAL OSCILLATION ON RAINFALL PRODUCING SYSTEMS OVER WEST AFRICA

BY

Ballo Abdoulaye

Bsc, Msc (MET/15/5743)

A thesis in the Department of Meteorology and Climate Science, Earth and Mineral Sciences, in Partnership with the West African Science Service Centre on Climate Change and Adapted Land Use (WASCAL), submitted to the School of Postgraduate Studies in Partial Fulfilment of the Requirements for the award of Doctor of Philosophy in Meteorology and Climate Science of the Federal University of Technology, Akure, Nigeria.

September 2019

DECLARATION

I hereby declare that this Thesis was written by me and is a correct record of my own research work. It has not been presented in any previous application for any degree of this or any other University. All citations and sources of information are clearly acknowledged by means of references.

Candidate's Name: Ballo, Abdoulaye

Signature: …… **Date: ……..**

CERTIFICATION

We certify that this thesis entitled "Influence of the Quasi-biennial Oscillation on Rainfall Producing Systems over West Africa" is the outcome of the research carried out by Ballo, Abdoulaye in the Department of Meteorology and Climate Sciences, the Federal University of Technology, Akure, Nigeria, in partnership with the West African Science Service Center on Climate and Adapted Land Use (WASCAL)

Major Supervisor's Name: Prof. J. A Omotosho

Signature: …… **Date: ……**

Co-Supervisor's name: Dr. N. A. B. Klutse

Signature: …… **Date: ……**

Adviser's name: Prof. B. J. Abiodun

Signature: …… **Date: ……**

ACKNOWLEDGEMENTS

This PhD programme is fully sponsored by the Bundesministerium für Bildung und Forschung (BMBF), which is the Federal Ministry of Education and Research of Germany, through the West African Service Center for Climate Change and Adapted Land Use (WASCAL) at the Graduate Study Programme on West African Climate Systems (GSP-WACS), Federal University of Technology, Akure (FUTA), Nigeria. I am therefore grateful to WASCAL for granting me financial support for the study and my research visit to the University of Cape Town (UCT) South Africa for providing me the computing facilities.

I sincerely thank the Executive Director and the staff of WASCAL Head office, Accra, Ghana and the Director, Prof. K. O. Ogunjobi and staff of WASCAL GSP-WACS FUTA, Nigeria for their strong support and encouragement throughout the period of the study. I am also grateful to Prof. A. A. Balogun, the Head, and the Staff of Meteorology Department, FUTA, Nigeria, for their cooperation.

I am most grateful to my supervisors Prof. J. A. Omotosho, for his interest, guidance, encouragement and support on the study and to my co-supervisor Dr. Nana A. B Klutse for her advice, guidance and contribution on this thesis.

My special thanks to my South Africa adviser Prof. B. J Abiodun whose invitation to UCT, guidance, support and fruitful discussions, both concerning my work and my attempts to write papers, helped me to understand the topic and also giving me the opportunity to improve my computational skills, which was required for this research. I am also grateful to his Peer Review Meeting Group including Sabina Omar, Koketso Molepo, Myra Naik, Mariam Nguvava, Michel Gore, Roland Takong and Molulaqhooa

Maoyi for their contribution on this work. My regards, to Mr. Phillip Mukwenha for its help in installing the climate tool software on my laptop. Many thanks to all my colleagues of the GSP WACS for your valuables contributions, especially to Sawadogo Windmanagda, Naomi Kumi and Abdoulatif Bonkaney with whom I spent my research field work at UCT. I would like also to thank you all the staff members of the Climate Science Analysis Group (Staff) at UCT for their contribution in the achievement of this work.

To my family, I am very grateful for your great patience, supports, never-lacking confidence and prayers. In this respect my beloved wife, Mms Ballo Melissa Esther Famba thank you for your infinite support, love and encouragement during the course of this work. I would like to thank you my deceased father Youssouf Ballo who passed away during the course of this work, thank you for giving me the chance to be educated. May your soul stay in peace in Paradise. Amen. And thank you for everything you have done for me. Many thanks, to my brothers and sisters especially Moussa, Mariam, and Aïssatou for their ever constant supports and prayers. I also want to thank all my colleague WASCAL PhD students for their moral and technical support throughout these years.

Finally, I would like to thank my external examiners for their important comments to improve this document.

I am most grateful to Almighty God above all for making this thesis a reality and a success. Thank you ALLAH for everything.

DEDICATION

To my wife Mme Ballo Melissa Esther Famba and daughter Nana

ABSTRACT

Rainfall is a major ingredient for economic development for most West African countries. It has serious implications on the socio-economic activities because more than 95% of its agricultural activities are rainfed and rain-fed agriculture serves as the main source of income for most of the economies. Therefore, rainfall variability in terms of amount and time can lead to good or poor agricultural production as either too much rainfall causes floods and water logging or very little rainfall results in inappropriate agricultural planning and activities. This study used ERA-Interim reanalysis and observational GPCP v2.2 to investigate the seasonal rainfall variability and relationship with the tropospheric jets. This work focuses on the Influence of the Quasi-biennial Oscillation on Rainfall Producing Systems over West Africa. This study analyses the relationship of the sub-tropical westerly jet (STJ) with the West African monsoon and its associated tropospheric jets. The association and relative influence of the low-level West African Westerly Jet (WAWJ), the AEJ and TEJ during wet and dry situation were also examined. Results showed that the sudden appearance of the TEJ in June and the intensification of the AEJ are linked to the weakening and disappearance of the stratospheric easterly flow (QBO) and the fast poleward retreat of the STJ. A close association between the northward movements of the AEJ core and rainfall belt was found. However, no clear relationship was seen between the northward advance of the rainfall distribution and the TEJ slow movement, as this jet core always lags the rainfall maximum. By considering rainfall variability causes, results also showed that the Sub-tropical jet (STJ) retreated poleward faster while the TEJ, WAWJ and ascending motion were all stronger, resulting in higher rainfall during wet years than dry. Furthermore, it

was found that the so-called monsoon jump and the reversal of the shape of the monsoon layer both occur in May/June and that this may be linked to the weakening of the QBO and the sudden poleward retreat of the sub-tropical jet in the same months.

The influence of stratospheric quasi-biennial oscillation (QBO) on the African Easterly Jet, Tropical Easterly Jet and West African precipitation was investigated through simulations using the Global Climate Model (GCM) using the Coupled Models Intercomparison Project Phase 5 (CMIP5). The performance of the CMIP5 models in reproducing the quasi-biennial oscillation was evaluated while the influence of the QBO on West African rainfall precipitation was studied using wavelet analysis over each zone of region (Sahel, Savannah, Guinea). Also, the composite of the effect during QBO and non-QBO years as well as of the QBO phases on rainfall variability were studied. The results show that all the models capture the general structure of the QBO but with some biases while HadGEM2-CC produced results closer to observation (ERAINT). It was also found that there is good coupling between QBO and precipitation over all zones of West Africa. The wavelet coherence analysis gives confirmation of the results. From this study it is concluded that the quasi-biennial oscillation has an important influence on West Africa precipitation that could lead to improved rainfall prediction over West Africa.

TABLE OF CONTENTS

LIST OF TABLES

LIST OF FIGURES

Table **Page**

ACRONYMS

AEW African Easterly Waves

AWJ African Westerly Jet

AMIP Atmospheric Model Intercomparison Project

AMO Atlantic Multi-decadal Oscillation

CAPE Convective Available Potential Energy

CMIP5 Coupled Models Intercomparison Project Phase 5

COI Cone of Influence

DGP Days of Growing Period

ECMWF European Center for Medium-Range Weather Forecasts

EK Equatorial Kelvin Waves

ENSO El Nino Southern Oscillation

ER Equatorial Rossby Waves

GCM Global Climate Model

GDP Gross Domestic Product

GPCP Global Precipitation Project

GWS Global Wavelet Spectrum

IFS Integrated Forecast System

IOD Indian Ocean Dipole

ISM Indian Summer Monsoon

ITCZ Intertropical Convergence Zone

ITD Inter-Tropical Discontinuity

LLW Low-level Westerly Jet

MCCs Mesoscale Convective Complexes

MCSs Mesoscale Convective Systems

NAO North Atlantic Oscillation

NASA National Aeronautics and Space Administration

PCMDI Program for Climate Model Diagnosis and Inter-comparison

QBO Quasi-biennial Oscillation

SAL Saharan Air Layer

SAO Semi-annual Oscillation

SLs Squall Line

SST Sea Surface Temperature

TEJ Tropical Easterly Jet

WAM West African Monsoon

WAWJ West African Westerly Jet

WPS Wavelet Power Spectrum

CHAPTER ONE: INTRODUCTION

1.0 Background to the Study

Rainfall is a major ingredient for economic development for most West African countries. It has serious implications on the socio-economic activities because more than 95% of its agricultural activities are rainfed and rain-fed agriculture serves as the main source of income for most economies. The variability in rainfall leads to either too much rainfall which causes floods and water logging or very little rainfall resulting in poor agricultural production. West Africa in recent decades has been affected by decreases in rainfall and its extended effect on variability of surface and sub-surface water. The combined effect of rainfall variability and low adaptive capacity could cause these changes to have significant impacts on people and the sectors that depend on the availability of adequate water in West Africa. However, over West Africa rainfall varies seasonally and spatially from the coastal to the Sahel zones in the north (Cooper et *al.*, 2008), so that the two types of variability, namely decadal and inter-annual (Nicholson, 1981), interact and interrelate. Over the region, the climate is dominated by a large-scale circulation known as the West African Monsoon (WAM), accounting for most of the total precipitation. The regional rainfall fluctuation responds to the strong seasonal influence of the West African Monsoon and associated deep convections processes. This is in agreement with Omotosho (1990) and Mathon and Laurent (2001). This response is related to the thermal gradient between the ocean and continental zone (Eltahir and Gong, 1996). WAM is associated with low level south-westerly winds and high rainfall (Hall and Peyrille, 2006) as well as the northward migration of the Intertropical Convergence Zone (ITCZ) (Hastenrath, 1991; Hourdin *et al.*, 2010).

In general, rainfall in the region especially over the land is mostly influenced by the migration of the Inter-Tropical Discontinuity (ITD). The ITD oscillates south to north

and back and so modulates the pressure system of the West African Monsoon (Mounier *et al.,* 2008; Nicholson and Grist, 2001; Sylla *et al.,* 2011; Amekudzi *et al.,* 2015). Southwesterly winds dominate the region south of the ITD. This carries moisture from the Atlantic Ocean into the region. In contrast, a North-East trade wind which is dry and hot dominates the region north of the ITD. WAM variability is characterized by complex interactions at different spatiotemporal scales during boreal summer, ranging from decadal (Lu and Delworth, 2005; Mohino et al., 2011) to intra-seasonal timescale (Nicholson and Grist, 2003; Redelsperger *et al.,* 2006). Nevertheless, the spatial-temporal distributions of West Africa rainfall is highly variable and difficult to predict because of the complex interactions between West African monsoon systems [African easterly jet (AEJ), Tropical Easterly Jet (TEJ) and the equatorial (6^oS-6^oN) Quasi-biennial Oscillation (QBO)] and various atmospheric teleconnections (like El Nino Southern Oscillation (ENSO), Quasi-biennial Oscillation (QBO), Indian Ocean Dipole (IOD), etc.) that influence the climate of the region. Numerous studies have tried to explain the monsoon rainfall variability over West Africa. Most of them have associated to various factor which include Sea Surface Temperature (SST) variations over the Pacific Ocean (e.g. El Nino Southern Oscillation, ENSO; (Janicot *et al.,* 1998; Okonkwo *et al.,* 2014), land-atmospheric feedbacks such as soil moisture, vegetation and albedo (Douville, 2002; Grodsky and Carton, 2001; Douville, 2002), large-scale circulation features (Jenkins *et al.,* 2005; Mounier *et al.,* 2008; Lavender and Matthews, 2009). Figure1 shows that the major components of this climatological system (WAM) are associated with atmospheric circulation features consisting essentially of the near-surface monsoon flow, the northeast trades, the intertropical discontinuity (ITD), the low-level westerly jet (LLW), the mid-tropospheric African Easterly jet (AEJ) and the upper-level Tropical Easterly Jet (TEJ). In addition, the unusual fluctuations in West

African rainfall can be attributed to various global systems which trigger this variation. Prominent among these triggering phenomena is the quasi-biennial oscillation.

The Quasi-biennial oscillation (QBO) first reported in the 1960s, is a major oscillation in the equatorial stratospheric zonal wind (Lindzen and Holton, 1968). It is a periodic oscillation in atmospheric waves on an average of 26 months. The alternating easterly and westerly wind regimes make up the QBO, which change from being strong at 10mb to relatively weak at 100mb. The quasi-biennial oscillation has been speculated to have some effect on West African precipitation (Gray *et al.,* 1992). Hence, there may be some interaction between the QBO and TEJ which is at 150-200hPa. The QBO affects the circulation at the Earth's surface and is an important consideration in extended-range weather forecasts (e.g., Baldwin et al., 2001). Recently, Yoo and Son, (2016) indicate the QBO exerts greater influence on the Madden–Julian Oscillation than does the El Niño–Southern Oscillation. It modulates the Indian summer monsoon rainfall through its influence on ENSO (Mukherjee *et al.,* 1985; Chattopadhyay and Bhatla, 2002). For example, Chattopadhyay and Bhatla (2002) associated the easterly phase of QBO with drought in India and the westerly phase with normal or strong monsoon rainfall. Indeje and Semazzi (2000); Hashim *et al.* (2010) found good relationship between QBO and seasonal rainfall anomalies in East Africa and showed that the relationship is strongest in boreal summer (June-August) and weakest in the winter (December-February). However, there is no such comparative study over West Africa although Folland (1986), Giannini (2003) reported that QBO could affect the Atlantic jet stream (one of the rainfall producing system in the Sahel region). But no study has investigated this further or linked the relationship with West African rainfall.

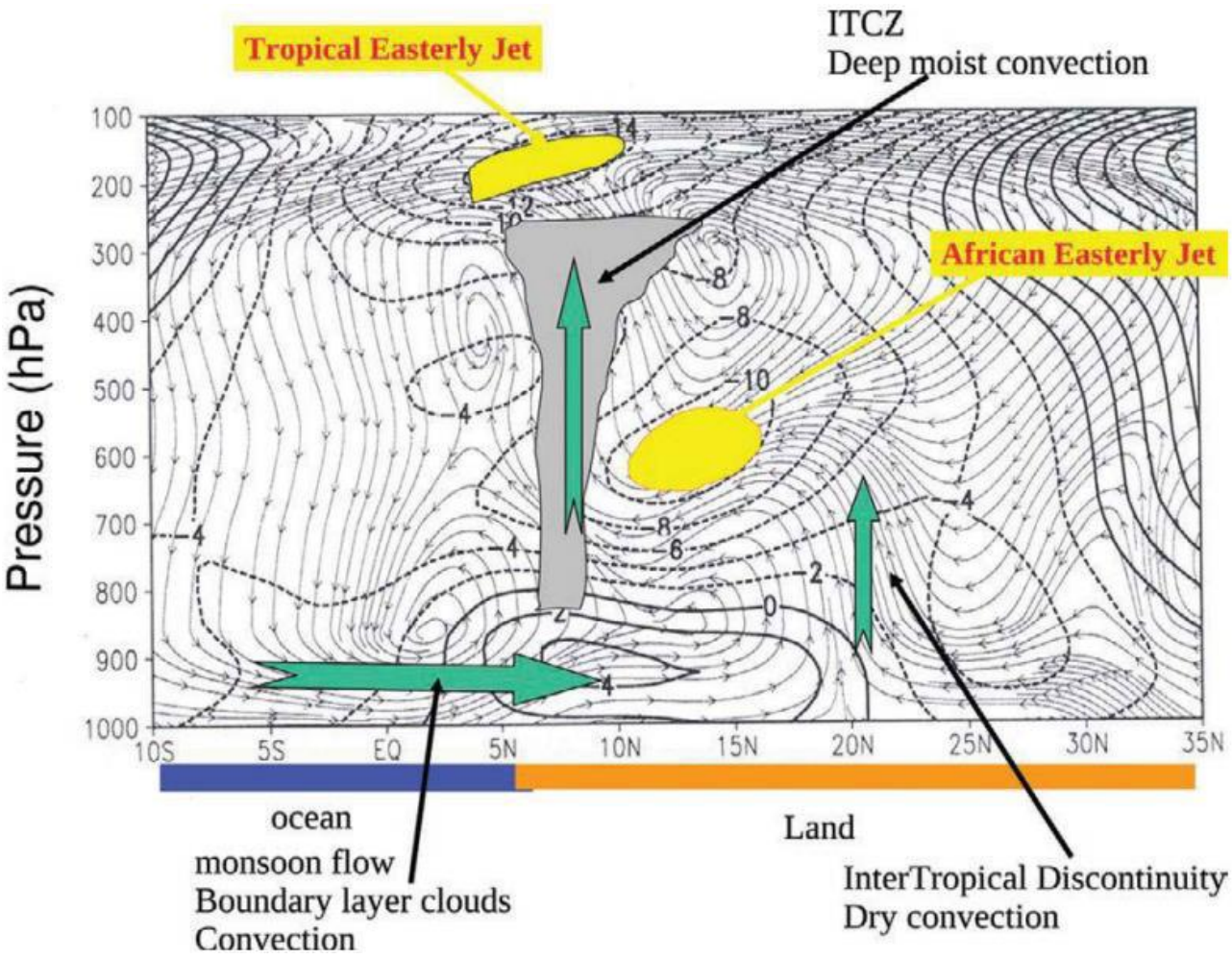

Figure1.1: Mean Meridional Circulation (stream lines) and associated mean zonal winds (m/s in contours) over West Africa during the summer season(Hourdin et al., 2010).

1.1 Statement of Problems

Understanding rainfall variability and its prediction has been a major challenge for agricultural production, transportation, hydro-electricity generation and water resource management. There has been a hash economic and social condition faced in many West African countries due to consistent rainfall variability (Manzanas *et al.*, 2014). Previous studies have focused on investigating WAM dynamics and its circulation features. Most of these studies are interested in reproducing the processes and mechanisms responsible for precipitation regimes in the region (Sylla et al., 2010; Diallo *et al.*, 2013) while others study the nature of the relationship between WAM circulation features (Zaroug *et al.*, 2014*;* Diallo *et al.*, 2014; Sylla *et al.*, 2015). However, not much work has been done on the TEJ, AEJ and atmospheric teleconnections QBO (Sharon E Nicholson, 2013).

Although some previous studies improved our understanding of the influence of TEJ on seasonal rainfall variability over West Africa (Lemaitre, 2014), the literature is scarse on the dynamics of TEJ, the effect of climate variability and change on it, as well as its interaction with other West Africa weather systems, especially the African Easterly Jet (AEJ) and Quasi-biennial Oscillation (QBO). Although some important results have been obtained on the West African Monsoon features and their relationship with convection and precipitation over West Africa, other factors such as the TEJ, a very important feature of the WAM, its relationship and interaction with the QBO and their overall influence on precipitation need to be properly investigated. Also, a clearer relationship and interaction between AEJ and TEJ is required.

1.2 Aim and Objectives

1.2.1 Aim

The aim of the study is investigate the impacts of the interactions between the Jets (AEJ, TEJ) and the Quasi-biennial oscillations on West African rainfall.

1.2.2. Specific objectives

The specific objectives of the research are to:

1. Provide a clear climatology of the characteristics (north/south extent, core speed, height variability and associated convergence/divergence and vertical velocity fields) of the Tropical Easterly Jet and African Easterly Jet over West Africa;
2. assess the impact of climate variability and change on TEJ and AEJ characteristics;
3. Determine the impact of the interactions of the QBO, TEJ, and AEJ on rainfall over West Africa and their potential for its prediction;
4. Simulating the Influence of QBO on West African rainfall;

1.4. Justification and Research Questions

Tropical easterly jet is an important meteorological system that which is also a controlling factor on the rainfall over West Africa. In this region the rain-producing systems play significant roles on socio-economic lives of the population as their economy rely mainly on rain-fed agriculture. Consequently, in West Africa, any intra-seasonal rainfall variability impacts severely on the agricultural and water resource sectors, with equally severe consequences on health. This is especially true for the population living in the semi-arid Sahel region. This region experiences the full impact of the TEJ, AEJ and African Easterly Waves (AEW) systems but is ill-equipped to mitigate the effects of their spatial and temporal variation as well as the intensity of rainfall that these systems bring (Kebe, 2015).

Presently, there is only little work in the literature on the Tropical Easterly Jet (TEJ), which has been the focus of studies in the Asian and East African regions. According to Nicholson and Webster (2007), the Africa Easterly jet (AEJ) at a more northerly latitude and Tropical Easterly Jet (TEJ) to the south are both important in determining the behaviour of the summer rainy season in the Sahel region. The AEJ and TEJ are linked to the inter-annual rainfall variability such that the wetter conditions in the Sahel are associated with weaker AEJ and stronger TEJ while drier situations are associated with stronger AEJ and weaker TEJ (Nicholson, 2008). The TEJ is also linked to the mean climate of West Africa (Cuesta *et al*., 2010). Therefore, it is important to investigate the exact role of Tropical Easterly Jet on convective systems, over West Africa.

However, the mode and direction of the interaction between AEJ and TEJ (e.g. the convergence /divergence vorticity and vertical motion) and, consequently the effect of these interactions on West African convective systems is not known. Also, as mentioned previously, the possible interaction of TEJ with the QBO as well as QBO and AEJ and their consequent influence convective precipitation have never been investigated. With all these, there is therefore the need to obtain a clearer understanding of the interactions and the influence of TEJ, AEJ and QBO together on West Africa rainfall, with special focus on the climatology, mechanisms and structure using both analysis and numerical modelling. In particular, the study will address the following questions:

i. Is there any interactions between QBO and TEJ, QBO and AEJ and if so, do these have any effect on West Africa rainfall?

ii. Is the Global Climate Model (GCM) able to simulate the evolution and circulations (convergence, divergence, vorticity and vertical motion fields) associated with the TEJ and its interactions with the AEJ and QBO?

1.5 Contribution to the Knowledge

At the end of this study, it is expected that:

a) The essential climatology of TEJ over West Africa would be produced.

b) A clear picture of the interactions of TEJ with AEJ and QBO will also be produced.

c) The relationships between the QBO phases in the stratospheric zonal wind and the West Africa monsoon will be produced,

d) Also, the prediction potential of the rainy season using information from the phases of the QBO will be determined.

e) The results of the study will lead to more skillful forecasts of the West African monsoon rainfall. Such long-range information should assist agricultural practices and water resources management

1.6 Thesis Structure

This thesis is structured as follows:

1) Chapter two presents the literature review
2) The third Chapter is on research methodology
3) The results and discussion are presented in Chapter four
4) Chapter five summarizes the main Conclusions and Recommendation.

CHAPTER TWO: LITERATURE REVIEW

Before assessing the influence of the Quasi-biennial oscillation on African Easterly Jet, Tropical Easterly Jet and rainfall over West Africa, it is important to understand the various features of West African climate system. The major characteristic of West African climate is the strong variability of its rainfall (Doherty *et al.,* 2001; Giannini *et al.,* 2003). West Africa has a very complex climate driven by local processes, such as tropical convection and alternation of monsoon and also by remote processes (e.g., El Nino-Southern Oscillation, Indian Ocean Dipole (IOD), Quasi-biennial Oscillation (QBO), etc.). Each of these processes highly influences the inter-seasonal, inter-annual and decadal variability of rainfall pattern in the region. Therefore, understanding the interactions between these processes is crucial to mitigating the negative effects of climate variability and change in West Africa. This chapter reviews the studies that have been carried out to date in this respect.

2.1. West African monsoon features

The West African Monsoon (WAM) is the key feature in the climatology of West Africa and the major factor of rainfall distribution. It is characterized by a large scale circulation modulated by two air mass systems in the lower atmosphere: the southwest monsoon blowing from the ocean to the continent and the northeast continental trades blowing toward the ocean, which are characterized by summer rainfall and winter dryness. Within these large-scale circulations are the African Easterly Jet (AEJ), the Tropical Easterly Jet (TEJ) (Grist and Nicholson, 2001; Nicholson and Grist, 2001), the African Easterly waves (AEWs) (Diedhiou *et al.,* 2001; Grist, 2002; Wu *et al.,* 2013) and the West African monsoon (Janicot *et al.,* 2011; Mohino *et al.,* 2011; Lu and Delworth, 2005). It is also well established that inter-annual variability of West African rainfall is associated with the changes in higher level circulation features (Wang and

Gillies, 2011). Two other low-level westerly jets are involved in the processes, the African Westerly Jet (AWJ) over the continent and West African Westerly Jet (WAWJ) over the Atlantic (Nicholson, 2013).

2.1.1. Monsoon and Harmattan flows

The basic driving forces of West African monsoon circulation are provided by the contrast in the thermal properties of land and sea surfaces (Martin *et al.,* 2016). Monsoon flow is a south-westerly moist convective flow blowing from the Atlantic Ocean throughout the continent which brings moisture into land (Hourdin *et al.,* 2010; Brandt *et al.,* 2010; Janicot *et al.,* 2010). This flow is established due to the meridional thermal gradients existing between the Atlantic Ocean and the continent in spring. This thermal gradient strongly contribute in strengthening the southerly trade wind which can cross the equator and deviated eastward by Coriolis force. West African climate can be generalized as having two main seasons, the dry season and wet (rainy) seasons (also known as the monsoon season (Figure 2.1), resulting from the interaction of two migrating air masses: tropical maritime and tropical continental air masses (Figure 2.2). The dry season is mainly influenced by the north-east trade's winds known as Harmattan (Prospero and Carlson, 1981). The dry season, which runs approximately from November and March/April, is characterized by the hot and dry tropical continental air mass from the northern hemispheric high pressure system. This wind blows over the Sahara to most countries in West Africa (Amekudzi *et al.,* 2015). The prevailing northeasterly winds bring dry and dusty conditions across the region. The maximum southern extension of this air mass occurs in January between 5^{o} and 7^{o}N (Figure 2.2). The wet season on the other hand is mainly influenced by the southwesterly wind which dominates the continent from March to October (Lamb, 1978; Leroux, 2001; Janicot *et al.,* 2008). The maximum northern penetration of this wet air mass is in August, averagely between 19^{o} and 22^{o}N (Figure 2.2). The confluence over land between these

two trade winds creates near the surface low pressure zone at a point known as the Inter-Tropical Discontinuity (ITD) over land and the Inter-tropical Convergence Zone (ITCZ) when it occurs over the ocean (Abiodun *et al.,* 2008; Amekudzi *et al.,* 2015)(Abiodun *et al.,* 2008; Aryee, 2015). The north and south migration of ITD (or ITCZ), which follows the apparent movement of the sun, influences the climate of the region (Figure 2.2; Nicholson and Grist, 2003; Redelsperger *et al.,* 2006; Omotosho and Abiodun, 2007)

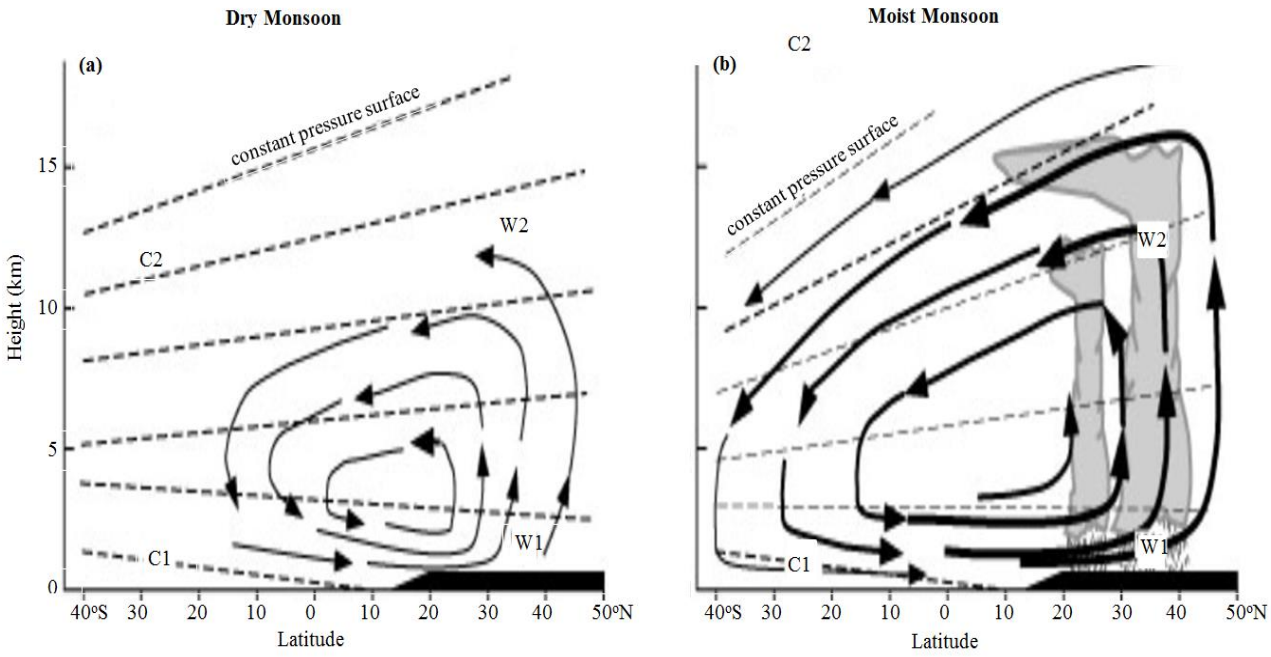

Figure 2.1: Two forms of monsoon systems (a) Dry monsoon and (b) Moist monsoon (Leroux, 2001)

2.1.2. ITD and ITCZ

The ITCZ (or ITD over land), is the most prominent meteorological phenomenon of the tropics and it marks the ascending branch of atmospheric Hadley cell where Harmattan and southwesterly trade wind converge producing intense convection and rainfall (Wang and Gillies, 2011). It plays an important role on the atmospheric energy balance. The ITD migrates northward in spring and southward in autumn with the apparent motion of the Sun, because it is located over areas of warmest surface temperatures. When the ITD moves northward, the monsoon flow penetrates deeply into the continent, bringing more moisture for the deep mesoscale convective systems which produce rainfall in the summer months. The ITD is most northerly in August at about 23^{o}N and most southerly in January to February between latitudes 5^{o} and 7^{o}N over Guinea zone.

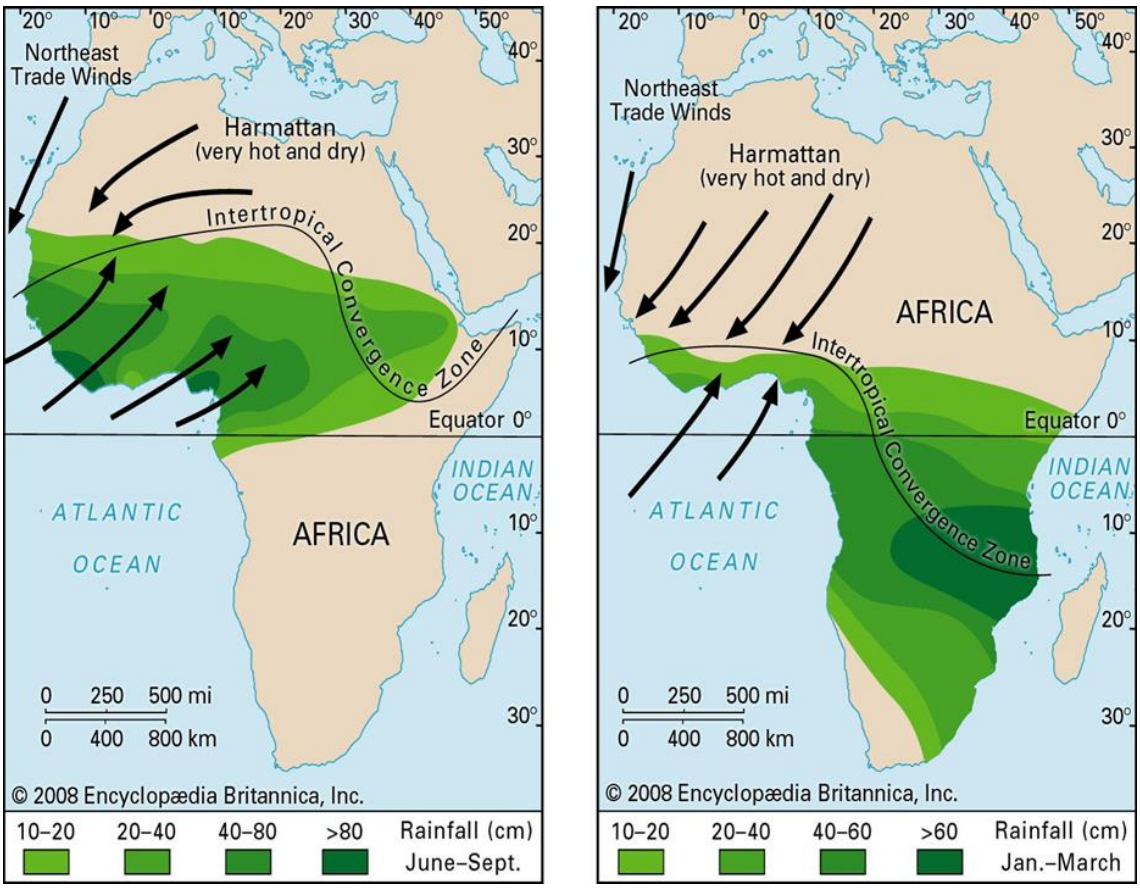

Figure 2.2: Wind and rainfall patterns of the West African monsoon during the boreal summer (left panel) and the boreal winter (right panel). Source: https://www.britannica.com/science/West-African-monsoon

The north-south displacement of the ITD brings two rainy seasons to Guinea region of West Africa, while the Sahelian area experiences only one pronounced dry and wet season (Williams and Kniveton, 2011). Dry years are generally associated with a delay of the ITD and southwestern monsoon moving northward. It should be noted that the position and the intensity of the ITD does not always imply the position of the rainbelt (East-West band of intense localized rainfall), as observed by Nicholson (2009). During the rainy season in West African Sahel, the ITD is associated with a large convective available potential energy (CAPE) and also horizontal moisture flux through the available abundant water vapor. These conditions with inherent conditional instability generate deep convection which constitutes the major rain-producing systems in that region (Omotosho, 1985).

By contrast, the ITCZ is a planetary-scale band of heavy precipitation close to the equator (Byrne *et al.,* 2018). It accounts for 32% of global precipitation (Kang *et al.*, 2018) and shapes climate and society in the tropics; any response of the ITCZ to climate change will have implications for tropical regions (Pierrehumbert *et al.,* 1995; Byrne *et al.,* 2018). It is located around 10^{o}N where most of the convective rainfall occurs, with a mean upward motion that reaches 200 hPa where the tropical easterly jet is found. However, the ITD mainly plays a crucial role in regions as the Sahel in which rainfall is of critical importance and explains more than 80% of Sahelian rainfall (Omotosho, 1985).

2.1.3 West African Monsoon Jump

The WAM jumps quickly northward from about 5° N in May-June to 10°N in July-August according to Sultan and Janicot (2000) and this determines the wet and dry seasons in West Africa following the northward movement of the Inter-tropical Convergence Zone (ITCZ). The monsoon jump can be described as the onset of intense convection and rainfall along latitude 10° N accompanied by a sudden termination along the Guinean Coast. Again, it is told that the continuous seasonal migration of the ITCZ gives rise to two rainy seasons along the Guinean Coast but results in a single rainy season over the Sahel (Hagos and Cook, 2007). The shift between the maximum at 5° North in the coastal phase and 10°N in the continental phase is very abrupt (Sultan et. al 2000), bringing about the term "monsoon jump". Various explanations have been proposed to account for the abrupt shift. Sultan and Janicot (2000) suggest it is triggered by westward propagating disturbances. Sijikumar et al. (2006) and Ramel et al. (2006) implicate the Saharan heat low, which intensifies and shifts northward at the time of the "jump" whilst Gu and Adler (2004) pointed out that the shift is associated with a northward shift of the African Easterly Jet and associated horizontal and vertical shear zones, as well as the development of westward-propagating waves. Again, it is suggested that the shift is related to the interaction of the Atlantic equatorial cold tongue and the African monsoon (Okumura and Xie 2004) whiles Sultan et al. (2003) suggests the complex interactions among convection, AEJ dynamics and local topography, especially the Ahaggar Plateau and Tibesti highland are also responsible for the jump. Their work also pointed out that when the heat low is sufficiently intense, it leads to a reversal in the potential vorticity gradient and, consequently, there is a generation of AEWs and convection. The shift begins with a release of potential instability leading to the inertial instability shifting the rain band to 10° N (Hagos and Cook 2007). The underlining of all these mechanisms is the northward shift and intensification of the

latitudinal temperature and pressure gradients over West Africa. Changes in the heat low and the instability mechanisms are probably direct consequences of the increased gradients. The northward shift of the AEJ, shear zones, wave's disturbances, and convection can be viewed as results of the aforementioned factors.

2.1.4. African Easterly Jet

AEJ is a thermally-driven wind system located above strong low-level meridional potential temperature and geopotential height gradients between the Sahara and the Gulf of Guinea (Hsieh and Cook, 2005). The Sahara Desert to the north creates a dry and dusty Saharan air layer, an elevated warm anomaly that is north of cooler air near the equator (Figure 2.4). Strong easterly geostrophic flow develops in response to the significant surface temperature and moisture gradient from the Gulf of Guinea to the Sahara. Low-level flow associated with the African monsoon is paramount to the development of AEJ. The AEJ exhibits large vertical and horizontal wind shears with a position of between 10^{o} to 16^{o}N. The vertical wind shear associated with the AEJ is crucial to the organization of moist convection and the generation of squall lines. According to Omotosho (1990) the vertical wind shear associated with the AEJ promotes the organization of mesoscale convective systems (MCSs) which produce 95% of the rainfall in the Sahel. It is very strong from April through August, when it vertical shears of roughly the same magnitude as the horizontal shear. The horizontal shear is particularly strong in August and September. Both the vertical and horizontal wind shears are important for the growth of AEWs (Nicholson and Grist, 2003).

The generation, maintenance and the factors that govern AEJ position and variability over West Africa have been investigated in many studies. Most of them have associated the AEJ with an ageostrophic circulation that enhances upward motion and deep convection south of the jet core and downward motion along and north of the jet. It is maintained by two separate diabatically forced meridional circulations (Tompkins *et al.*,

2005). Cook, (1999) showed that the AEJ is related to the negative meridional soil moisture gradient. The meridional circulation caused by the ITCZ convection also play significant role in AEJ maintenance (Schubert *et al.,* 1991). Many studies have shown a consistent link between AEJ and West Africa rainfall variability. Sylla et al. (2010a) showed that AEJ location in higher latitude would lead in general to more precipitation over West Africa while a lower latitude position of jet mostly favors less precipitation. Mohr and Thorncroft (2006) also found that the intense convective systems follow the seasonal migration of the AEJ northwards. Hagos (2014) show that much change in precipitation is related to changes in circulation, particularly to the response of the intensity and latitudinal position of the AEJ, which varies with the changes in meridional surface temperature gradients. AEJ plays vital role regarding the large-scale interactions in the West African monsoon system because it is often subject to barotropic and baroclinic instabilities. The instabilities are sources of perturbations at synoptic scale such as African Easterly Waves (Kiladis et al., 2006)

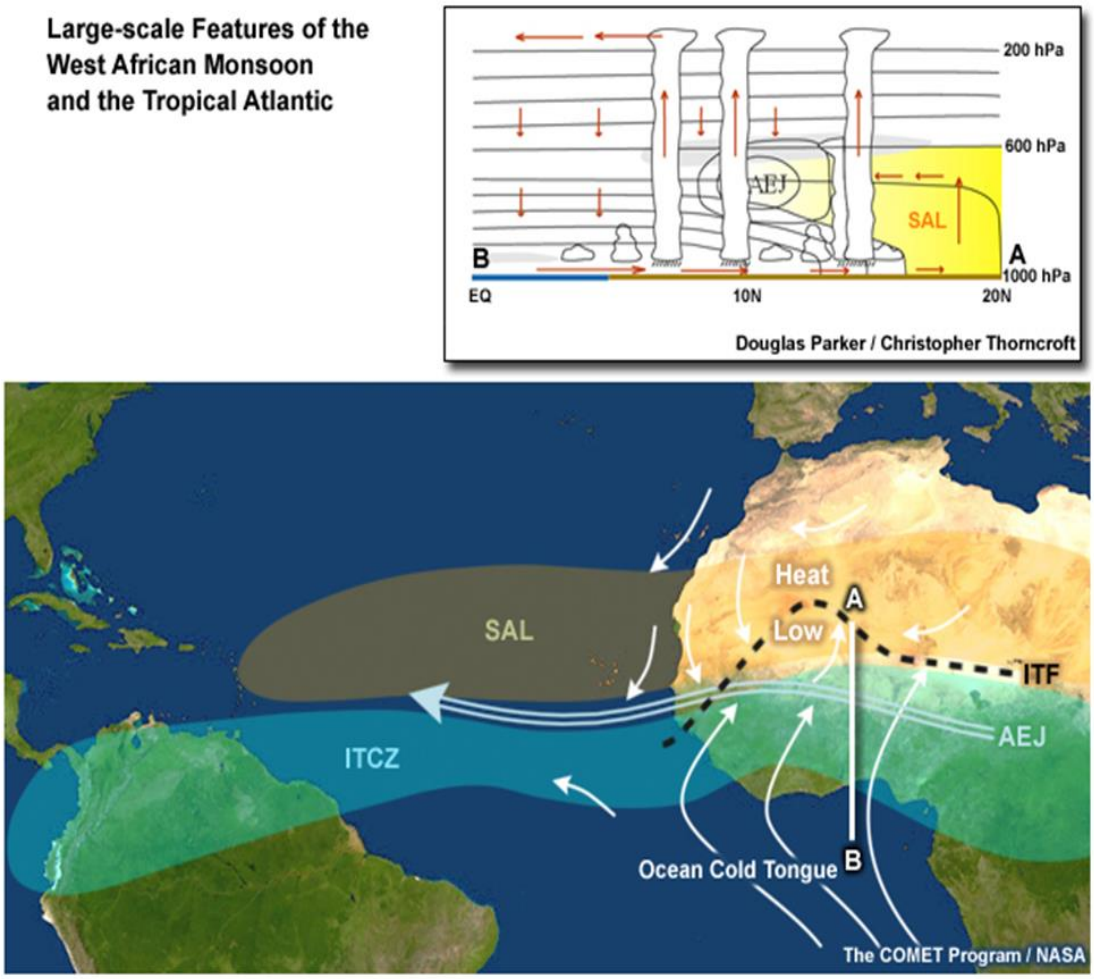

Figure 2. 3: Major large-scale features of the West African Monsoon and tropical Atlantic ocean; inset is a schematic of N-S vertical cross section along the Greenwich Meridian highlighting the heat low-AEJ-ITCZ system, Saharan Air Layer (SAL), and meridional variation the atmospheric boundary layer.

Source:

http://kejian1.cmatc.cn/vod/comet/tropical/jetstreams/navmenu.php_tab_1_page_3.2.0_type_text.htm

2.1.5. Tropical Easterly Jet

The Tropical Easterly Jet (TEJ) is a dominant feature of the northern hemispheric summer over southern Asia and northern Africa. It affects the summer rainfall over West Africa. The TEJ is located between 5^{o} and 10^{o}N with wind speeds 20-30m/s. This strong flow is due to the existence of strong meridional temperature gradient between the Himalaya plateau and the Indian Ocean (Krishnamurti and Bhalme, 1976). Variability in the structure, intensity, and location of the TEJ can influence the development of deep, moist convection over West Africa. The right entrance region of TEJ happens to correspond to upward branch of the Walker circulation that extends from Southeast Asia eastward across the Pacific Ocean and is associated with deep convection (Figure 2.3, Besson and Lemaitre, 2014). The TEJ is associated with the African monsoon and it is weak when the monsoon is weak but strong when the monsoon is strong, suggesting that variability in the monsoon also modulates variability in the strength of the TEJ (cook, 1998; Nicholson et al., 2001; Grist and Nicholson, 2001; Nicholson, 2013). It is an important feature of the tropics, which occurs only during northern hemisphere summer. Deep, moist convection forms preferentially in the right entrance and left exit regions of the jet, located over central to western Africa. The association between the TEJ and rainfall appears to be primarily upper-level divergence associated with the jet core. The divergence results from strong meridional components of the TEJ over Africa (Nicholson and Grist, 2003). This pattern is particularly pronounced in wet years in the Sahel and appears to play a role in its impact on rainfall (Nicholson, 2009). TEJ is linked not only to more rainfall in the Sahel, but also a more intense rainbelt. Other studies (Nicholson *et al.,* 2003; Thorncroft *et al.,* 2011) have shown that a weak AEJ with a strong TEJ correlates well with Sahel rainfall. Lembur*g* e*t al*., (2017) found a substantial correlations between Sahel rainfall and TEJ strength on decadal time scales, but on shorter time scales, the correlations become weaker and the relationship between the

TEJ and Sahel rainfall is less clear. Lemburg *et al*. (2019) also showed that initiation, intensity and size of Mesoscale convective systems, major rainfall producing systems over West Africa, are not associated with TEJ-related upper level divergence or its anomalies.

2.1.6. African Easterly Waves

African easterly waves (AEWs) are synoptic-scale perturbation on the African easterly jet (AEJ) over northern Africa during the boreal summer season between June and October, propagating westward across the Atlantic (Burpee, 1972; Kiladis *et al.,* 2006, DeLonge *et al.,* 2006). It results from the increase instabilities associated with the AEJ. They have wavelengths of approximately 3000 km, a period of 3-5 days and propagate westward at about 5-8m/s. They are particularly important for rainfall over the Sahel (Diedhiou, 1999; Wu et al., 2013). However, Pytharoulis and Thorncroft (1999) suggested that some AEWs may exhibit periods of 6-9 days. Their largest amplitude is obtained near the west coast of Africa and decays after emerging over the eastern Atlantic Ocean 6-8 days after their formation. The biggest amplitude is obtained at around 650 hPa and exhibit a vertical tilt against the shear vector such that AEWs tilt eastward with increasing height (Cornforth *et al.,* 2009). The AEWs are important for organizing precipitation patterns, influenced by the effect of Sahara Desert which causes a reversal of meridional surface temperature gradient in the mid-troposphere during the boreal summer (Diedhiou et al., 1999). This meridional temperature gradient reversal is responsible for the African Easterly Jet generation. The studies of Burpee (1972) and Reed *et al.* (1977) showed that this jet satisfied the necessary conditions for barotropic and baroclinic instability. This instability generates perturbation and therefore assists in the development of AEWs. Many studies have shown AEWs as seed disturbances for Atlantic tropical cyclones (Thorncroft and Hodges, 2001), and the interannual variability of AEWs may modulate Atlantic tropical cyclones on similar timescales. Gaye et al.

(2005) and Mekonnen et al. (2006) show that AEWs modulate summer rainfall through the initiation and organization of mesoscale convective systems (MCSs) and squall lines during the monsoon season. Other studies suggest that the variation of convection is the more important factor controlling periods of active and inactive AEWs than the state of the AEJ. For instance, Hsieh and Cook (2005) demonstrated that AEWs without the AEJ develop more readily in their simulation with strong ITCZ than the opposite. Leroux *et al.* (2010) proved that the increase in AEWs is associated with an increase of moist convection in East Africa. Kiladis *et al.* (2006) assert that convection with AEWs is initiated by dynamical forcing associated with the wave, which forces vertical motion at low levels and couples the wave to deeper convection as it matures. Leroux and Hall (2009), highlight that AEWs develop most readily when the AEJ has a strong Potential Vorticity (PV) gradient over a large region. Overall, the AEWs play a crucial role in establishing the most favorable synoptic conditions for the development of intense rainfall event over West Africa (Diedhiou *et al.*, 1999; Cretat *et al.*, 2015).

2.1.7. Mesoscale Convective Systems (MCS) and Squall Line (SLs)

2.1.7.1. Mesoscales Convective Systems (MCS)

Mesoscale Convective Systems (MCS) can be defined as complexes of thunderstorms which become organized on a scale larger than the individual thunderstorms and normally persist for several hours or more. The overall cloud and precipitation pattern of an MCS may be round or linear in shape and includes weather systems such as tropical cyclones, squall lines, lake-effect snow events, polar lows and Mesoscale Convective Complexes (MCCs). MCS is often used to describe a cluster of thunderstorms that does not satisfy the size, shape, or duration criteria of a Mesoscale Convective Complex (NWS, 2012). The MCS are essential for the earth equilibrium as they modify the environment on a scale many times larger than the visible cloud (Moncrieff, 1995). They

regulate the transport of energy, heat, moisture and momentum in the atmosphere (Schröder *et al.* 2009) and play an important role in the input of energy to the climate system through the radiative effect of the upper-tropospheric cloud and water vapor and enhanced surface fluxes (Moncrieff, 1995). It is well known that MCSs often produce severe weather and over half of the annual warm season precipitation is associated with MCSs. MCSs are often prolific producers of cloud-to-ground lightning. Over West Africa, many studies prove that large MCSs play a crucial role in rainfall variability (Mathon *et al.,* 2002; Fink *et al,* 2006; Laing *et al.* 2008). Heavy rainfall over sub-Saharan northern Africa is usually related to the generation of MCSs. Mathon et al. (2002) and Mohr (2004) showed that MCSs contribute up to 95% of the boreal summer rainfall over this region and that the diurnal cycle of rainfall is related with MCS activity. Over West Africa Sahel, it is estimated that between 50 and 95% of the total rainfall occurred during the peak of the rainy season which can be explained by about 12% of the total number of MCS (Lebel *et al.,* 2003; Mohr, 2004). However, the contribution of MCSs to annual rainfall ranges from 16% to 32% along the shore of the Gulf of Guinea (Acheampong, 1992; Omotosho, 1985), about 50% in the Sudanian zone (Eldridge, 1957; Omotosho, 1985) but more than 80% in the Sahelian region (Mohr *et al.,* 1999). This rainfall has been shown to be strongly modulated by the organization and intensity of deep convection within these MCSs (Fink and Reiner, 2003, Cretat *et al.,* 2013). As mention in the last section favorable large-scale dynamical forcing for the generation of rainfall through the organization of MCSs may be provided by AEWs. Over West Africa, MCSs are usually integrated in AEW, but they propagate faster than most AEWs, suggesting that an individual AEW can embed several MCSs (Gaye *et al.,* 2005; Mohr and Thorncroft, 2006). However, the MCSs are also linked with AEJ since it transport them westward over West African region. According to Grist and Nicholson (2001), the intraseasonal oscillations of the AEJ have an impact on the latitudinal

oscillation of the MCSs. A more northern (southern) location of the AEJ lead to shift of the MCs tracks northward (southward) (Nieto-Ferreira *et al.,* 2009). Mohr and Thorncroft (2006) found also that in September during the MCSs event the most intense convective system occurred south of the AEJ. By contrast, fewer studies have focused on the role of the TEJ (Lavaysse *et al.,* 2006; Nicholson, 2009). According to Besson and Lemaitre (2014), this is not surprising since the TEJ maximum is usually along the Guinea Coast, while most MCSs are much farther north and closer to the AEJ maximum. When the monsoon is well developed, the TEJ is over West Africa and is correlated with the monsoon peak, with MCs activity linked to the TEJ (Diongue *et al.,* 2002; Redelsperger *et al.,* 2002).

2.1.7.2. Squall Lines (SLs)

Squall line is a form of MCSs and defined as a narrow band of active thunderstorms (Newton, 1950). It is shown to be associated with about 75% of the tropical North Africa rainfall (Omotosho, 1985, 1990). Squall lines can extend to hundreds of miles in length, simultaneously affecting several states at a time. They also can travel fast at speeds up to 60 mph. Squall lines typically form in unstable atmospheric environment in which low-level air rise unaided after being initially lifted (e.g. by a high ground) to the point where condensation of water vapor occurs. Heat is released during condensation, resulting in the rising air becoming lighter than nearby air at the same height. This leads to an increase in the speed of the rising air which sometimes reaches speeds above 30 mph (WW2010, 2019). However, many squall line are observed in association with MCCs in West Africa (Leroux, 2001), although short periods of very heavy rain, sometimes associated with squall lines, need not to be from cumulonimbus embedded in mesoscale cloud systems (Fink and Reiner, 2003). The contribution of squall lines to Sahel rainfall is not uniform everywhere in West Africa. Mathon et al. (2002a) indicated that the westward-propagating squall lines contribution to the total rainfall varies

significantly with respect to latitude, accounting for a much as 80% - 90% of the annual rainfall in the Sahelian climate zone. In the wetter climate zones to the south, squall lines account for about half of the rainfall in the Sudanian climate zone (Eldridge, 1957; Omotosho, 1985) and as little as 16% - 32% along the Guinea coast (Acheampong 1982; Omotosho, 1985). Prominent squall lines genesis maximum over highland of the central Nigeria (e.g. Jos Plateau) has been shown by Omotosho (1984), while the Dahomey Plains in Benin Republic is found to be for less-favorable zone for the squall lines genesis (Aspliden *et al.,* 1976; Vollmert *et al.,* 2003). However, Fink et al. (2006) hypothesized that the strong organizations of organized convective systems over Nigeria may be related to local factors (e.g., terrain, height, moist static stability, and upper level outflow) that help developing squall lines attain the necessary strength of the self-sustaining mesoscale circulation.

2.2. Rainfall variability in West Africa

West Africa rainfall variability has serious implication on socio-economic activities. This is because more than 95% of its agriculture activities are rainfed and many other management decisions such as agricultural practices, hydro-electric power generation, and water resource management in the region are also rainfall dependent. Rain-fed agriculture serves as the main source of income for most economies in the region. For instance, Jalloh et *al.* (2011), Suhas et *al.* (2009), World Bank (2017) reported that more than 60% of the population in most West African countries make a living from rainfed agriculture, which account more than 35% of the Gross Domestic Product (GDP) and about 40% of the exports of the region. The variability in rainfall will therefore have serious consequences on agricultural practice, water resource management and hydroelectric power generation. Consequently, any rainfall variability that results in

droughts or floods usually reduces agricultural productivity, thereby threatening food security, water management at both household and national levels.

West Africa region is divided in to climatic zones which includes the arid, semi-arid, sub humid and humid zones. The arid zones include Mali, Burkina Faso, Senegal and Niger which forms the Sahel and Saharan regions in West Africa. The rainfall begins in Savanna zone from May/June and it receives higher annual rainfall of up to 2000mm. Over the Sahel, the annual rainfall is less than 750 mm in most area and becomes even less than 200 mm, with an extended dry season that lasts for about 10 months (Kessler and Breman, 1991; Casenave and Valentin, 1992). The semi-arid zone of West Africa is grassland and is located at the northern parts of Mali, Senegal, Niger, Burkina Faso, Nigeria and Cameroun. This zone also receives annual rainfall that range from 250 to 500 mm (Casenave and Valentin, 1992). The Semi-humid zone includes the Sudan Savannah which is shrub and grassland with mean rainfall values ranging from 500 to 900 mm. The semi-humid zones include southern parts of Mali, Burkina Faso, Niger, Senegal, and the north of Nigeria, Togo, Cameroon and Benin. The humid zone consists of two sub zones such as Guinea savannah zone and the Forest zone (Boffa, 1999; Valentin *et al.,* 2004; Jalloh *et al.,* 2011). The Savannah sub zone which has an annual rainfall of between 1500 mm and 2000 mm divided into two alternating dry and wet seasons. This sub zone includes southeast Guinea, middle of Nigeria and Ghana, parts of Cote d'Ivoire, and parts of Cameroon. The Forest zone has rainfall of about 1500 mm to more than 2000 mm with a bimodal pattern. This forest zone includes Ghana, Togo, Benin, Cameroon, Congo, the southern zone of Cote d'Ivoire, east of Sierra Leone, Eastern Nigeria and Gabon (Jalloh *et al.*, 2011).

The climate of West Africa is made of two main seasons such wet and dry seasons. The maximum of its rainfall is observed during the period June-August which occurs in the peak of the WAM. Numerous studies has focused on West Africa rainfall variability especially the Sahel region, which has been the most vulnerable due to severe droughts and famine in the last century (e.g., in the 1970s and 1980s, Janicot, 1992; Nicholson *et al.*, 2000; Vizy and Cook, 2001; Hulme, 2001; Camberlin and Diop, 2003; Giannini *et al.*, 2003; Rowell, 2003). Most of them have associated this variability to the global climate teleconnections and regional climate systems, which include the ITD, monsoons, the tropical Atlantic Sea Surface Temperature (SST) anomalies, subtropical anticyclones, atmospheric winds, the jet streams etc. The global teleconnections include those associated with El Nino Southern Oscillation (ENSO) and the North Atlantic Oscillation (NAO). The rainfall patterns of many parts of Africa respond significantly to different phases of the ENSO cycle forcing.

2.3. West African Rainfall and Sea Surface Temperature (SST)

2.3.1. Role of Sea Surface Temperature (SST)

Sea surface temperature (SST) is defined as a basic measure of ocean surface conditions. It usually refers to water temperature measured within the upper 10 meters of the ocean. In these waters, after variation due to seasonal changes, the oceanographic process called upwelling is a major cause of sea surface temperature variation. Over West Africa many studies have demonstrated that the variability of the SSTs influences the variability of West African rainfall (Rowell *et al.*, 1992; Paeth and Hense, 2004; Lu and Delworth, 2005; Fink *et al.*, 2006; Biasutti *et al.*, 2008). These showed that the change in latent heat release over the West African monsoon region have great impact on the large scale tropical circulation. There have also been many studies that examined the impact of teleconnection between the SST anomalies in the Pacific, Indian and Atlantic

Oceans on Sahelian rainfall (Giannini *et al.,* 2003; Lu and Delworth, 2005; Caminade and Terray, 2010). While it has been concluded that SST patterns play a crucial role in West African rainfall variability (Biasutti et al., 2008; Giannini et al., 2008), there is still a debate regarding the major drivers (e.g., NAO, AMO, QBO, IOD etc.). Several results found that an increase of the Sahel rainfall coincides with an oceanic pattern that resembles a configuration of Pacific Niña, Atlantic Niño and western Indian Ocean cooling (Losada *et al.,* 2010). They further found that this mode accounts for 54% of the squared covariance between West African rainfall and tropical SST anomalies. According to Zheng *et al.* (1998), in 1994 the abundant rainfall observed in West Africa was linked with the warm SST anomaly. Hoerling *et al.* (2006) also showed that regional weather patterns forced by the SST of the North Atlantic have more influence than hydrological impact of land use on the local climate in the Sahel region. An understanding of observed variability in precipitation therefore requires both SST and land-atmosphere interaction (Wang *et al.,* 2004). Camberlin *et al.* (2002) found that ENSO (El Niño southern oscillation (ENSO) and Atlantic SST (predominantly south Atlantic) contribute to different parts of the rainfall variance in West African Sahel.

2.3.2. The El Niño Southern Oscillation (ENSO)

ENSO is a naturally occurring phenomenon with significant impact on the worldwide climate (Ropelewski and Halpert, 1987, 1996). It has positive and negative effects on society and environment; but to a greater extent, disadvantageous impacts (Guzman et al., 2009). ENSO refers to El-Niño and La Niña. El-Niño refers to a warming pool over the Pacific Ocean that occurs usually every three to seven years, lasts 12-18 months and dynamically associated to the Southern Oscillation. During El Niño conditions, the usually present east to west winds weaken and anomalous west to east flow develops. The west to east flow transport warm equatorial waters from the western Pacific towards the eastern Pacific and northern South America (see Figure 2.5; IRI, 2019). On the other

hand, La Niña represents a colder than normal SST over the Pacific, is characterized by an unusually high pressure in the Western Pacific and low pressure over the Eastern Pacific. Over West Africa several works pointed out the role of ENSO and Pacific Ocean in modulating Sahel precipitation (e.g., Rowell, 2001; Janicot and Sultan, 2001). The limiting role of ENSO on rainfall variability only on eastern Sahel has also been suggested (Bader and Latif, 2003). One of their findings is that the interannual to decadal variability in precipitation over West Africa is controlled by competing physical mechanisms (also, Druyan, 2011). Many studies also associated its role in drought occurrence in Southern Africa (Philippon *et al.,* 2012) and Eastern African (Ropelewski and Halpert, 1987). However, over Western Africa, its impacts are still under debates. Among some studies on the matter, no agreement was found on the effects of ENSO on Sahel drought. For example, while Janicot *et al.* (2001) and Okonkwo *et al.* (2014) suggested that ENSO have a relationship with Sahel rainfall and this impact has strengthened after the 1970s, Bader and Latif (2003) suggested its effects are localized to the Eastern Sahel. However other studies by Okonkwo and Demoz (2014); Hansen et al. (2016) have also associated ENSO and others climatic indices Such as the Atlantic Multi-decadal oscillation (AMO), Quasi-biennial oscillation (QBO) etc. as sources of rainfall variability over West Africa.

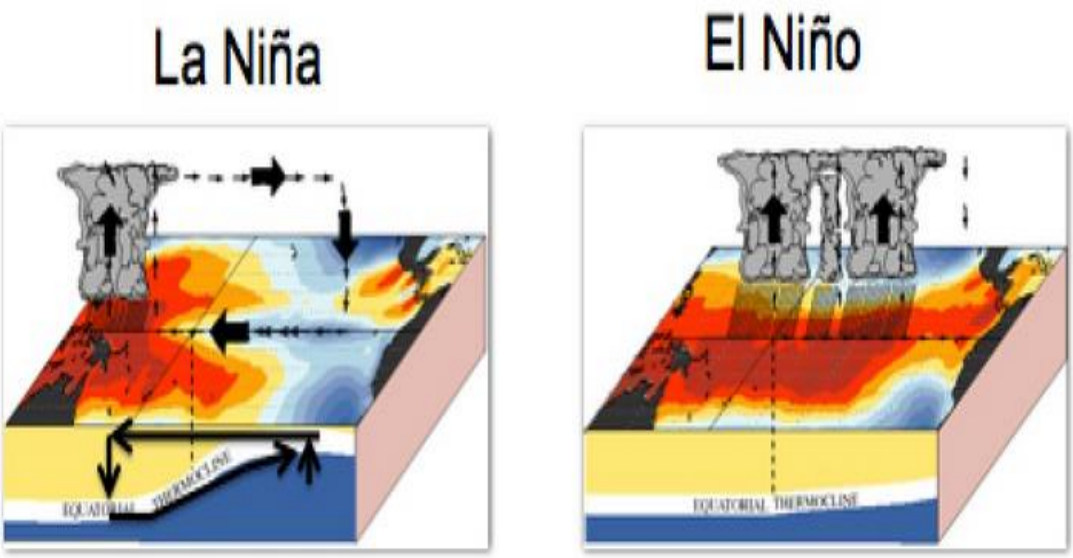

Figure 2.4: Illustration of normal vs. El Nino condition with the migration of the warm pool eastward and attendant precipitation patterns (TAO_Project_Office 2016)

2.4. The theory of the quasi-biennial oscillation

The quasi-biennial oscillation (QBO) was first reported in the 1960s. It is a major oscillation in the equatorial stratospheric zonal wind (Lindzen and Holton, 1968). It consists of an alternating pattern of easterlies and westerlies that slowly descend from the stratopause to the tropopause (Baldwin *et al.,* 2001). The QBO is mainly driven by vertically propagating waves with easterly and westerly phase speed that dissipate in the corresponding shear zones, leading to easterly acceleration in easterly shear zones (where easterlies increases with height) and westerly acceleration in westerly shear zones (Holton and Lindzen, 1972). These tropically-trapped waves are of various horizontal scales, ranging from planetary scales to a few kilometers or less (Baldwin *et al.,* 2001; Kim and Chun, 2015). The oscillation has a cycle (average period) of about 26 months and maximum amplitude of about 20 m/s with a periodic change in its zonally symmetric wind regimes, i.e., the easterlies and westerlies. The downward propagation with speed of around 1 km/month through lower stratosphere is a key feature of this oscillation (Holton, 1968; Quiroz, 1981). The maximum amplitudes are observed in the middle and lower tropical stratosphere, with the easterly phase having larger amplitudes compared to the westerly phase. The region of QBO winds is confined to the latitude band between about 15^{o}S and 15^{o}N and is observed mainly at stratospheric altitudes between about 18 and 40 km. In the upper stratosphere and large parts of the mesosphere the situation is different. In this altitude region the zonal mean zonal wind is dominated by a semi-annual oscillation (SAO). The wind changes between strong easterlies and strong westerlies with a dominant period of 6 months. In the upper mesosphere the zonal mean zonal wind is again dominant by the QBO (Baldwin *et al.*, 2001). In the past few decades, a number of theories have been developed to explain the QBO. It has been shown by Lindzen and Holton (1968) and Holton and Lindzen (1972) that the QBO is a wave driven oscillation. Waves of both global scale (equatorial wave's mode like Kelvin

waves, equatorial Rossby waves, or Rossby-gravity waves) as well as mesoscale gravity waves contribute to the observed reversals. According to Dunkerton (1997), the total wave fluxes should be about 2-4 times as high as the flux of the global scale wave modes alone. This means that the impact of mesoscale gravity waves in the forcing of the QBO should be about 50-75% of the total wave forcing. There has been some debate as to the type of waves that are involved, i.e., large scale Rossby-gravity waves or Kelvin waves and/or mesoscale internal gravity waves. The gravity waves fluxes have been recognized to be a generator of a large vertical momentum flux for driving QBO. The QBO is forced by the interaction of long-period vertically propagating tropical atmospheric waves, including Kelvin, Rossby-gravity, gravity, and inertia-gravity waves that are tied to tropical convection (Holton and Lindzen, 1968). These waves deposit their momentum in the stratosphere to force the QBO cycle (Baldwin et al., 2001). The QBO is driven by equatorial waves interacting with the stratospheric mean flow (Holton and Lindzen, 1972).

2.5. Equatorial Wave Theory

Equatorial waves is an important class of tropical atmospheric disturbance (Fathullah *et al.*, 2017). It has been recognized that the tropical thermocline (the sharp boundary between warm and deeper cold waters) provides a wave guide many types of large-scale ocean waves. The existence of this waves guide is due to two key factors. The mean ocean vertical stratification in the tropics which facilitates waves propagation. Secondly, the Coriolis parameter vanished exactly at 0^o of latitude, the equator works as a natural boundary, suggesting an analogy between coastally trapped and equatorial waves (Fedorov and Brown, 2009). The equatorial waves are atmospheric phenomena that propagate parallel to the equator; it is mainly generated by tropical convection and is trapped within an equatorial waveguide produced by the change in Coriolis parameter

with latitude (Garcia and Salby, 1987; Hayashi and Golder, 1997). In some circumstances they may also propagate energy and momentum vertically. Equatorial waves are solutions to the "shallow water" equations, characterized by meridional mode number, frequency, planetary zonal wavenumber, and "equivalent depth" h of the shallow layer of fluid (Wheeler and Kiladis, 1999). The equivalent depth $c = \sqrt{gh}$, links the shallow water equations and vertical structure equation through a separation constant (Wheeler and Kiladis, 1999). The relationship between phase speed and equivalent depth implies that deeper waves have faster speeds. According to Matsuno, (1966), the latitudinal extent of the waves is characterized by$(c/\beta)^{1/2}$, where c is the phase speed and β is the variation of the Coriolis force in the meridional direction suggesting that faster equatorial waves have greater latitudinal extent. The most well-known examples of equatorial waves are eastward propagating Kelvin waves and westward propagating Rossby waves. The Kelvin waves and Rossby waves are important due to their associated large-scale flow and low-frequency characteristics, as well as the ability to transmit information from the Indo-pacific warm pool to the West African monsoon region. Equatorial waves are divided into two regimes by Wheeler and Kiladis (1999): symmetric and asymmetric. Mixed Rossby-gravity waves are antisymmetric about the equator, while equatorial Rossby waves and Kelvin waves are symmetric about the equator. Inertia-gravity waves fall into both regimes.

2.5.1. Equatorial Rossby Waves (ER)

Rossby-gravity waves (first reported by Yanai and Maruyama, 1996) propagate westward and transport easterly momentum upward. Rossby waves in the mid-latitudes arise out of the meridional variability in the potential vorticity field. Over the tropics they can be generated by the meridional variability of the Coriolis parameter (Gruber, 1974; Zangvil, 1975). Equatorial Rossby waves are associated with twin vortices on either side of the equator; such vortices occur most often in the western Pacific Ocean

and Indian Ocean. The direct effects of equatorial Rossby waves are strongest over the Asian monsoon and West Pacific warm pool. Rossby waves have a period of about 4 to 5 days, and propagate westward with a vertical wavelength of about 4 – 8 km. It plays pivotal role in controlling disturbance in the equatorial stratospheric (e.g., QBO) and tropospheric circulation and precipitation (Setiawan, 2010; Lubis and Jacobi, 2015).

2.5.2. Equatorial Kelvin Waves (EK)

The Kelvin waves (first reported by Wallace and Kousky, 1968a) propagate eastward and transport westerly momentum upward. Among the two equatorial wave models, the existence of Kelvin waves has been documented fairly well compared with Rossby-gravity, because the kelvin wave mode has much longer horizontal and vertical scales than the Rossby-gravity wave mode. Kelvin waves are large-scale waves that propagate along a physical boundary such as a mountain range or coastline. Kelvin propagate eastward with a vertical wavelength of about 6 – 10 km, with periods ranging from 10 to 20 days and 6 to 10 days which are classified as slow and fast waves, respectively. These eastward propagating planetary scale waves carry eastward momentum upwards but are damped by various processes like radiative cooling, small scale disturbance and critical level interactions. After the waves are damped, they lose momentum and accelerate the westerly mean flow of the QBO (Das and Pan, 2013). In the tropics, the southern and northern hemispheres act as a trapping barrier, such that equatorial Kelvin waves are considered to be “equatorially-trapped” waves. The Kelvin waves are thought to be important to the El Niño Southern Oscillation (ENSO) and the QBO. Several studies demonstrated that the lower stratospheric Kelvin wave activity is observed mostly during the transition from the easterly to the westerly phase of the QBO, suggesting that the role of Kelvin wave is by far the dominant global scale equatorial wave mode during QBO easterly phase and is responsible for the largest part of the wind reversals from QBO easterlies to westerlies (Wallace and Kousky, 1968b; Maruyama,

1979, 1991; Miller et al., 1976; Ern and Preusse, 2009). Kelvin wave are also known to affect the dynamics, cloud physics and transport around tropical tropopause layer (Fueglistaler *et al.,* 2009). Their effects on deep, moist convection over Africa, South America, and the western Indian Ocean exhibit strong seasonal variability. Kelvin wave have a horizontal length scale of about 2000 km and as such have a direct impact on deep, moist convection within approximately 10^{o} latitude of the equator.

CHAPTER THREE: RESEARCH METHODOLOGY

3.1 STUDY AREA

The study area of this research is West Africa which is located below 20^{o}N. Following Omotosho and Abiodun, (2007), Abiodun *et al.* (2012) and for the purpose of weather and climate application, three climate sub-regions, Guinea Coast (4^{o}N-8^{o}N, 18^{o}W-18^{o}E), Savannah (8^{o}N-12^{o}N, 18^{o}W-18^{o}E) and Sahel region (12^{o}N-16^{o}N, 18^{o}W-18^{o}E) (Figure 3.1) were selected for more detail analysis. The region is however among the wettest on the continent with mean annual rainfall values ranging from 200 to 4500 mm (Jalloh *et al.,* 2011). This Guinea zone has sub-humid climate with an average annual rainfall is between 1250mm and 3000mm. The numbers of days of growing period (DGP) varies between 180-270 days. The Savannah zone is a semi-arid zone (Sahelio-Sudan) with an average annual rainfall between 750 mm and 1250 mm in a season. The Sahel or Sahelian zone is an arid zone and has up to 750 mm of rain in a single but short rainy season from June-September with a mean GDP of 90 days. The choice of dividing the zone is based on the local population's high dependency on rain-fed agriculture for their economy and the need to understand and bring a clear picture on the influence of QBO on the West African rainfall variability, since the QBO is an essentially equatorial climate system.

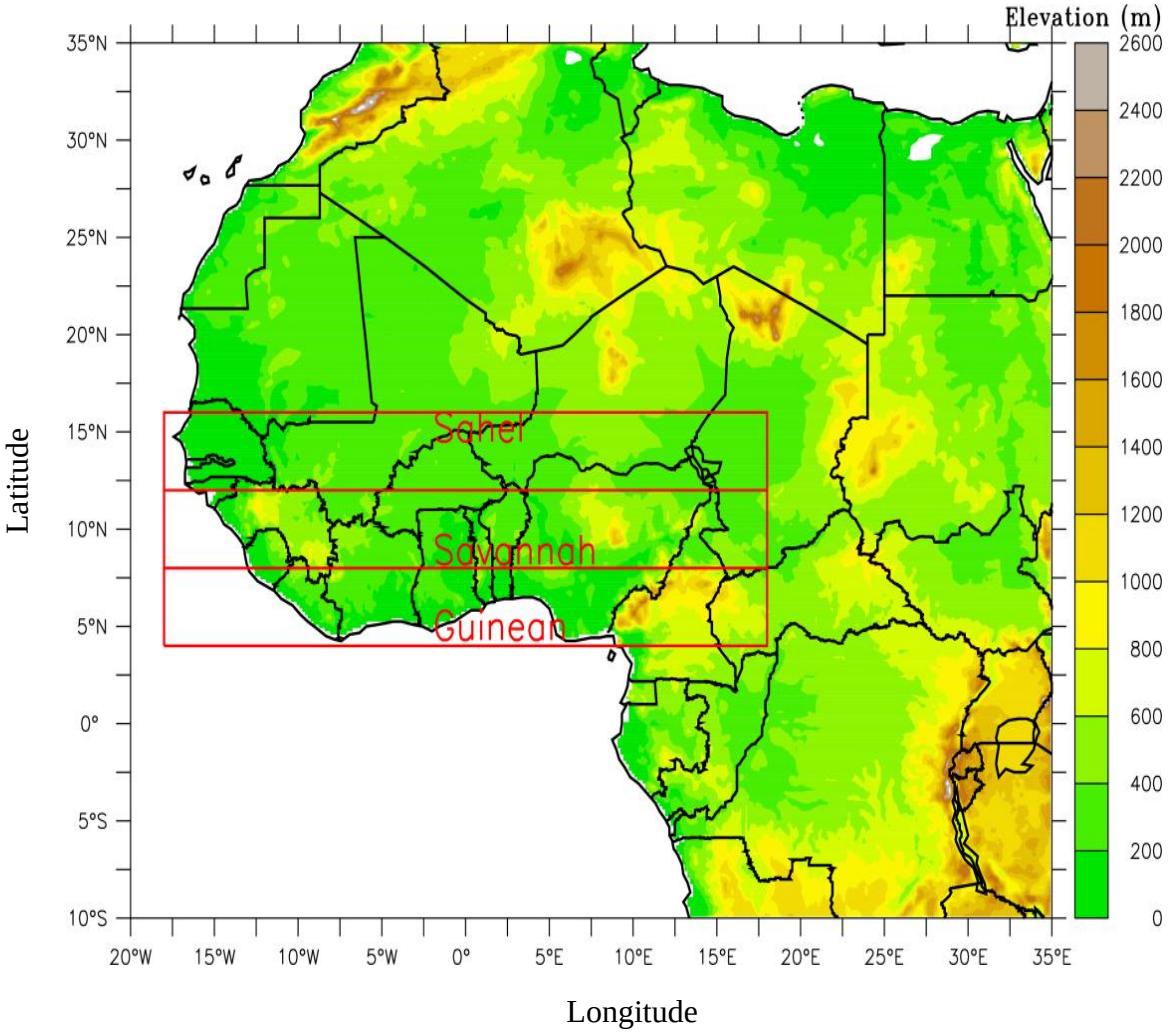

Figure 3.1: West African domain showing the topography and regions designated as Guinea, Savannah and Sahel zones.

3.2 DATA

In this study different types of dataset are used for different purposes. The model CMIP5, reanalysis and observed datasets were used to simulate West African monsoon systems and its relationship with the QBO. The observational and reanalysis data were used to evaluate the capability of the model to reproduce climate variability.

3.1.1 ERA-Interim Reanalysis

The European Center for Medium-Range Weather Forecasts (ECMWF), ERA-Interim is the primary dataset utilized in this study. It is a reanalysis of the global atmosphere beginning in 1989 and continuing in real time (P. Berrisford et al., 2011; Dee et al., 2011). It corresponds to new version of ECMWF model with the objective to fill the gap between the old and new generation reanalysis. ERA-Interim is a coupled wind-wave reanalysis produced at ECMWF covering the period 1979 onwards. It is also from the Integrated Forecast System (IFS), which is operational since 2006. The model has 79 km of horizontal resolution and 60 vertical levels. The available data have a temporal resolution of 00h, 03h, 06h, 12h, and 18h, with 0.75^{o} in longitude and latitude also with 37 pressure levels from 1000 hPa to 0.1 hPa (Berrisford et al., 2009). The purpose is to overcome the problems of data assimilation and provide meteorological variables needed for a better understanding of West African rainfall variability. It also improve the quality of the reanalysis products relating to quality control, bias correction, and performance monitoring to be consistent with observations given the estimated uncertainties (Dee *et al.,* 2011).

3.1.2 Observation Data

In this work the Global Precipitation Project (GPCP) version 2.2 was utilized due to lack of quality observation datasets and accessing the existing one is still a challenge in the region. It is needed to support a variety of studies, including global change, surface

hydrology, and numerical weather and climate model initialization and validation. GPCP is maintained by the National Aeronautics and Space Administration (NASA) and provides daily rainfall. The GPCP Monthly product provides a consistent analysis of global precipitation from an integration of various satellite data sets over land and ocean and a gauge analysis over land, and was initially described by (Huffman *et al.,* 1997). GPCP incorporates a blend of the six best quasi-global datasets (Huffman *et al.,* 2001). In particular, these datasets are: 1) Special Sensor Microwave/Imager (SSM/I; fractional occurrence of precipitation), 2) GPCP Version 2.1 Satellite-Gauge (monthly accumulation of precipitation), 3) geosynchronous orbit IR brightness temperature histograms, 4) low-orbit IR GOES Precipitation Index (GPI), 5) Television and Infrared Operation Satellite (TIROS) Operational Vertical Sounder (TOVS), and 6) Atmospheric Infrared Sounder (AIRS). The GPCP v2.2 consists of monthly precipitation estimation data at 2.5^{o} x 2.5^{o} horizontal grid resolution. The use of high resolution precipitation data over West Africa is important to account for topographical variances and the sharp moisture gradient between the Gulf of Guinea and the Sahara. Additionally, GPCP provides an alternative to ERA-Interim precipitation and provides a precipitation dataset to supplement the measure of convection provided by CLAUS, which improves the robustness of the study.

3.1.3 Global Circulation Models outputs

Also utilized was the numerical simulation carried out in the framework of the Atmospheric Model Intercomparison Project (AMIP) and historical experiments as part of the Coupled Models Intercomparison Project Phase 5 (CMIP5) simulations (Taylor *et al.,* 2012, CMIP5 recommended data, 2013). CMIP5 is the most current and the most extensive of the CMIPs. It is defined by experiment suites divided into three categories: 1) Decadal Hindcasts and Predictions simulations; 2) “long-term” simulations; and 3) “atmosphere-only” (prescribed SST) simulations for especially computationally-

demanding models (NCAR/UCAR, 2019). The CMIP5 includes 24 distinct models, data from which are available through the program for climate Model Diagnosis and Inter-comparison (PCMDI) Earth Grid (https://esdf-node.llnl.gov/search/cmip5/). The purpose of the use of AMIP and CMIP5 in this study is to undertake the systematic Intercomparison and validation of the performance of atmospheric Global Climate Models (GCMs) on seasonal and interannual time scales. The GCMs are among the most advanced tools, which simulate climatic conditions on earth hundreds of years into the future (Anandhi *et al.*, 2008).The GCMs may be useful tools to explore stratosphere/troposphere coupling mechanisms (e.g. Yoden *et al.*, 2017). However, many GCMs fail to generate the QBO due to coarse stratospheric vertical resolution (e.g. Charlton-perez *et al.*, 2013). There were few models generating QBO in the CMIP5. An overview of the models with the ensemble members, horizontal resolutions and further details are listed on Table 3.2.

Table 3.1: *Summary of reanalysis and observed datasets used in the present study*

Dataset	**Variables**	**Temporal coverage**	**Spatial coverage**
ERA-Interim	P, q, w, ua, va,	1979-2012, monthly mean	Global, ~0.75^{o} x 0.75^{o}
GPCP v2.2	P	1979-2012, monthly mean	Global, ~2.5^{o} x 2.5^{o}

Note: Variables are precipitation (P), specific humidity (q), vertical velocity (w), zonal wind (ua), meridional wind (va)

Table 3.2: Summary of model datasets used in the study

Model	**Reference**	**Resolution**	**Institute**
CMCC-CMS	Manzini *et al.* (2006) Giorgetta *et al.* (2006)	T63L95	Centro Euro-Mediterraneo per I Cambiamenti Climatic
HadGEM2-CC	Osprey *et al.* (2013) Hardiman *et al.* (2006)	1.25^{o} x 1.875^{o} L60	Met Office Hadley Centre
HadGEM3-A	Vautard *et al.* (2018) Christidis *et al.* (2012)	N216 L85 (~60 km)	Hadley Centre near-real time attribution system
MPI-ESM-MR	Schmidt *et al.* (2013) Krismer and Giorgetta (2014)	T63L95	Max Planck Institute for Meteorology (MPI-M)
MIROC-ESM-MR	Watanabe *et al.* (2011) Watanabe and Kawatani (2012)	256 x 128	Model for Interdisciplinary Research on Climate

3.2 METHODOLOGY

The methodology of this work consists of characterizing both the monthly and seasonal climatology of rainfall using observational data set and the zonal wind using reanalysis dataset. The positions of TEJ and AEJ during each month of the year were identified. To examine the monthly averaged structure of the African and Tropical Easterly Jets, monthly zonal winds at 600 hPa and 200 hPa where the jet is maximized were utilized. These fields were analyzed for all the months. This study also applied the wavelet transform to estimate the power spectrum or power spectral relationship between QBO, AEJ, TEJ and West African precipitation. Specifically, wavelet power spectrum, and bivariate and conditional wavelet transform using the Morlet wavelet analysis were employed. The wavelet power spectrum (WPS) provides time-frequency information about the cyclical characteristics of individual variable while wavelet coherence provides quantitative time-frequency information about the coupling between different variables, helping to identify strong periodicity between different variable (e.g. rainfall over West African zones, AEJ, TEJ and QBO at different stages). Also used was the composite method to describe evolution of QBO (e.g. west and east phase, QBO and Non-QBO year).

3.2.1 Wavelet Analysis Techniques for Rainfall variability

3.2.1.1 Wavelet Analysis

Wavelet analysis is a mathematical technique based on dilating and translating an analyzing function, called wavelet, at different scales and positions, in order to decompose non-stationary signals (e.g. time or space-series) into their frequency components, allowing the identification and analysis of dominant localized variations of power, i.e., where the variance of the time series is largest for a given frequency (Daubechies, 1992; Torrence & Compo, 1998; Grinsted *et al.,* 2004; Keener *et al.,* 2010). By wavelet analysis, one is able to determine both the dominant modes of variability of a time series and how they vary in time (Torrence and Compo, 1998). In natural phenomena, signals frequency present intermittent or transit features forming non-stationary data series to which classical Fourier analysis cannot be applied, requiring instead time-resolved methods (Furon *et al.,* 2008). The advantage of wavelet analysis is that the window size is not fixed, varying as a function of frequency (i.e. time resolution is intrinsically adjusted to the scales). It allows analyzing different scales of temporal variability and it does not need a stationary series. In this context, a main purpose of using the wavelet analysis technique is to quantify and visualize statistically significant changes in the QBO and rainfall over a mutli-decadal time scale. Since its theoretical development in 1984 by Grossmann and Morlet (1984), wavelet analysis have been applied in several fields such as in meteorology and climate as well as oceanography (Furon *et al.,* 2008; Labat, 2010). Meteorological forecasts with reasonable skill offer useful information of rainfall estimation with antecedence ranging from some days to one year. Therefore, this study can be considered an important tool for time series analysis, especially when used in rainfall forecasts, which can helps the studies concerning the coupling between rainfall, jet stream and quasi-biennial oscillation.

3.2.1.2. Application of Wavelet analysis in Rainfall variability studies

Wavelet analysis has been used by several studies for studying rainfall variability over the world in general and particularly over West Africa (e.g. Santos et al., 2001; Santos and Freire, 2012; Okonkwo *et al.,* 2014; Li *et al.,* 2016; Chang *et al.,* 2018). In the studies by Chang et al. (2018) wavelet analysis was applied to characterize the effects of monsoons and climate teleconnections on precipitation over China. It found that on the intra-annual, inter-annual and decadal timescales, the Indian Summer Monsoon (ISM) many affects precipitation in the Northeastern and Central China. Santos et al. (2001) used wavelet analysis on monthly rainfall in order to analyze rainfall variability. It's founding reveal that using global wavelet spectrum (GWS) that the monthly rainfall of Matsuyama city is composed mainly by an annual frequency. In the same founding the wavelet power spectrum showed a big power concentration between 8-16- month bands, revealing an annual periodicity. Santos *et al.* (2013) recommended that the global wavelet power spectrum should be used to describe rainfall variability in non-stationary hyetographs. For the regions that do not display long-term changes in hyetograph structures, global wavelet spectra are useful for summarizing a region's temporal variability and comparing it with rainfall in other regions. Over Nigeria, rainfall variability has also been studied using wavelet analysis. However, in this case both monthly and annual total rainfall were used describe the time frequency of rainfall. High variance were found at both monthly and annual variation of rainfall and the most outstanding frequencies of variation of monthly and annual rainfall were 8 -16 month band, showing that the these time series have strong annual signals(Adepitan and Falayi, 2019).

Over the Sahel wavelet transform and coherency analysis have been used by Okonkwo (2014) to determine the inter-annual and decadal to multi-decadal rainfall variability. Its founding revealed that, Sahel rainfall is associated to ENSO, Atlantic Multi-decadal

Oscillation (AMO) and Indian Ocean Dipole (IOD) at different time scales. An antiphase relationship existed between ENSO and the rainfall of Sahel at the 3-4 year band during 1982-1983 El Niño episodes indicating a cause effect relationship between the 1983 drought and the 1982-1983 El Niño. The wavelet coherence analysis also revealed a relatively anti-phase relationship between AMO and Sahel rainfall. However the control of the IOD on Sahel rainfall variability was limited to the east (Okonkwo, 2014). In addition, according to Xu et al. (2005) wavelet analysis can be used as an alternate approach to multi-time scale analysis of climate and short term climate variation forecast.

3.2.2 Wavelet Transform

Wavelet transform is a new instrument for signal analysis. It is considered as oscillation that decays fast with zero mean localized frequency and time. The concept was introduced in 1982 by Jean Morlet (Torrence and Compo, 1998). In this study an R package "WaveletComp" (Rösch and Schmidbauer, 2018), was used for the spectral analysis, wherein the Morlet wavelet transform of a time series is defined as the convolution of the series with a set of "wavelet daughters" as follows:

$$Wave(\tau, s) = \sum_{t} x_t \frac{1}{\sqrt{s}} \psi^{\star}\left(\frac{t-\tau}{s}\right) \qquad 3.1$$

Where x_t denotes the data point at time t of the time series to be decomposed and $\psi^{\star}$ denotes the complex conjugate, the scaling parameter s determines the daughter wavelet's coverage of the series in the frequency domain, and the localizing time parameter τ determines the daughter wavelet's location in the time domain. Ψ is the Morlet "mother" wavelet defined as:

$$\psi(t) = \pi^{-1/4} e^{i\omega t} e^{-t^2/2} \qquad 3.2$$

where the dimensionless frequency ω is set as 6 to ensure that the Morlet function has zero mean and is localized in both time and frequency space (Farge, 1992).

3.2.3 Wavelet power spectrum

The wavelet power spectrum describes the evolution of the variance of a time-series at different frequencies. Concerning the fact that the WPS gives more information in one picture, it is often practical to show the information as the averaged value of the result in the range of scale or time. The wavelet power spectrum can be defined as:

$$Power(\tau, s) = \frac{1}{s}|Wave(\tau, s)|^2 \qquad 3.3$$

3.2.4 Global wavelet power spectrum (GWS)

Torrence and Compo (1998) showed the average variations of the whole time series on every scale, called the global wavelet spectrum (GWS) (time-averaged wavelet spectrum). Eq. (3), can be used to calculate a time-averaged wavelet power at a given scale parameter s, by measuring the relative contribution of the variation at a given frequency to the total variation. The higher the time-averaged wavelet power, the more significant the frequency is in the entire spectrum window. The global wavelet spectrum is defined as:

$$\acute{W}^2(s) = \frac{1}{N}\sum_{n=0}^{N}|W_n(s)|^2 \qquad 3.4$$

The scales are a series of fractional power of 2 and are defined as:

$$s_j = s_0 2^{k\delta_j} k = 0,1,\ldots\ldots,J \qquad 3.5$$

Were s_0 is the least resolvable scale and J determines the highest scale (Torrence and Compo, 1998). However, the scale $\delta_j = 0.25$ is used, which will do 4 sub octaves per octave. But the smaller values of δ_j give a finer resolution (Torrence and Compo, 1998). A δ_j of 0.5 is the largest value required to provide adequate sampling in scale for the Morlet wavelet.

3.2.5 Cone of influence (COI)

Error occurs at both the beginning and the end of wave power spectrum when considering a time series of finite length (Torrence and Compo, 1998). The time series is therefore padded with sufficient zero before applying the wavelet transform in order to limit the edge effects and seed up the Fourier Transform. The padding reduced the amplitude at the edges, as more zeros were involved in the analysis. The region of the wavelet spectrum in which the edges effects become important is referred to as the cone of influence (COI). And it is defined as the e-folding time for the autocorrelation of wavelet power at each scale (Torrence and Compo, 1998). The e-folding time is chosen such that the wavelet power at the edge drops by a factor e^{-2} to ensure a negligible edge effect.

3.2.6 Wavelet Coherence

The wavelet coherence describes the degree of coherence of wavelet transform in time-frequency space. Following Torrence and Webster (1999), the wavelet coherence coefficient can be defined as follows (Grinsted *et al.*, 2004; Hao *et al.*, 2016):

$$Coherence = \frac{|sWave.xy|^2}{sPower.x * sPower.y} \qquad 3.6$$

Where s is a smoothing operator, which is given as:

$$S = S_{scale}(S_{time}(Wave(\tau, s))) \qquad 3.7$$

where S_{scale} and S_{time} represent smoothing along the wavelet scale axis and in time, respectively.

The statistical significant level of wavelet coherence was estimated through Monte Carlo method. The Monte Carlo estimation of the significance level requires more than 1000 surrogate dataset pairs with the same first order autoregressive coefficients as the input datasets. The significance level for each scale was estimated using only the values

outside the Cone of Influence, which is the region of the wavelet spectrum in which edge effects become important (Torrence and Compo, 1998). The number of scales per octave should be significantly high to capture the rectangle shape of the scale smoothing operator while minimizing computing time. An empirically satisfactory parameter, i.e., 12 scales per octave, was used with reference to Torrence and Compo (1998). In addition, in this study the coherence for which the confidence level was greater than 95% were analysed.

CHAPTER FOUR: RESULTS AND DISCUSSIONS

4.1 Influence of Tropical and African easterly jets on West African precipitation

This section discusses the results of the first and second objectives of the thesis. This study provides more comprehensive climatology of the AEJ and TEJ and investigates their dynamics and interactions leading to the observed rainfall variability of the region. It also establishes the climatology of two major wind structures over the study area during all the months from January to December and also during the wet and dry years. The characteristics were defined by the north/south movements and extent as well as their core wind speed at the assigned pressure level. The locations of the wind cores in terms of longitude, latitude, and pressure also were noted. These monthly averages cover the duration of the study period from 1979 to 2012.

4.1.1 Climatology of the jets and precipitation

We will first discuss the relationship of sub-tropical westerly jet with the West African monsoon structure and its associated tropospheric jets. The association and relative influence of the AEJ, TEJ and the West African Westerly Jet (WAWJ) on the regions rainfall (wet and dry) conditions are also examined.

4.1.1.1 The West African Monsoon Structure

The month-by-month vertical structure of the West African monsoon is given in Figure 4.1. The figure shows the monthly ITD position and the associated monsoon depth and strength. Of crucial importance are the deepening monsoon layers, the intensifying WAWJ and the AEJ, as well as the rapidly weakening but poleward retreating STJ. It can be seen that, as the AEJ advances northwards from about 700hPa around the equator in January, it also strengthens reaching maximum speed of greater than 12m/s and reaching the 580hPa level in August. The AEJ being present all year round is an annual

and not a summer system only. It also changes its height, as found by (Afiesimama, 2006). In this month and also in July, the WAWJ has attained a speed of greater than 5m/s with the monsoon now at almost 700 hPa, thus pushing the AEJ to higher pressure level. The STJ remained very strong and reaches down to 800 hPa until May when it suddenly retreats both poleward and in height to below 400 hPa. This leads to the intensification of the AEJ and the sudden appearance of the TEJ in June. It is interesting to note that the so-called "monsoon jump" which marks the onset of rainfall in the Sahel (Sultan and Janicot, 2003) also occurs in May. This is a strong coincidence. The reverse takes place in October. TEJ is therefore a June to September phenomenon only (Sylla et al., 2010; Nicholson, 2013; Besson and Lemaitre, 2014). This sudden TEJ appearance (disappearance) may be linked to the equally sudden weakening (strengthening) and disappearance (appearance) of the stratospheric Quasi-biennial Oscillation (QBO). The QBO begins its appearance in October, strengthens and attains maximum easterly speed of greater than 8m/s and extends to about 13N in April. It then weakens quickly thereafter giving way to TEJ appearance in June. Hagos and Cook (2007) explained the monsoon jump in May/June using a regional climate model by considering moisture, momentum and energy budget analyses. Their results showed an agreement with those in Sultan and Janicot (2003) that the monsoon jump involves the release of potential instability due to moisture supply by southerly surface winds and also that surface heating drives the pre-onset southerly wind. A new question from the results of the present study may be raised: is there any link between the QBO disappearance, the sudden STJ withdrawal and the monsoon jump? This requires future study. The possible QBO influence on West African precipitation is the focus of the last objective of this study.

Another interesting aspect of the monsoon structure is under section 4.2 the shape of the monsoon depth between January and June compared with its shape from July to

October. While WAWJ is not far from the ITD and is north of the AEJ core in the former months, it shifts to the south of the jet core between July and October. The reason for this is however beyond the scope of the present study.

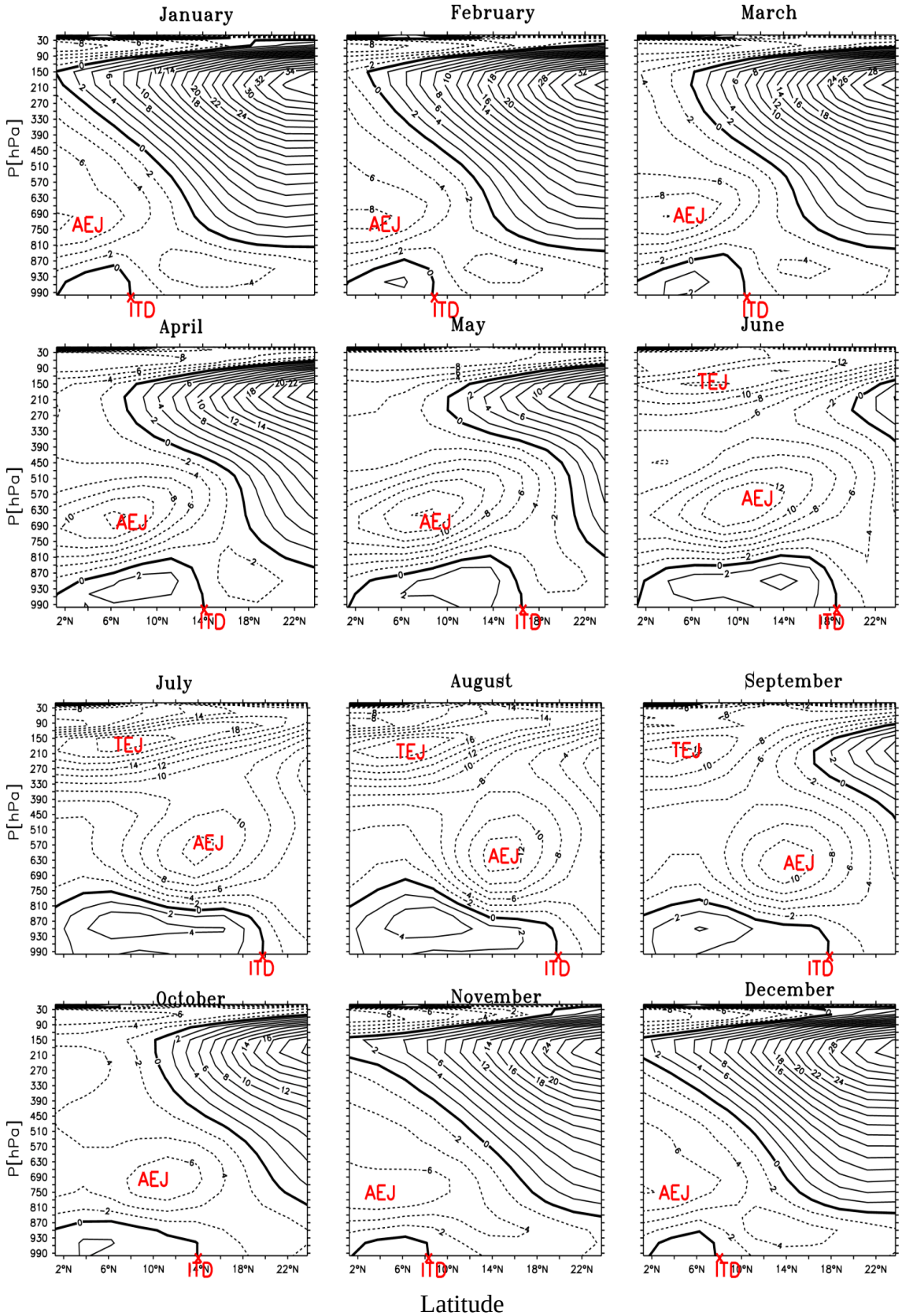

Figure 4.1: Cross section of mean monthly monsoon structure averaged between 10W and 10E showing the position of the ITD, the West African Westerly Jet (WAWJ), African easterly jet (AEJ), Tropical easterly jet (TEJ), the monsoon layer and Quasi-biennial Oscillation (QBO).

4.1.1.2 The Relative influence of the Tropospheric Jets (AEJ & TEJ) on West African Rainfall

Figure 4.2 shows the monthly mean wind distribution at the AEJ level. The precipitation pattern over West Africa is given in colour. It can be seen that the AEJ advances northward from the equator from January, its core arriving over West Africa by March/April. The jet core reaches about 15^{o}N in July/August, retreating rather fast southward between September and October. In a similar manner, the rainfall pattern also follows behind and parallel to the AEJ core in every month, with the about 5mm/day isoline always coinciding with the jet core from March to September. Maximum rainfall is observed in July and September, especially over southern Nigeria, Sierra Leone, Liberia and Guinea region. The northward movements of the AEJ core and rainfall distribution indicate a close link between them. This will be further shown shortly.

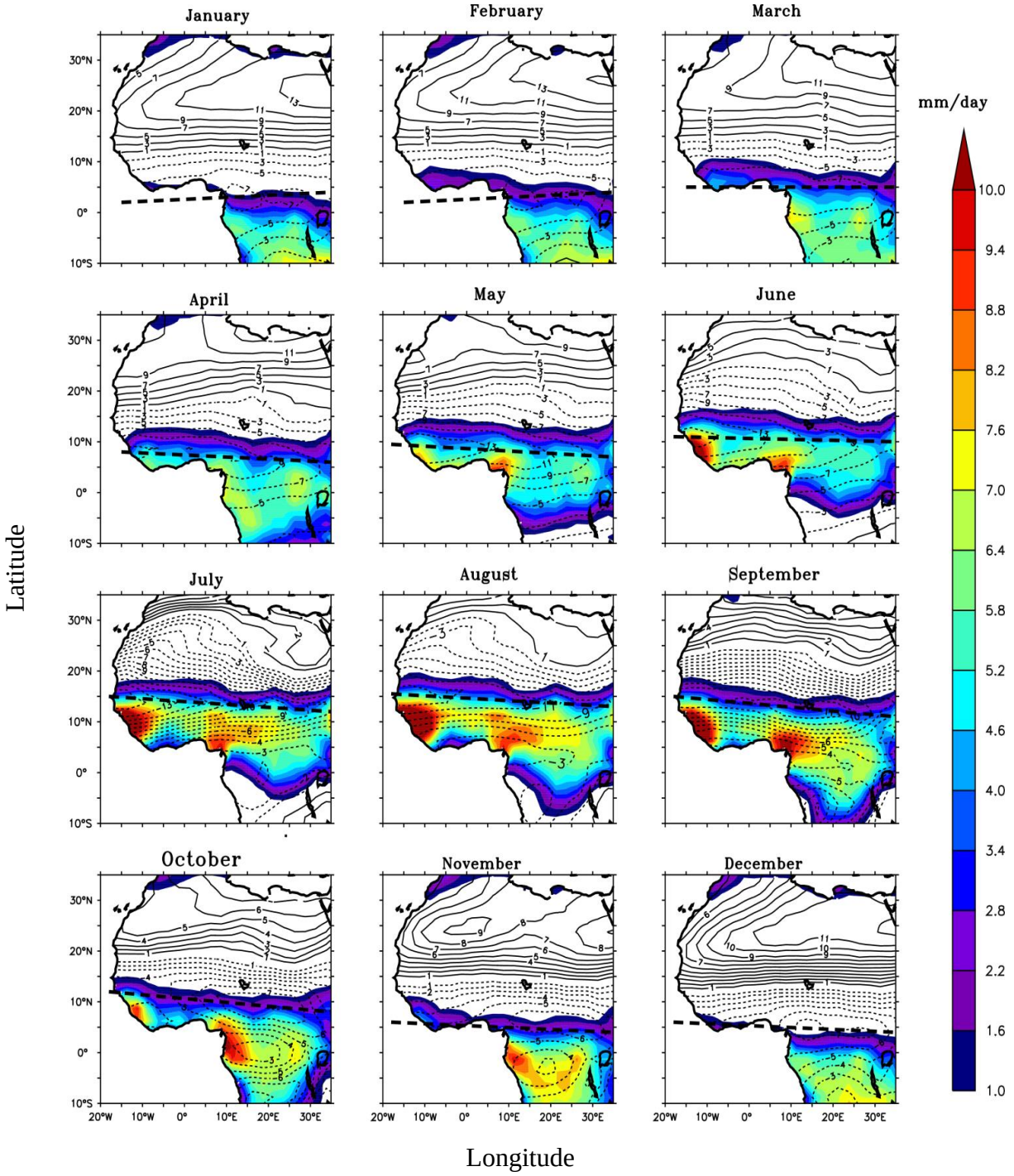

Figure 4.2: Monthly 600 hPa mean wind (isotachs) and precipitation (colour). The jet core is denoted by thick dashed lines.

The pattern of the upper tropospheric jet (TEJ) in relation to that of rainfall is given in Figure4.3. Starting from south of the equator, a slow northward advance can be seen, the jet reaching a maximum position of about 7-9^{o}N in August. It is noteworthy that the TEJ core does not arrive over West Africa until June, coinciding with a rapid poleward retreat (the zero isotach) of the sub-tropical westerly jet (STJ) between May and June. This was linked to the weakening of the stratospheric quasi-biennial oscillation (QBO) in section 4.1.1.1. The equatorward retreat is similarly rapid between August and September. However, it is clearly seen that the northward advance of the rainfall distribution shows no relationship with the TEJ movement as was found with the AEJ. TEJ core always lags the rainfall maximum. The TEJ therefore has little influence on rainfall development over West Africa, as will be further shown next.

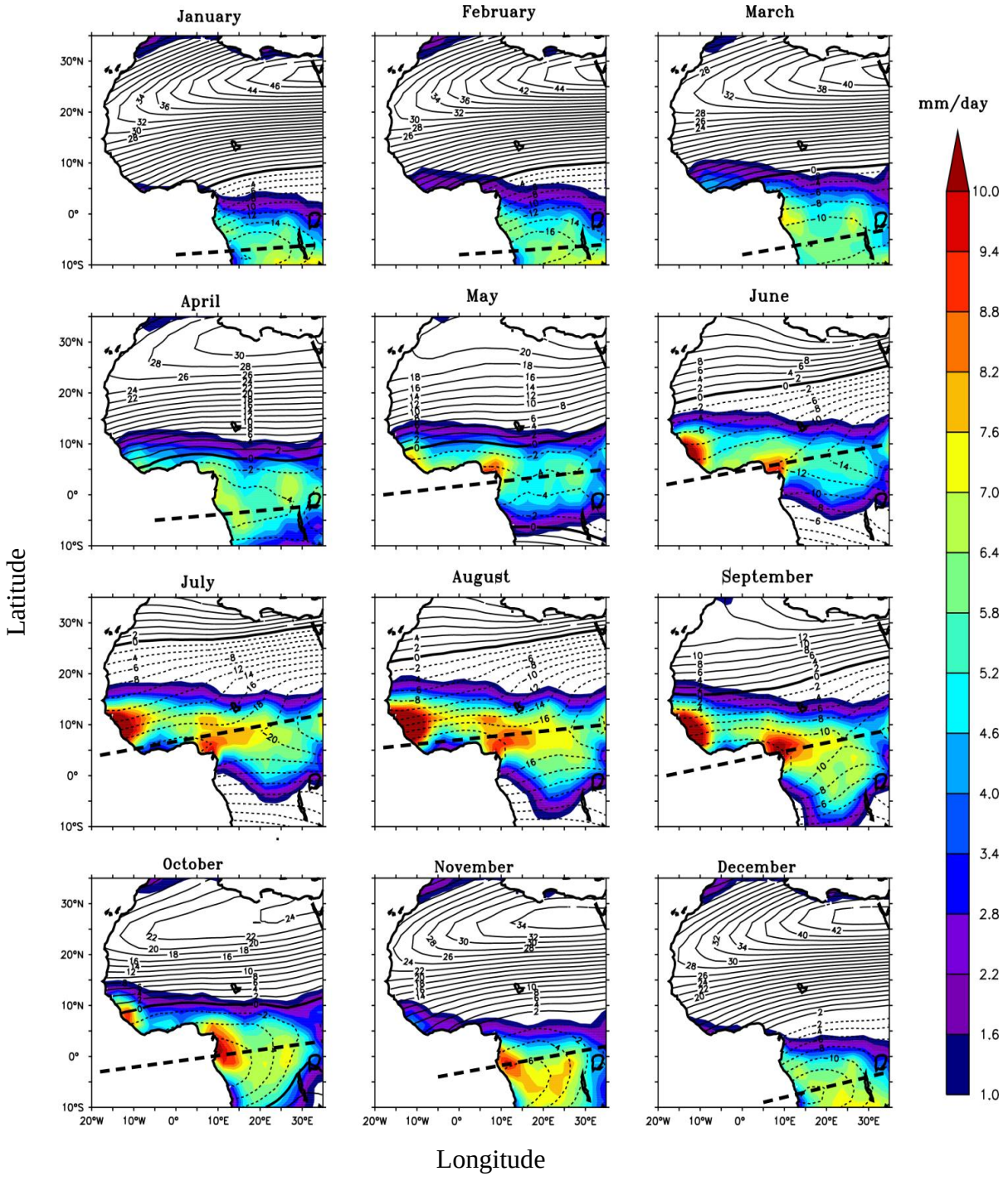

Figure 4.3: Monthly 200 hPa mean wind (isotachs) and precipitation (colour). The jet core is denoted by thick dashed lines.

The above results are investigated in another way. A latitude-time (monthly) cross-section of the jets with the rainfall pattern is obtained. These are depicted in Figures 4.4a and b, for the AEJ and TEJ, respectively. In order to investigate the influence of each jet on the east-west rainfall variability across West Africa, five longitudinal cross-sections were considered: 10W, 5W, 0, 5E and 10E. The cores of the jets are again indicated. First, while one long rainy season is observed at 10W with a high July/August peak and an almost similar pattern at 10E with a September/October peak, there are two rainy seasons between longitudes 5W and 5E, with less rainfall maxima. The pattern of rainfall is as found by previous authors (Sultan and Janicot, 2003), with rainfall generally starting in late February/March and advancing to reach about latitude 16-17N in August before retreating southward. The monsoon jump is seen only between about 5E to 5W, occurring late May/June. Of particular interest here is the orientation of the core of the two jets. While the TEJ core is oriented north-south at all longitudes (Figure 4.4a), showing no particular relationship with the rainfall pattern, it is clearly seen that the AEJ core is always leading the rainfall maximum. As observed previously, the AEJ core is almost aligning with the 5-6 mm/day isoline. This is essentially so even for the second (secondary) rainy season (September-November). However, it is noted that increased (maximum) rainfall occurs after the TEJ has attained maximum strength. This suggests there may some interaction between the AEJ and TEJ resulting in increased rainfall.

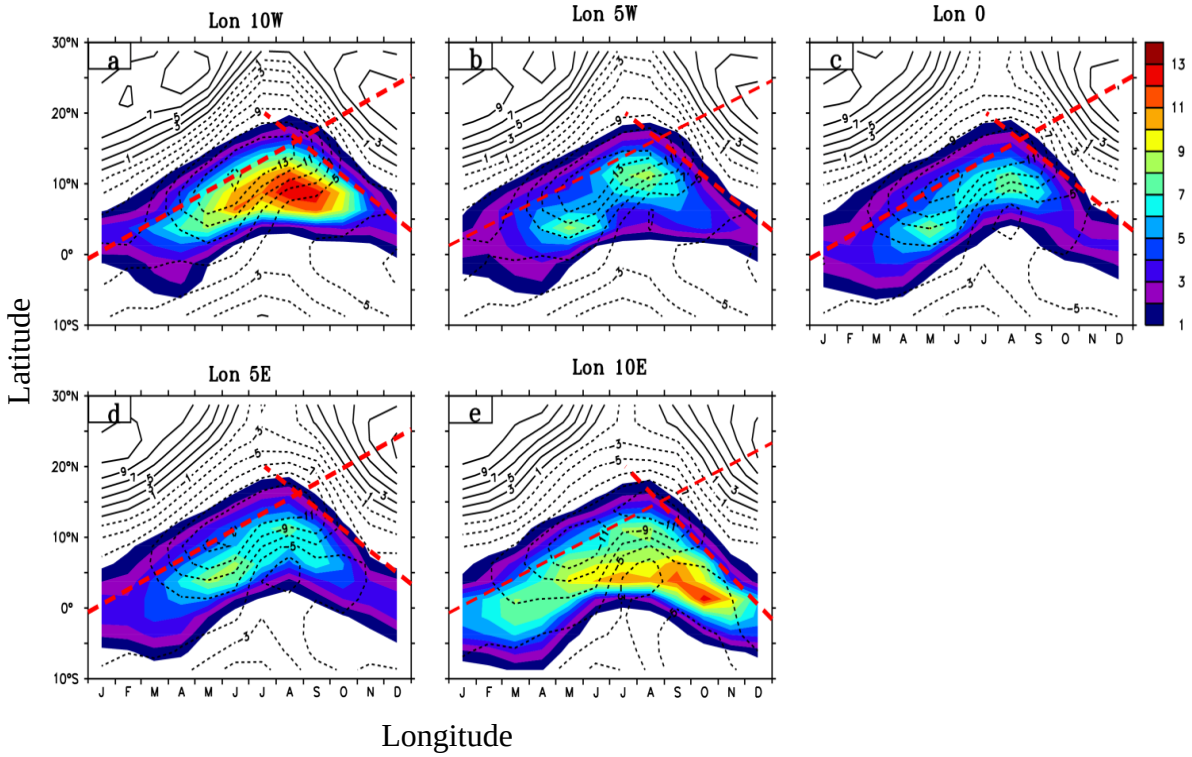

Figure 4.4a: Time-latitude cross section of zonal wind at 600hPa (contours) and rainfall pattern (color). Jet core indicated by thick dash red line.

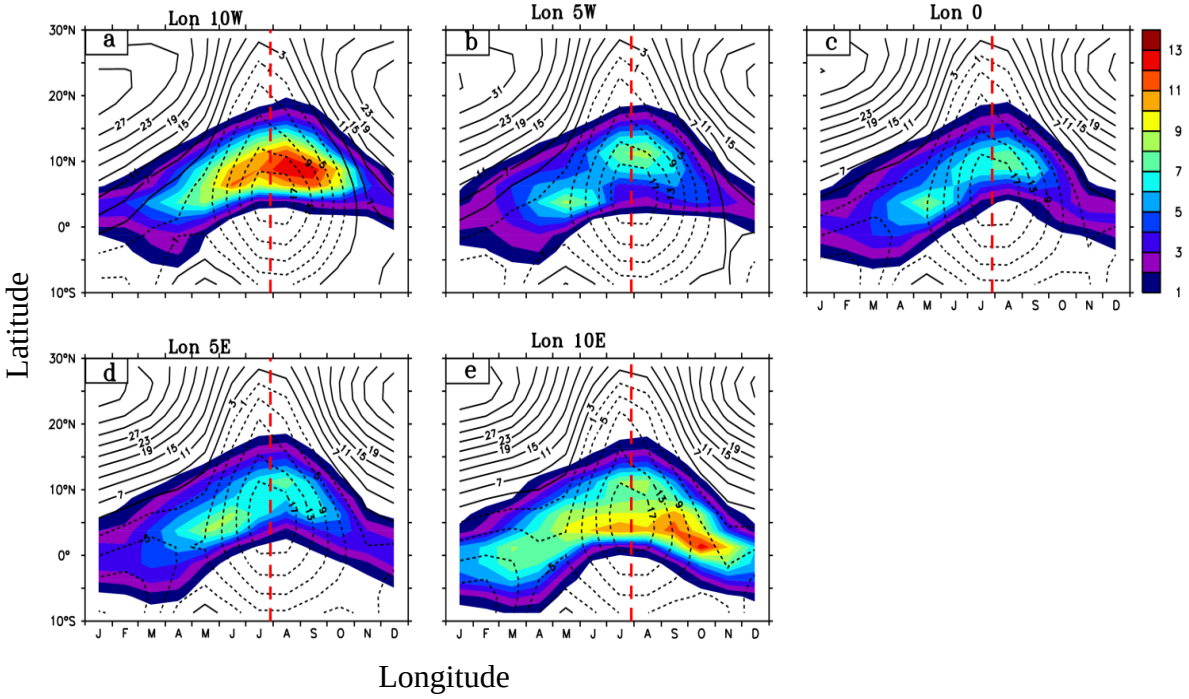

Figure 4.4b: As for Figure 4.4a but for TEJ

4.1.1.3 Effects of WAWJ, AEJ and TEJ on Rainfall Variability

Several methods have been employed to study the variability of precipitation over West Africa. A common method is the characterization of rainfall over the region into wet and dry periods (Nicholson and Grist, 2001; Omotosho, 2007; Omotosho and Abiodun, 2007). The method is adapted in this study.

Figure 4.5 gives the standardized rainfall index. It shows the well-known drought years of 1982-1987 and the so-called recovery period of 1994-2000 (Sanogo *et al.,* 2015). The wet and dry years were as defined in Omotosho (2008) and are given in Table 4.1

$$\text{Dry years} - RR < RRm - 25\%$$

$$\text{Wet years} - RR > RRm + 25\%$$

where RR_m is the rainfall average over West Africa between 10^oW-10^oE, these are indicated by dash lines on Figure 4.5. In order to allow the relationship of the monsoon component and the associated vertical motion field with the rainfall to be properly examined, the stratospheric flow (QBO) has been removed in Figures 4.6-4.8. The rainfall is shown in the bottom panel. It is must be stated that all features noted in Figure 4.1 in section 4.1.1.1 are also clearly evident here.

First, it can be seen that there is little or no difference in the latitudinal positions of the Inter-tropical discontinuity (ITD) during both wet and dry years, as previously noted by Nicholson and Grist (2001), Rufus et al. (2013), Almazroui *et al.* (2017). Secondly, the shape of the monsoon depth at the beginning of the rainy season, with the deepest layer closer to the ITD and associated rainfall peak far southward over zone of shallow moisture depth changed in the later part of the raining season. It reversed position of deepest moist layer and associated rainfall now to south of the AEJ core but still over region of shallow monsoon depth this very interesting situation was noted in the previous section. Here again, it may be asked: is the shape change related to the monsoon jump in May/June?

Zipser (1969), Robert (1977), Tompkins *et al.* (2005), and Dione et al. (2019) have shown that a very moist boundary layer overlain by a relatively dry mid-layer (800-600 hPa) is an important condition for intense convective systems which deliver most of West African rainfall. The speed of the monsoon flow, here termed West African Westerly jet (WAWJ), reaches a maximum of about 6m/s in August during the wet years but is weaker during dry years from May to September. On the other hand, the African easterly jet is slightly stronger during dry period but remains almost at same height in wet years between June and August. During dry years, the core of AEJ is always a little further south than in the wet cases. The opposite is the case for the TEJ, which remains consistently much stronger during wet than dry periods from its appearance in June till September. The jets both remain at same level in both wet and dry years.

The present results show two other findings. One is that while the STJ reaches to higher pressure levels (870 – 850hPa) in April and May than in dry years, its withdrawal is also faster than in the dry case, although the retreat is still sudden in both situations. Secondly, it can be clearly seen in Figure 4.6 that, from its appearance in June till September, the distance between the two jet cores gets wider. It is noted that while the AEJ advances northward, the TEJ has negligible corresponding shift. The effect of this on precipitation is at present unclear.

The associated vertical motion shows stronger ascent during wet years through all months. The upward motion occurs both north and south of the AEJ core but strongest to the south, while it is always north of the TEJ core in both cases. It has been well noted that a weaker AEJ with a stronger TEJ enhances Sahelian rainfall (Nicholson, 2013; Steinig *et al.*, 2018; Pante and Knippertz, 2019). While the present study applies to entire West Africa, the results of this work are still consistent with those findings. However, from the results of this study it can be stressed that mesoscale convective systems (squall lines and thunderstorms) which are responsible for at least 80 percent of

West African rainfall, are not dependent on the TEJ for their development and maintenance. This can be seen from the results in section 4.1.1.1, particularly 4.1.1.2 and bottom panel Figure 4.6, all showing that significant rainfall is observed in April and May and also March and October months (see Appendix 1) when the TEJ is completely absent over the region. Lemburg et al. (2017) found substantial correlations between Sahelian rainfall and TEJ strength on decadal time scales but weaker and less correlations on shorter time scales. They also showed that the initiation, intensity and size of West African mesoscale convective systems are not associated with TEJ-related upper level divergence or its anomalies. From all the results presented in this section, it may be concluded that the AEJ is far more important for West African rainfall, even though increased rainfall is observed during TEJ presence in June to September. It is also seen that precipitation is higher in all months during wet than dry years with maximum rainfall in the zone of strongest upward motion and again to the north of deepest moist layer, as previous noted.

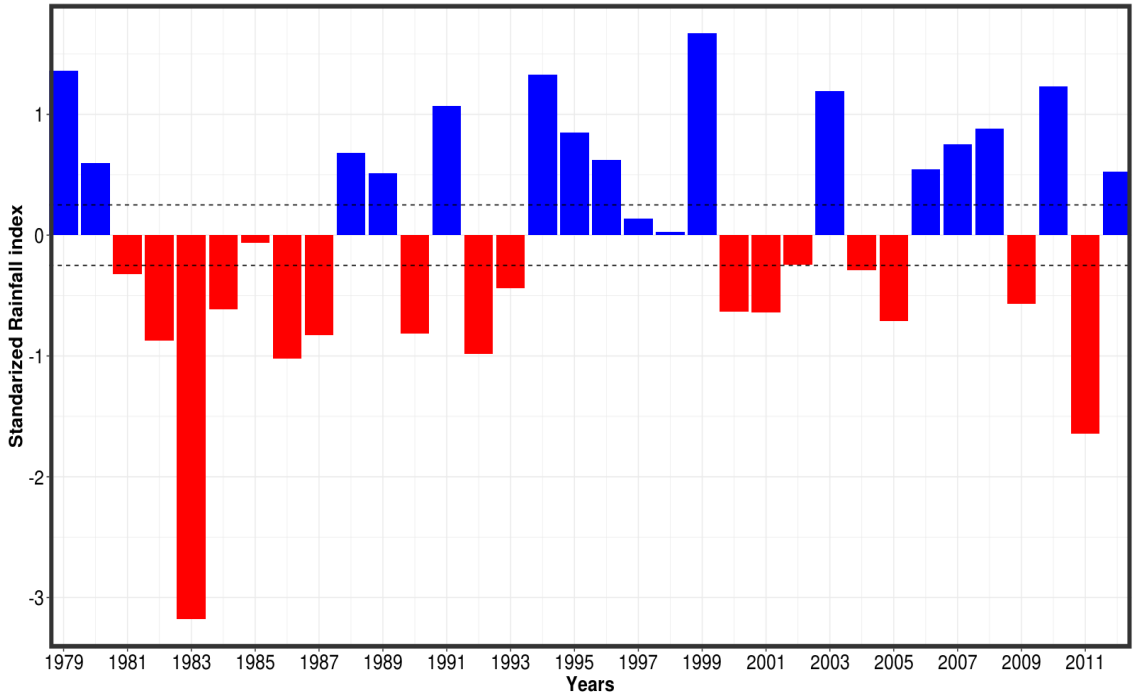

Figure 4.5: Extraction of wet and dry years of rainfall average at longitude 10W-10E and latitude 4N-16N

Table 4.1: Dry and wet years of rainfall

Wet Years	1979,1980,1988,1989,1991,1995,1996,1997,2000,2004,2006,2007, 2008,2010,2012
Dry Years	1981,1982,1983,1984,1986,1987,1990,1992,1993,2000,2001,2002, 2004,2005,2009,2011

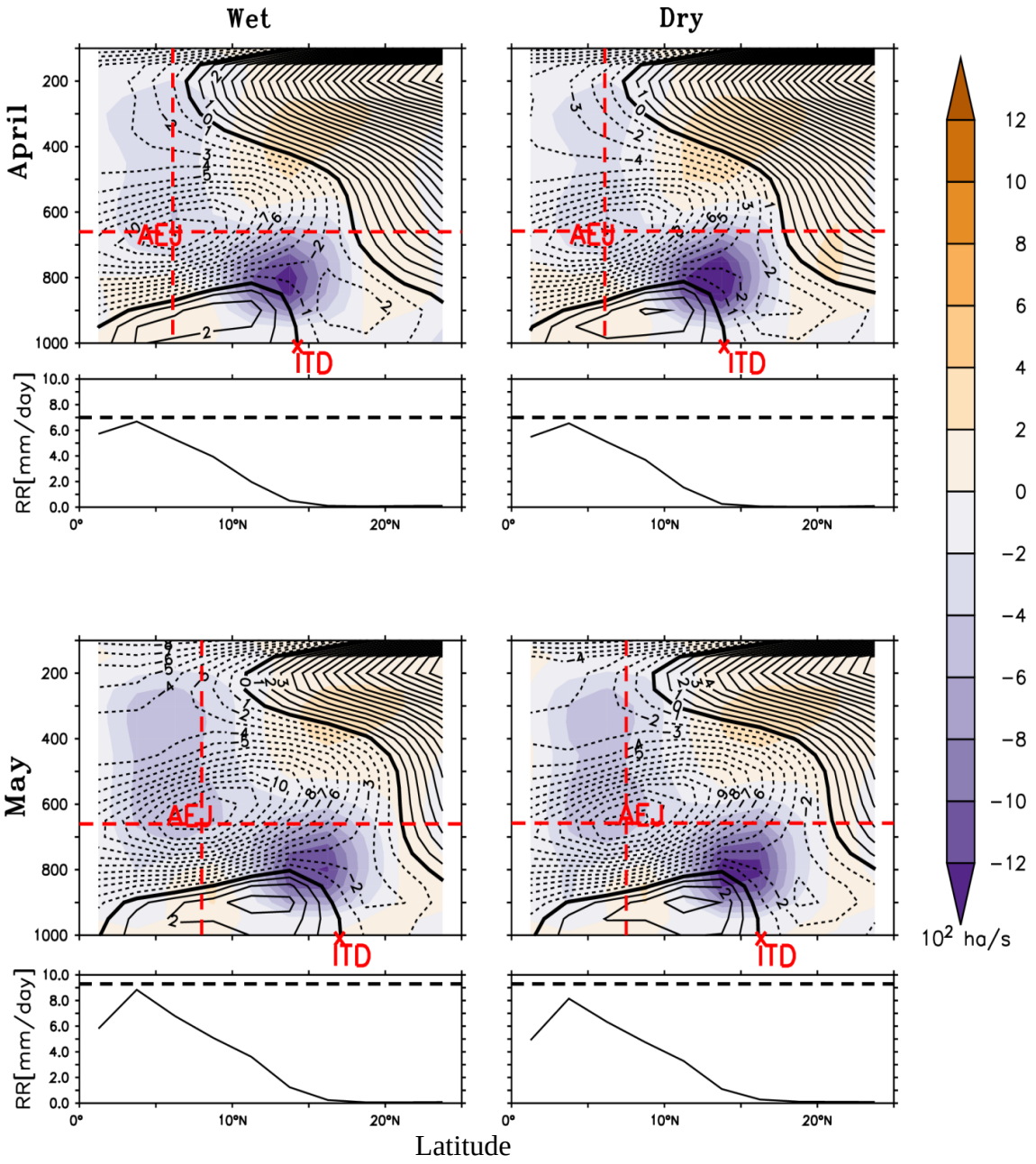

Figure 4.6: Cross section of composite evolution of wet and dry years cross section averaged at longitude 10W-10E. Wind speeds in isotachs. Latitudinal and vertical positions of jet cores in tick dash lines, the shaded is the vertical velocity (omega).

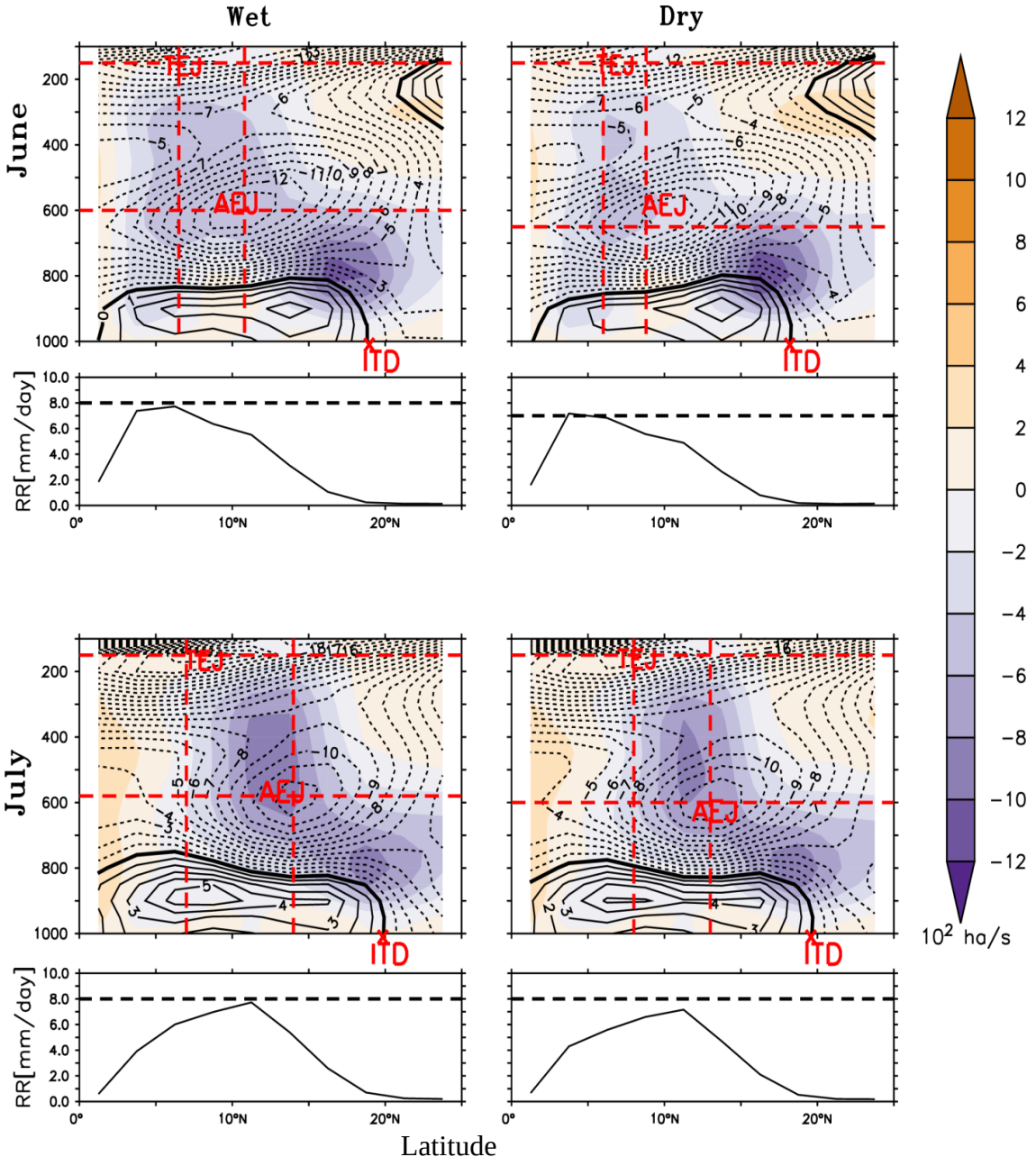

Figure 4.7: same as Figure 4.6 but for June and July

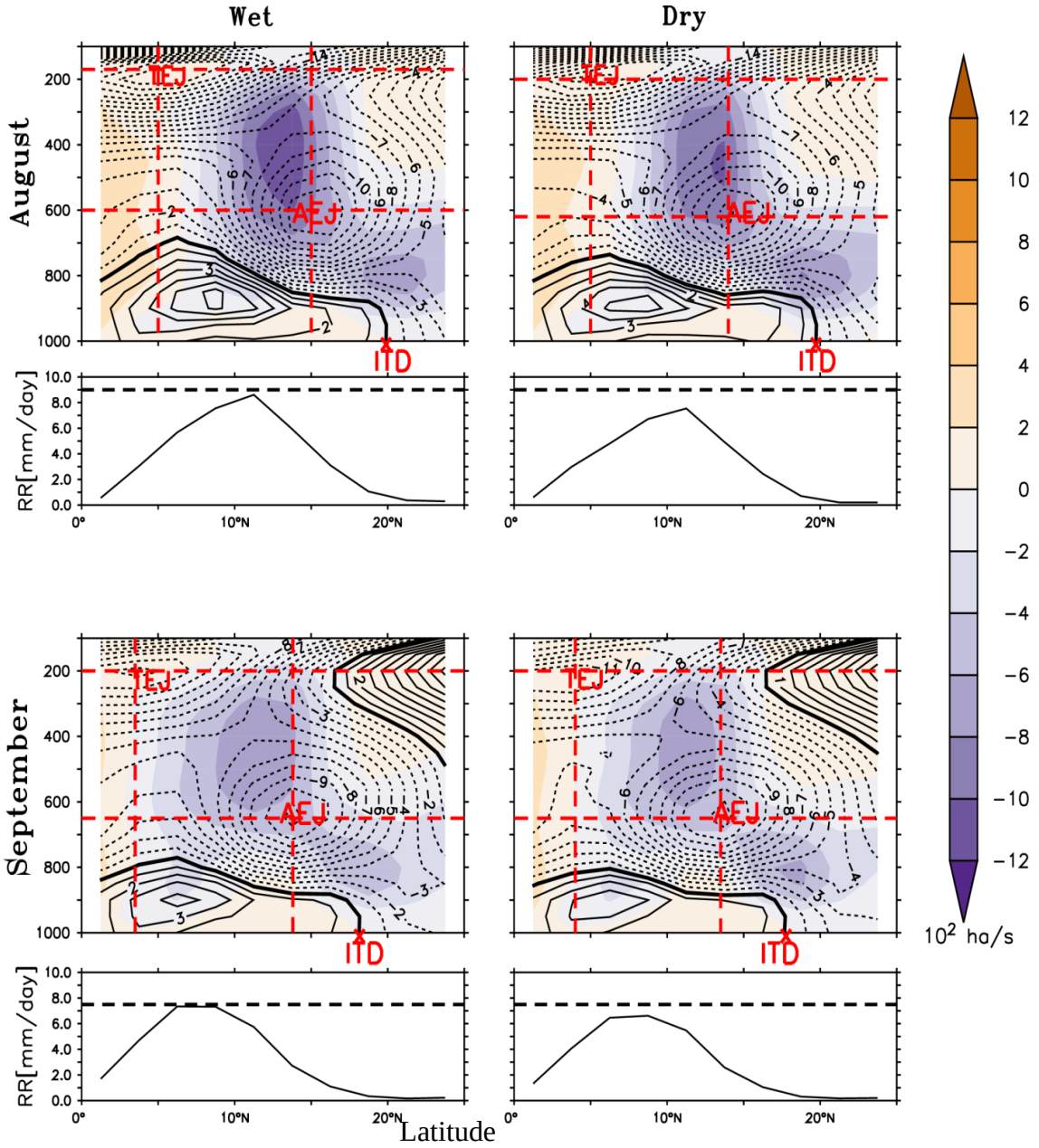

Figure 4.8: same as Figure 4.6 but for August and September

4.2 Investigation of the influence of Quasi-biennial Oscillation on West African Rainfall

This section examines the third and fourth objectives of the thesis. The purpose of this section is firstly to investigate the influence of the stratospheric QBO (zonal component) on precipitation over West Africa and also on the African easterly jet and Tropical easterly jet. Secondly, to evaluate the skills of Model CMIP5 in reproducing the equatorial mean zonal wind time-height, the influence of QBO, TEJ, and AEJ on rainfall over West Africa and their potential for its prediction. Then the composite of model during the west (east) phase and QBO (Non-QBO year) is addressed and compared to observation. The analysis focused on the HadGEM2-CC from the CMIP5 model for the period of 1979-2005.

4.2.1 Wavelet analysis

Figure 4.9, exhibits a higher power of global wavelet spectrum over the West African zones. For each zone, the global wavelet spectrum (GWS) shows peaks in 1-year band. However less than 1-year band also show some significant variability, but since these periods represent seasonal variability, they will not receive further attention in this study. For the Sahel (Figure 4.9a) the GWS shows peaks in 1-year band, but the wavelet power spectrum (WPS) indicates that this band has a high intermittent power in 1979-2005. However, in 2-4 year band and 4-8 year band the WPS shows significant power (Figure 4.9a), but the GWS indicates that this band has no peaks in that period of year. For example, the 2-4 year band shows significant power in 1986-1994 and 2000-2005. According to Torrence and Webster (1999), the climate variability in 2-4 year band is usually attributed to QBO, consistent with the result of this study (see Figure 4.14 showing West African rainfall with significant coherence to QBO). The 4-8 year band also shows significant power in 1984-2005. Climate variability in 8-year band is usually attributed to ENSO event (Santoso *et al.*, 2017; Abdul Malik *et al.*, 2019). The GWS and

WPS of Savannah (Figure 4.9b) show rather similar structures to that of the Sahel, but with notable difference, especially in the 2-4 year and 4-8 year period. The Savannah WPS 4-8 year band show significant power for shorter periods while the GWS over Guinea is the same for the Sahel and Savannah, the WPS differ from those of Sahel and Savannah, especially in the 2-4 year period. However, the results of the wavelet analysis confirm that rainfall variability over West Africa have different temporal characteristics. It is therefore necessary to understand the dynamics and teleconnection that control rainfall over the region.

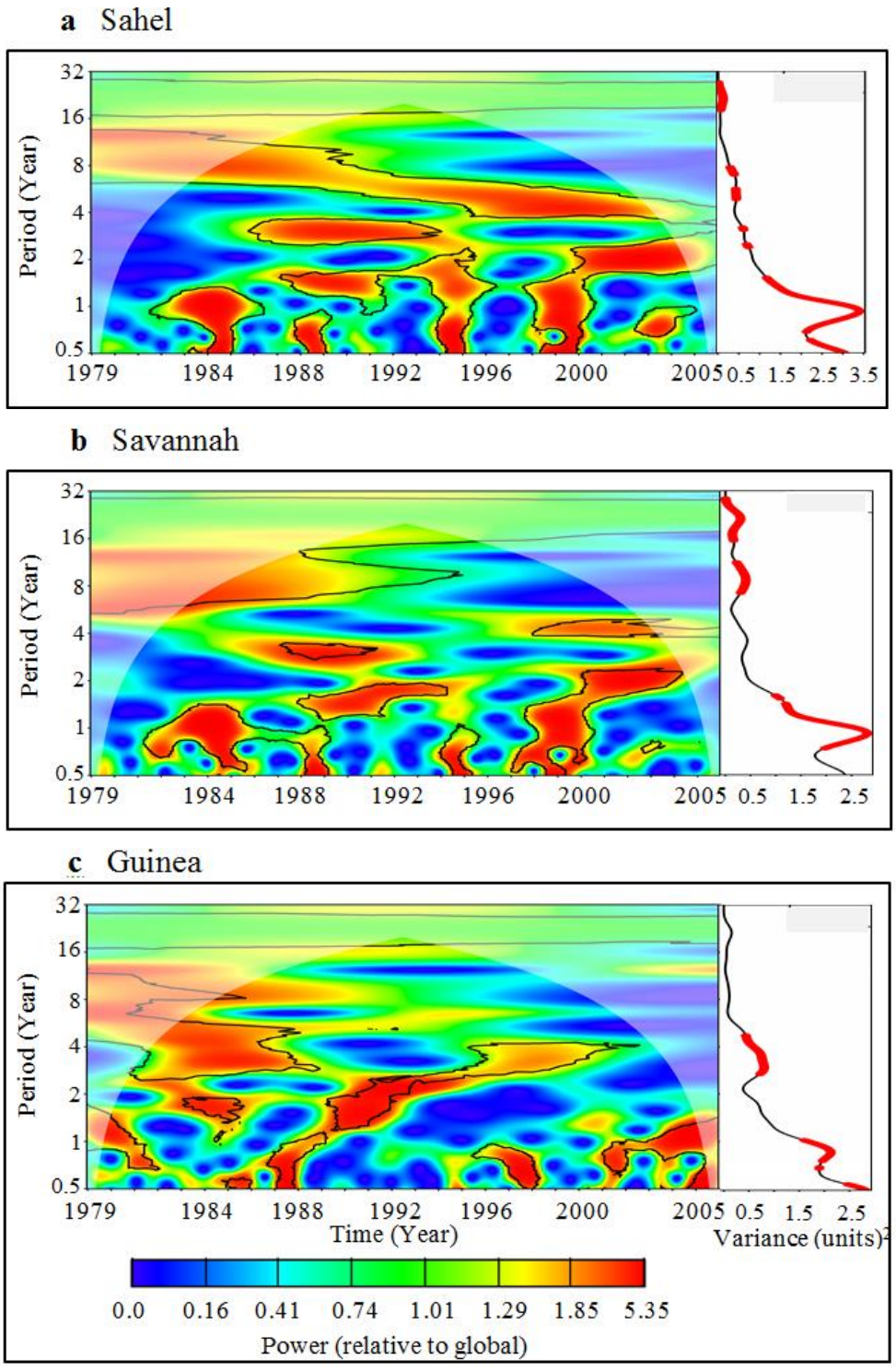

Figure 4.9: The wavelet power spectrum (left panels) and the corresponding global wavelet spectrum (right panels) of rainfall over West Africa zone a Sahel, b Savannah and c Guinea. The wavelet power has been scaled by the global wavelet spectrum. Black contour is the 10% significant level using the global wavelet as the background spectrum. The red color on global wavelet is 95 % significant.

Figure 4.10, shows several energy bands from the annual to interannual periods. For instance in Figure 4.10a, the GWS features a peak of 1-year band and lower variance at 6 and 16 year band, but the WPS shows three periods of significant variance. The first is the 1-year period with intermittent power; the second is the 2-4 years with significant power in 1992-2000 and the 6-16 year period with high power from 1988-2005. The GWS and WPS of TEJ (Figure 4.10b) differ from those of AEJ. The most pronounced variability within the WPS for the TEJ was observed during the periodicity band of 2-3 years and 4-8 years, with an oscillation from 1979-2005.

The wavelet analysis of QBO (Figure 4.11) shows several energy bands from the annual (2-3 years) and interannual scales (4-6 years). In both 30 and 50 hPa a frequency of 2 years is more identified. These 2 years is characterized by the continuities of significant power during 1979-2005 (Figure 4.11a, b). However, the discontinuities are also observed at 4-6 year band during 1981-1988 and 1996-2005 (Figure 4.11a). In figure 4b, this discontinuity is observed only in 1996-2005. Consistent with the observed period (Baldwin *et al.,* 2001; Paluš and Novotná, 2006)

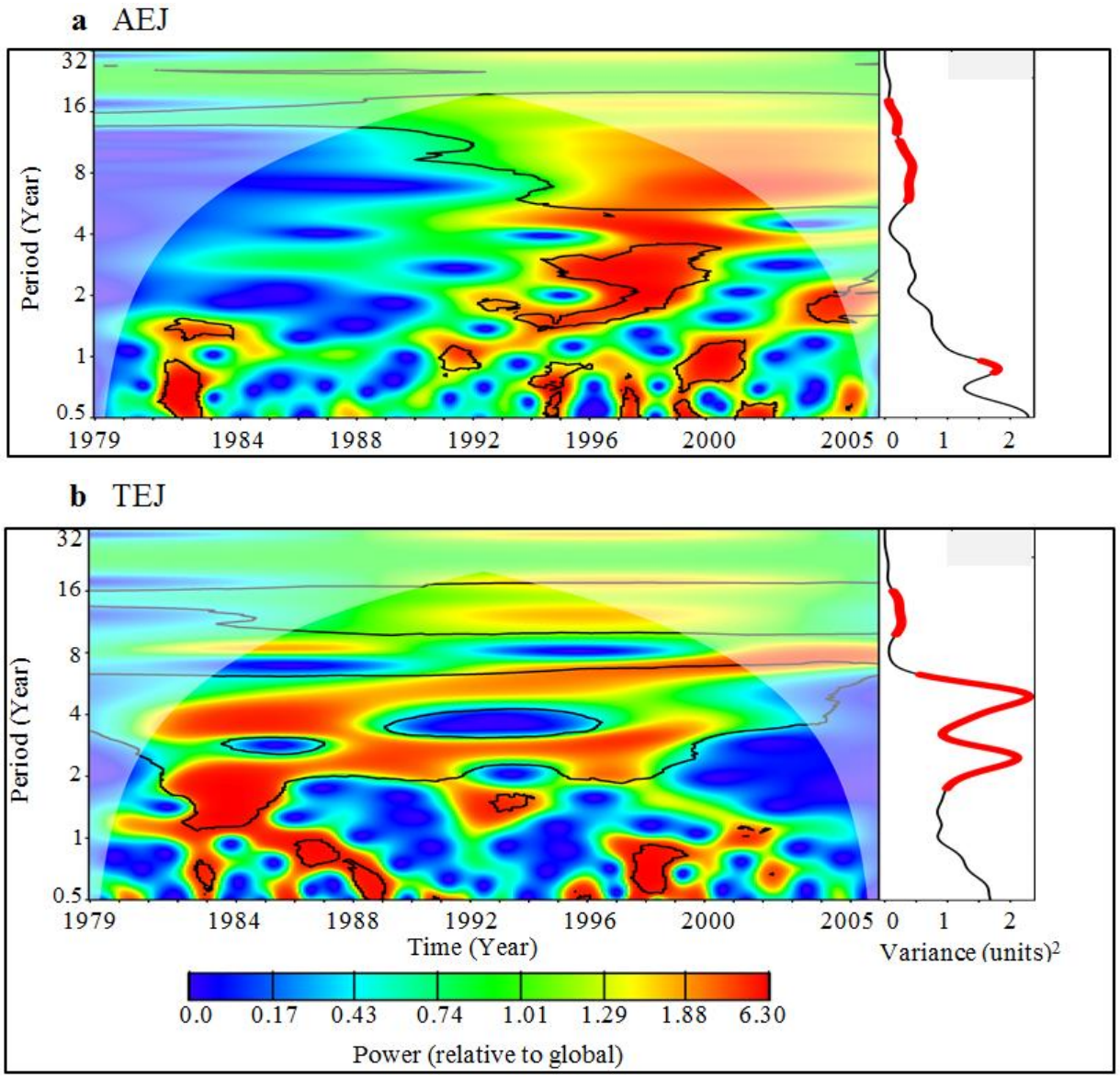

Figure 4.10: The wavelet power spectrum (left panels) and the corresponding global wavelet spectrum (right panels) of (a) AEJ and (b) TEJ. The wavelet power has been scaled by the global wavelet spectrum. Black contour is the 10% significant level using the global wavelet as the background spectrum.

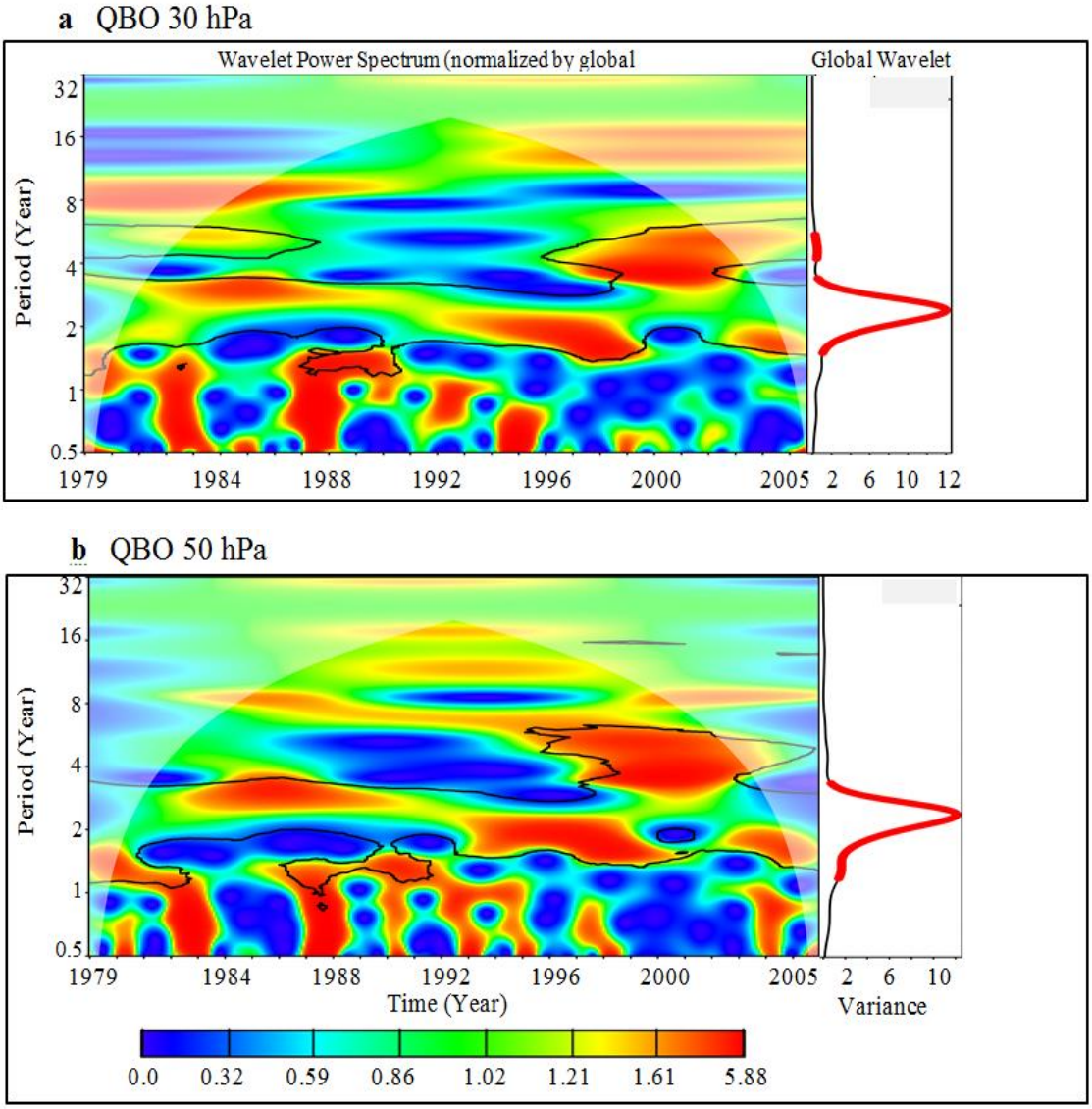

Figure 4.11: Same as Figure 4.10, but for a) QBO at 30 hPa and b) QBO at 50 hPa.

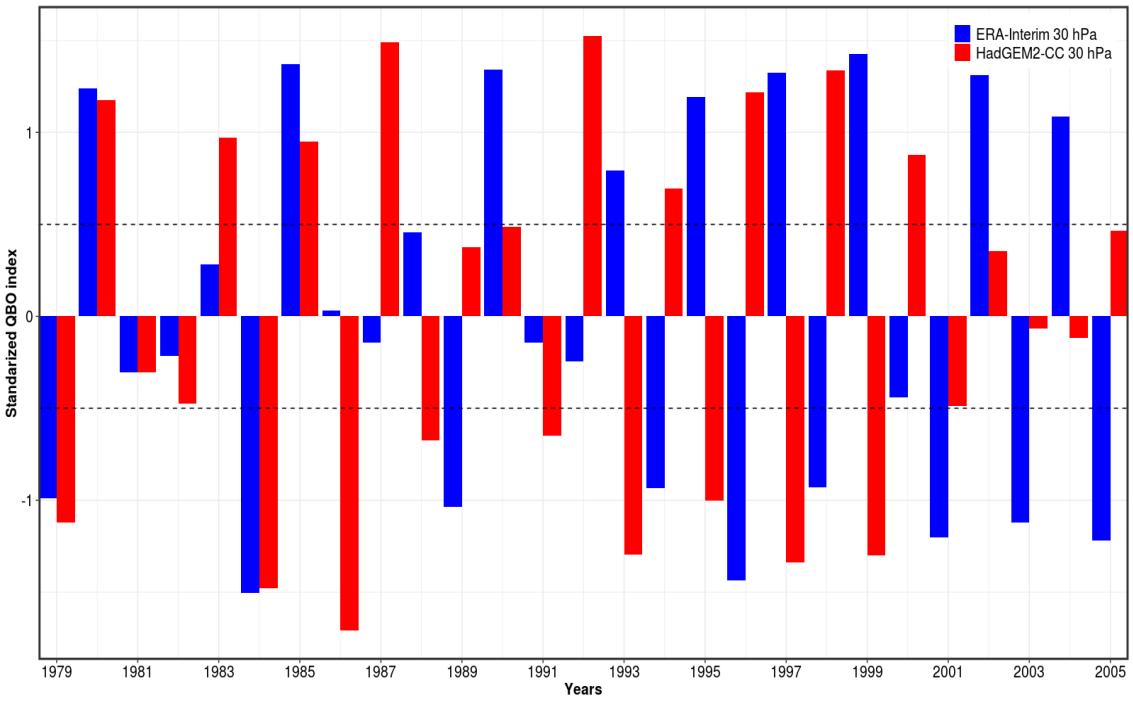

Figure 4.12: Extraction of east and west phase of QBO at 30 hPa using Era-Interim and model HadGEM2-CC

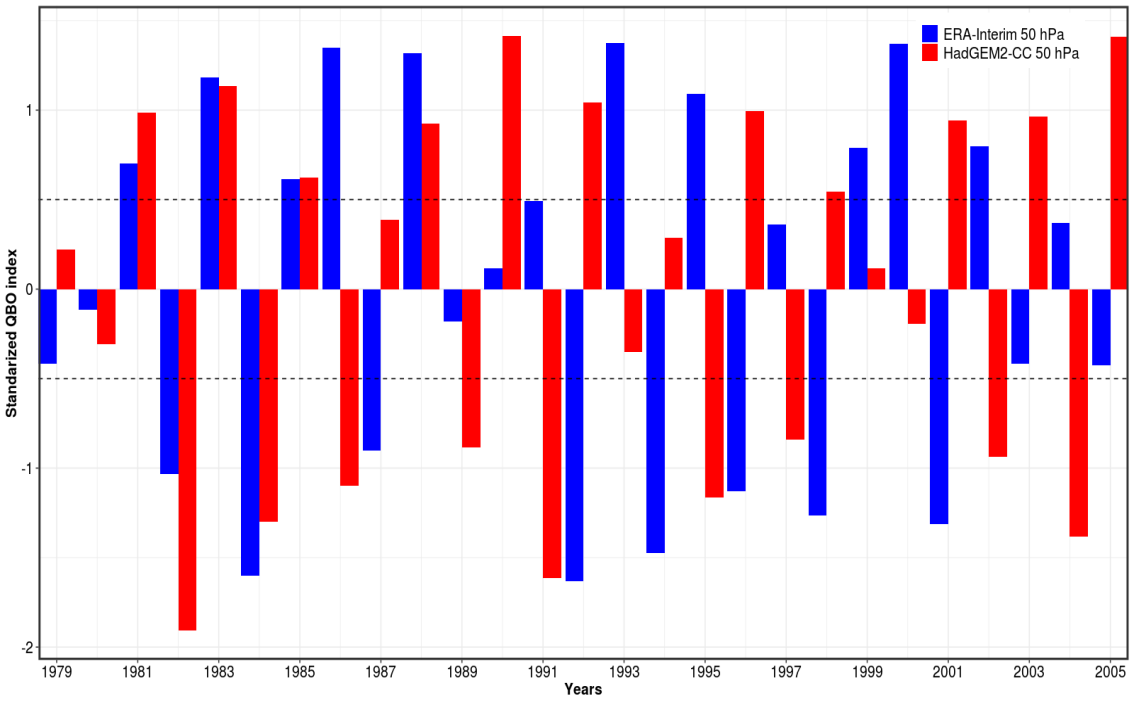

Figure 4.13: Extraction of east and west phase of QBO at 50 hPa using ERAI and model HadGem2-cc

Table 4.2a: Phases of QBO at 30 hPa in ERAINT

West Phase	1980, 1985, 1990, 1993, 1995, 1997, 1999, 2002, 2004
East Phase	1979, 1984, 1989, 1994, 1996, 1998, 2001, 2003, 2005
Non-QBO	1981, 1982, 1983, 1986, 1987, 1988, 1991, 1992, 2000
QBO-Year	1979, 1980, 1984, 1985, 1989, 1990, 1993, 1994, 1995, 1996, 1997, 1998, 1999, 2001, 2002, 2003, 2004, 2005

Table 4.2b: Phases of QBO at 50 hPa in ERAINT

West Phase	1981, 1983, 1985, 1986, 1988, 1991, 1993, 1995, 1999, 2000, 2002
East Phase	1982, 1984, 1987, 1992, 1994, 1996, 1998, 2001
Non-QBO	1979, 1980, 1989, 1990, 1991, 1997, 2003, 2004, 2005
QBO-Year	1981, 1982, 1983, 1984, 1985, 1986, 1987, 1988, 1992, 1993, 1994, 1995, 1996, 1998, 1999, 2000, 2001, 2002

Table 4.2c: Phases of QBO at 30 hPa in HadGEM2-CC

West Phase	1980, 1983, 1985, 1987, 1992, 1994, 1996, 1998, 2000
East Phase	1979, 1984, 1986, 1988, 1991, 1993, 1995, 1997, 1999, 2001
Non-QBO	1981, 1982, 1989, 1990, 2002, 2003, 2004, 2005
QBO-Year	1979, 1980, 1983, 1984, 1985, 1986, 1987, 1988, 1991, 1992, 1993, 1994, 1995, 1996, 1997, 1998, 1999, 2000, 2001

Table 4.2d: Phases of QBO at 50 hPa in HadGEM2-CC

West Phase	1981, 1983, 1985, 1988, 1990, 1992, 1996, 1998, 2001, 2003, 2005
East Phase	1982, 1984, 1986, 1989, 1991, 1995, 1997, 2002, 2004
Non-QBO	1979, 1980, 1987, 1993, 1994, 1999, 2000
QBO-Year	1981, 1982, 1983, 1984, 1985, 1986, 1988, 1989, 1990, 1991, 1992, 1995, 1996, 1997, 1998, 2001, 2002, 2003, 2004, 2005

4.2.2 Capability of GCM models to reproduce QBO

The models reproduce the general structure of the QBO, but with some biases (Figure 4.14). The biases, however, vary widely among the models. Of all the models HadGEM2-CC has the least but negative bias (Table 4.2), indicating that the HadGEM2-CC is more representative than CMCC-CMS, MPI-ESM-MR, MIROC-ESM-MR and HadGEM3-A. The behaviour of the QBO in HadGEM2-CC, HadGEM3-A and MPI-ESM-MR simulations have very good agreement with the reanalysis over the period of 1979-2005, showing the quasi-regular oscillation of easterly and westerly phase, with mean period of 22 months, which is consistent with the observed. The average period is 28 months, which varies between 22-34 months for individual cycles (Baldwind et al., 2001). The HadGEM2-CC reproduced QBO easterly and westerly phase show best agreement with the reanalyses and has the least bias. According to Schmidt *et al.* (2013) this is likely due to a better representation of the stratospheric physics and dynamics in the model.

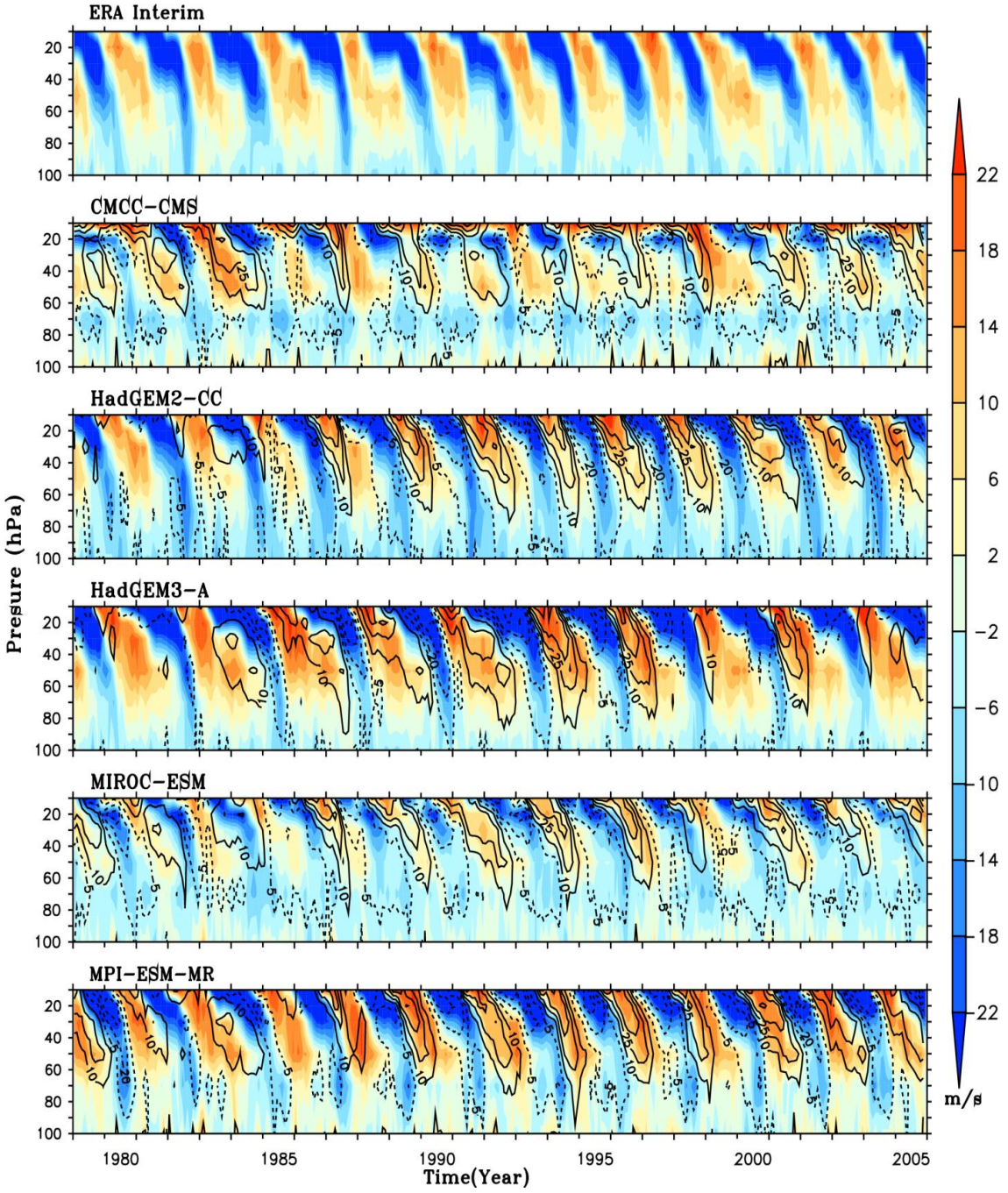

Figure 4.14: Equatorial zonal mean zonal wind time-height series from model (CMCC-CMS, HadGEM2-CC, HadGEM3-A, MIROC-ESM, MPI-ESM-MR) and the ERA-Interim reanalysis. Easterlies are blue and Westerlies orange, contour line indicate the bias with an interval of 15 m/s

Figure 4.15 show that three of the models generally overestimate the observed annual precipitation over the region (biases ranging from 0.08 to 0.39) but others underestimate the observed precipitation. However, among the five models, HadGEM2-CC and MPI-ESM-MR simulated precipitation close to the observed precipitation over most parts of West Africa. Therefore, because of its ability of to reproduce the annual climatology (wind and precipitation) over West Africa, HadGEM2-CC simulation is used for further analyses.

Table 4.3: Model Bias

Model	**Year Mean Bias**	
	Zonal wind (m/s)	**Precipitation (mm/day)**
CMCC-CMS	4.524	0.39
HadGEM2-CC	-0.7934	0.08
HadGEM3-A	1.281	-0.17
MIROC-ESM	1.642	0.16
MPI-ESM-MR	2.743	-0.06

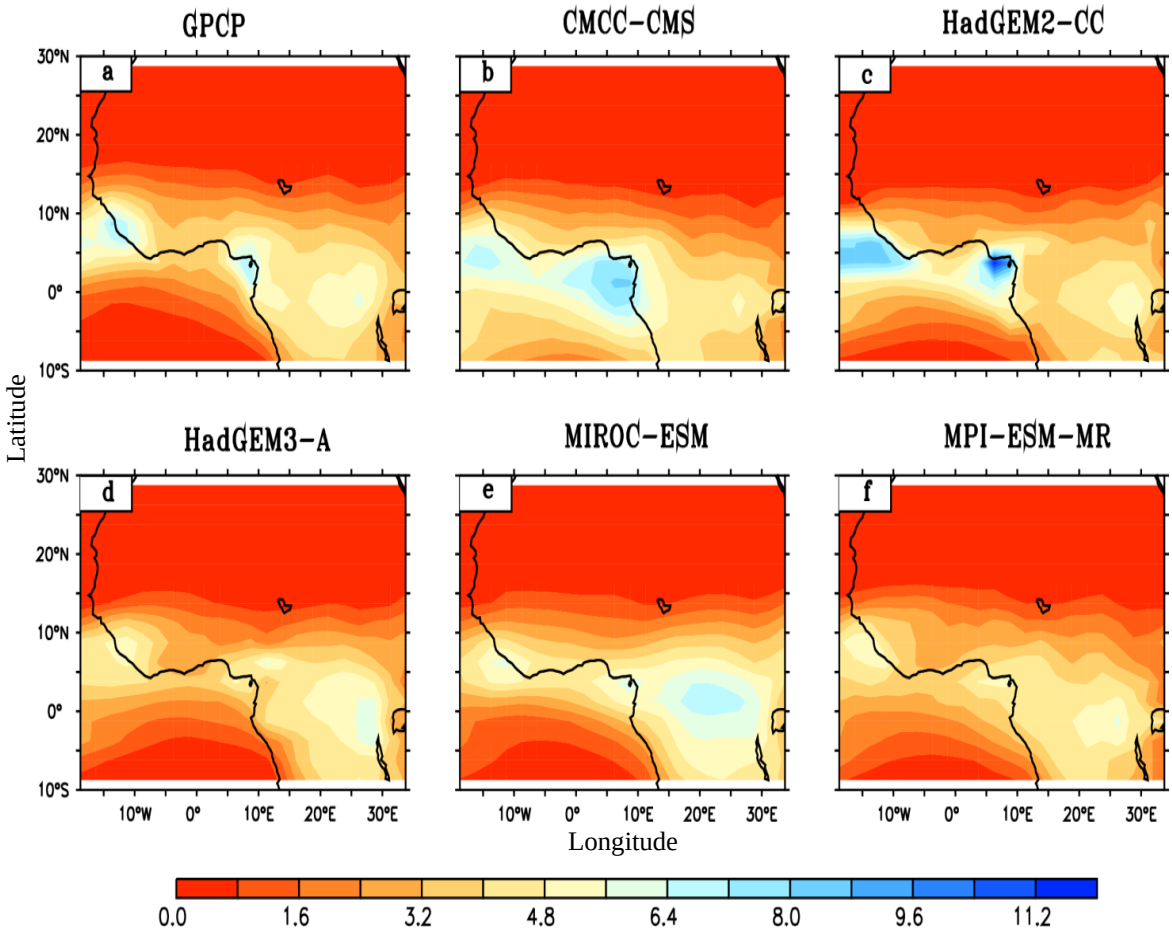

Figure 4.15: Spatial distribution of annual rainfall

4.2.3 Wavelet Coherence Analysis

The coupling between the stratospheric zonal winds and rainfall over West Africa as given by the models are shown in Figure 4.16. The coupling varies with period. In general, all model show there is coherence at annual time scale, indicating the significant effect of QBO on precipitation across all the zones. However, the HadGEM2-CC simulation (Figure 4.16(g,h,i)) are closer to the observed compared to other models. At both 30 and 50 hPa levels, a high coherence (0.6-0.8) is observed in both ERA-Interim and HadGEM2-CC for the intra-annual (i.e., 0.7-1.0 year) time-scale during the entire 27 year. This is particularly so during the 1992-2005 period. However, while HadGEM2-CC shows strong coherence in the 2.0-4.0 year band across all zones and at both 30 and 50hPa levels (also in other models), such are very weak in the ERA-Interim. That QBO has significant influence on West African rainfall, at both levels and across almost all models, is a very important result. The coherence for the 2.0-4.0 year band is also produced by all models at both 30 hPa and 50hPa, but is not continuous as for the intra-annual time scale and is also weakly so in the ERA-Interim.

In summary, the results from wavelet coherence analysis have shown that QBO has significant and persistent influence on Sahel, Savanna and Guinea rainfall in both model simulation and observed. Indeje and Semazzi (2000) noted that though the coherence between QBO and rainfall during East African long-rains is significantly high; there are some wet/dry years for which the relationship between the long rains and lower equatorial zonal wind are not significant. This has also been observed in the present study.

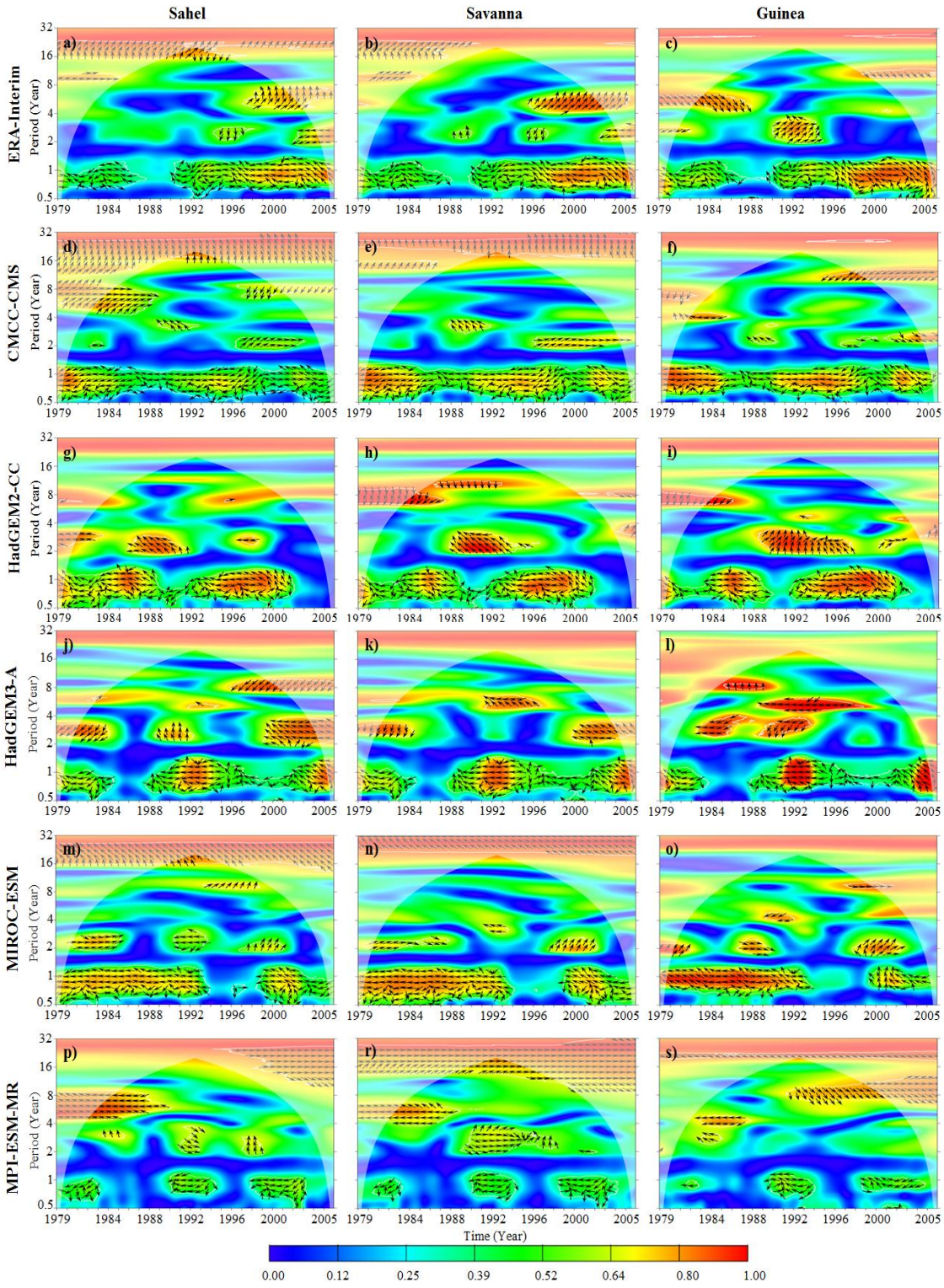

Figure 4.16: Wavelet coherence between precipitation and the QBO at 30 hPa

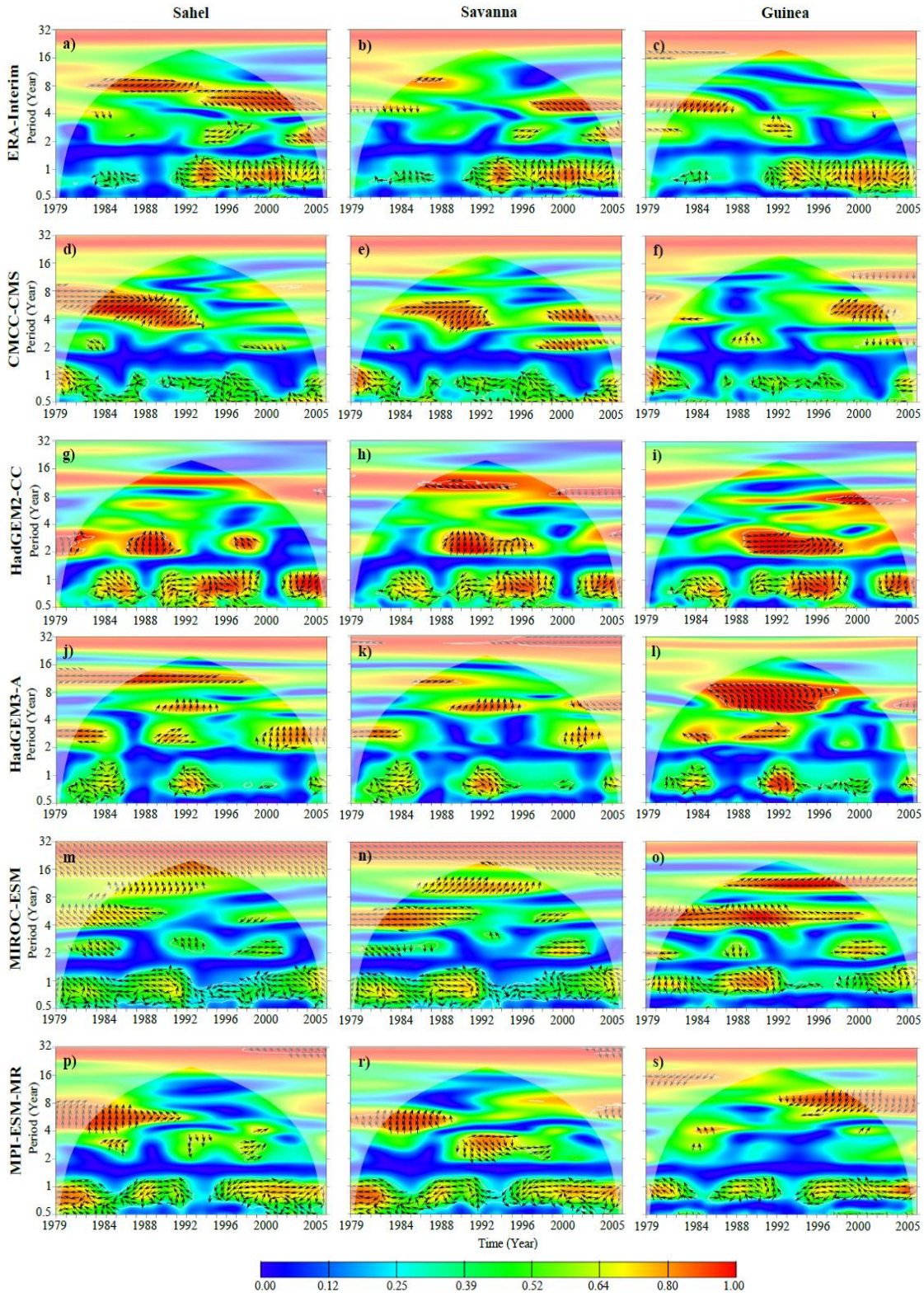

Figure 4.17: Wavelet coherence between precipitation and the QBO at 50 hPa

The coupling between the stratospheric zonal wind and tropospheric jet (AEJ and TEJ) over West Africa as given by the models are shown in Figure 4.18. In general, all model shows there is coherence at annual time scale, indicating the significant effect of QBO on AEJ and TEJ over the region. However, the HadGEM2-cc simulation at 50 hPa is closer to the observed ERAINT. Nevertheless, the model fails simulate the coherence at 50 hPa for both AEJ and TEJ. At 30hPa a high coherence (0.6 – 0.8) is observed in both ERAINT and HadGEM2-CC for the interannual (i.e., 0.7-1.0 year) time scale during the entire 27 years period. This is particularly so during the 1992-2005 period, consistent with the rainfall pattern (see Figure 4.16 and 4.17). However, while the ERAINT shows higher coherence in the 2 years and 4-8 years period at both 30 and 50 hPa also in other models, such are very weak in HadGEM2-CC model.

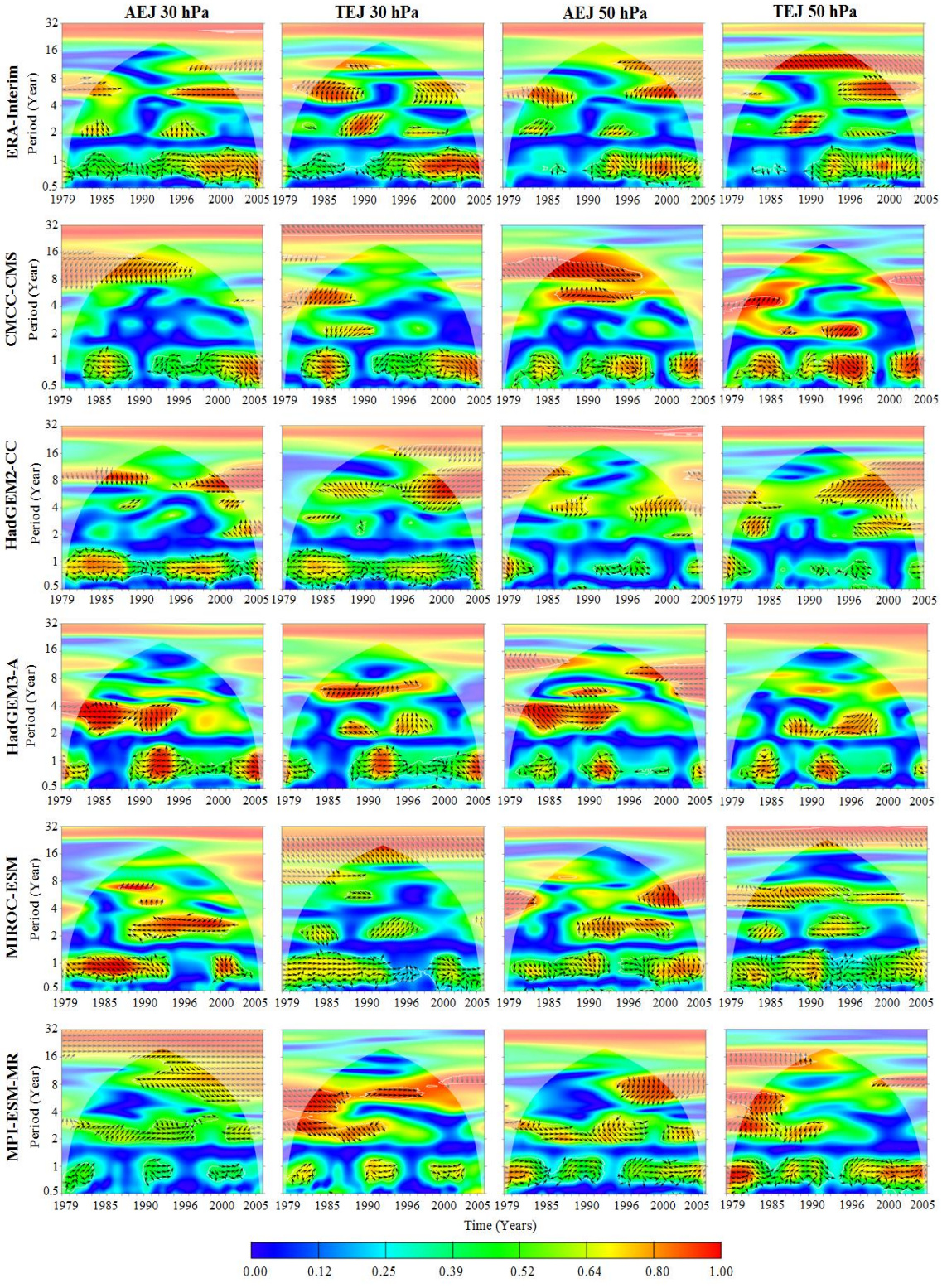

Figure 4.18: Wavelet coherence between tropospheric jet (AEJ, TEJ) and the QBO at 30 and 50 hPa

4.2.4 Composite

Further in this study, we split the region into 0-15^{o}E and 0-15^{o}W to better investigate the influence of QBO. Having shown that HadGEM2-CC has produced simulations that are similar to observation (ERAINT), the focus is now on comparison of its result with the ERA-Int. Here two simulations are considered: rainfall composites during QBO and non-QBO years (see Table 4.2) and the two phases (west and East) of QBO (also Table 4.2).

4.2.4.1 QBO and non-QBO years

In Figure 4.19-4.22, the composite at 50hPa (4.19 and 4.20) for longitude band 0-15^{o} and 0-15^{o}W respectively are shown while those at 30 hPa are in Figures 4.21 and 4.22. It can be seen from Figure 4.19 and 4.20 that there is generally more precipitation during QBO than in non-QBO years, although these are of order less than 1mm/day. This general situation is also observed at 30 hPa. However, while ERAINT shows greater rainfall during QBO years over all three zones and across whole West Africa, the model does not really produce these. From the observed (ERAINT), the influence of QBO is better felt over the eastern half of West Africa.

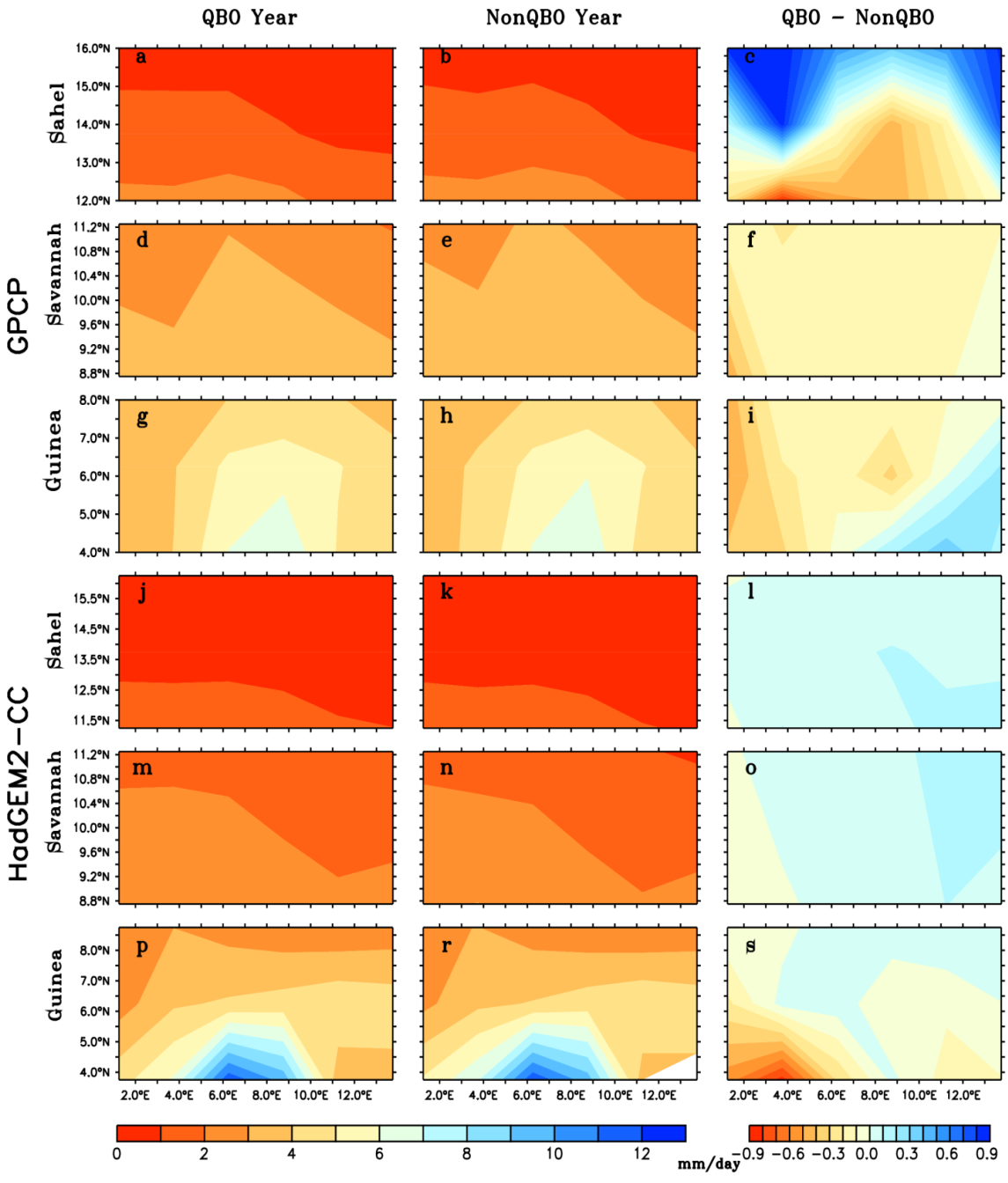

Figure 4.19: Composite evolution of rainfall at 50 hPa for 15E-0

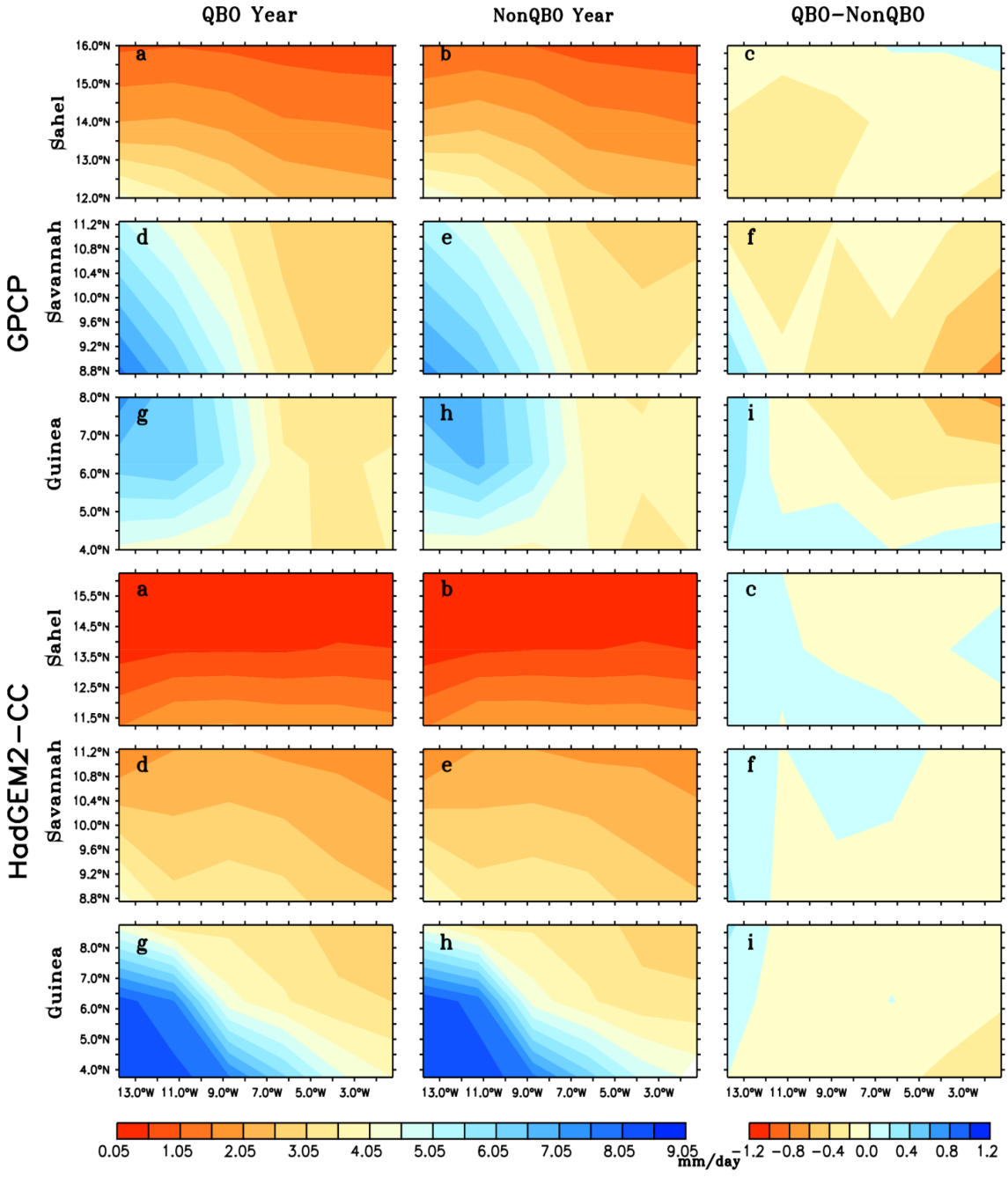

Figure 4.20: same as Figure 4.19 but for 15W-0

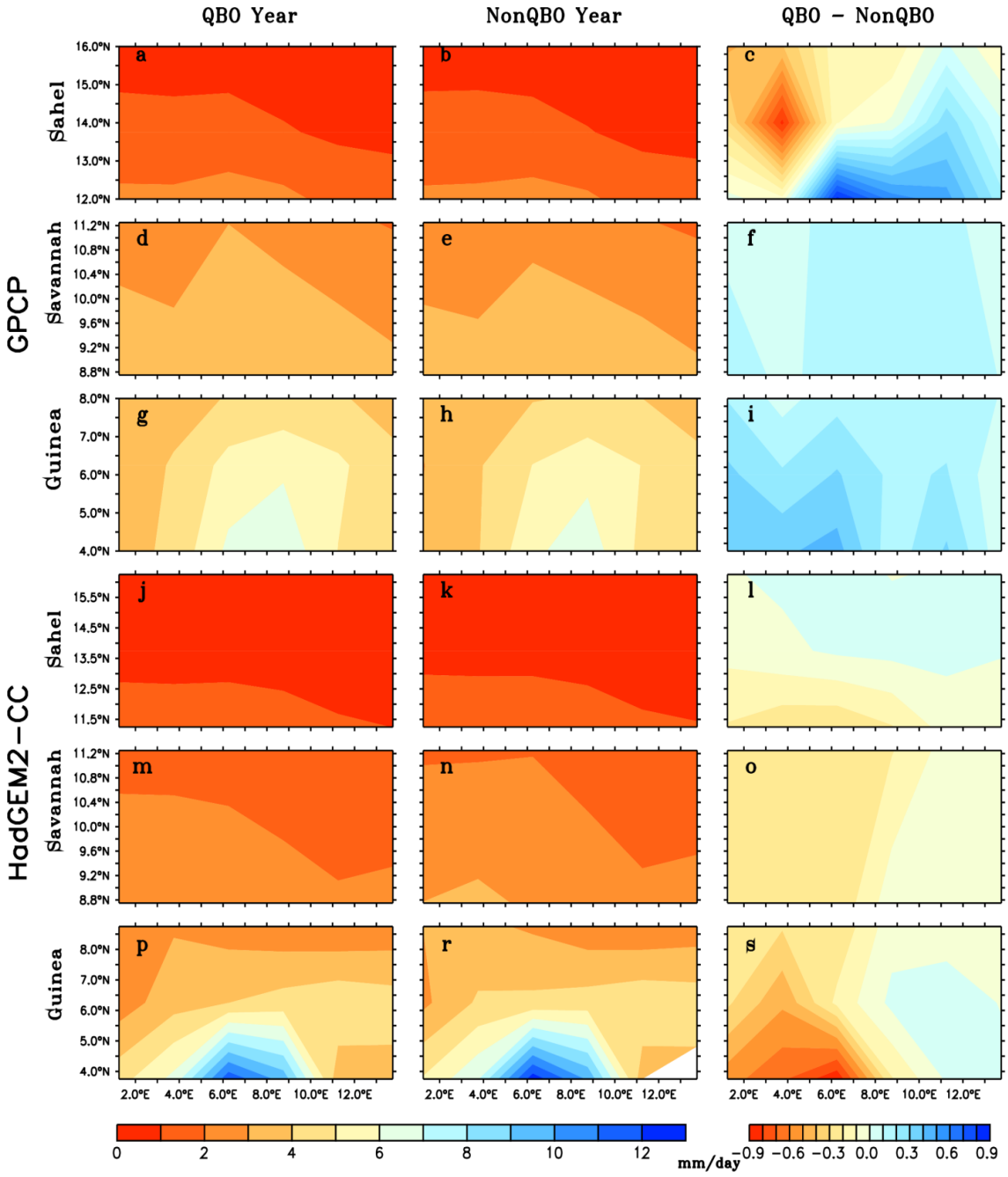

Figure 4.21: same as Figure 4.19, but at 30 hPa for 0-15E

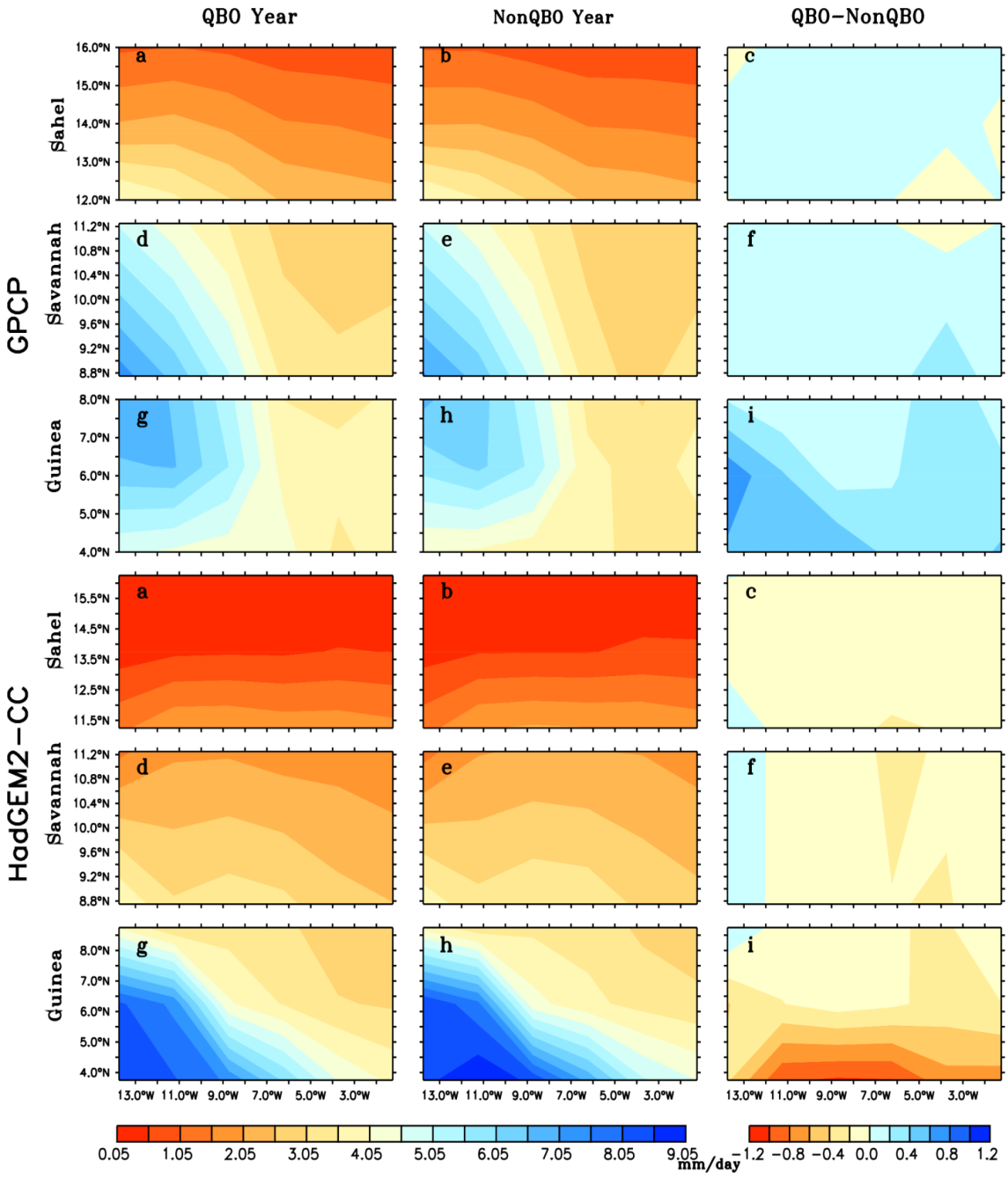

Figure 4.22: same as Figure 4.19, but at 30 hPa for 0-15W

4.2.4.2 Composites for East and West Phases of QBO

The east and west phases of the QBO at 50hPa are given in Figures 4.23 and 4.24 while at 30 hPa they are shown in Figures 4.25 and 4.26. At the 50hPa level, both model (HadGEM2-cc) and ERAINT show increased precipitation across the three zones entire West Africa (Figure 4.23). The excess precipitation is again greater over the Guinea zone, but more so in ERAINT than in HadGEM2-cc. The highest magnitude is about 0.8mm/day, representing 7-10 percent increase across the zone. The influence decreases rapidly towards the Sahel everywhere. The composite pattern is similar at the 30hPa, again with decreasing QBO influence towards the Sahel over the eastern half of West Africa. From both model and the observed (ERAINT, Figure 4.26), it can be seen that there is virtually no QBO effect west of the 0^{o} long at this higher level. The results of this present study is consistent with those of Chattopadhyay and Bhatla (2002) who associated the easterly phase of QBO with drought in India and normal to strong monsoon rainfall with the westerly phase.

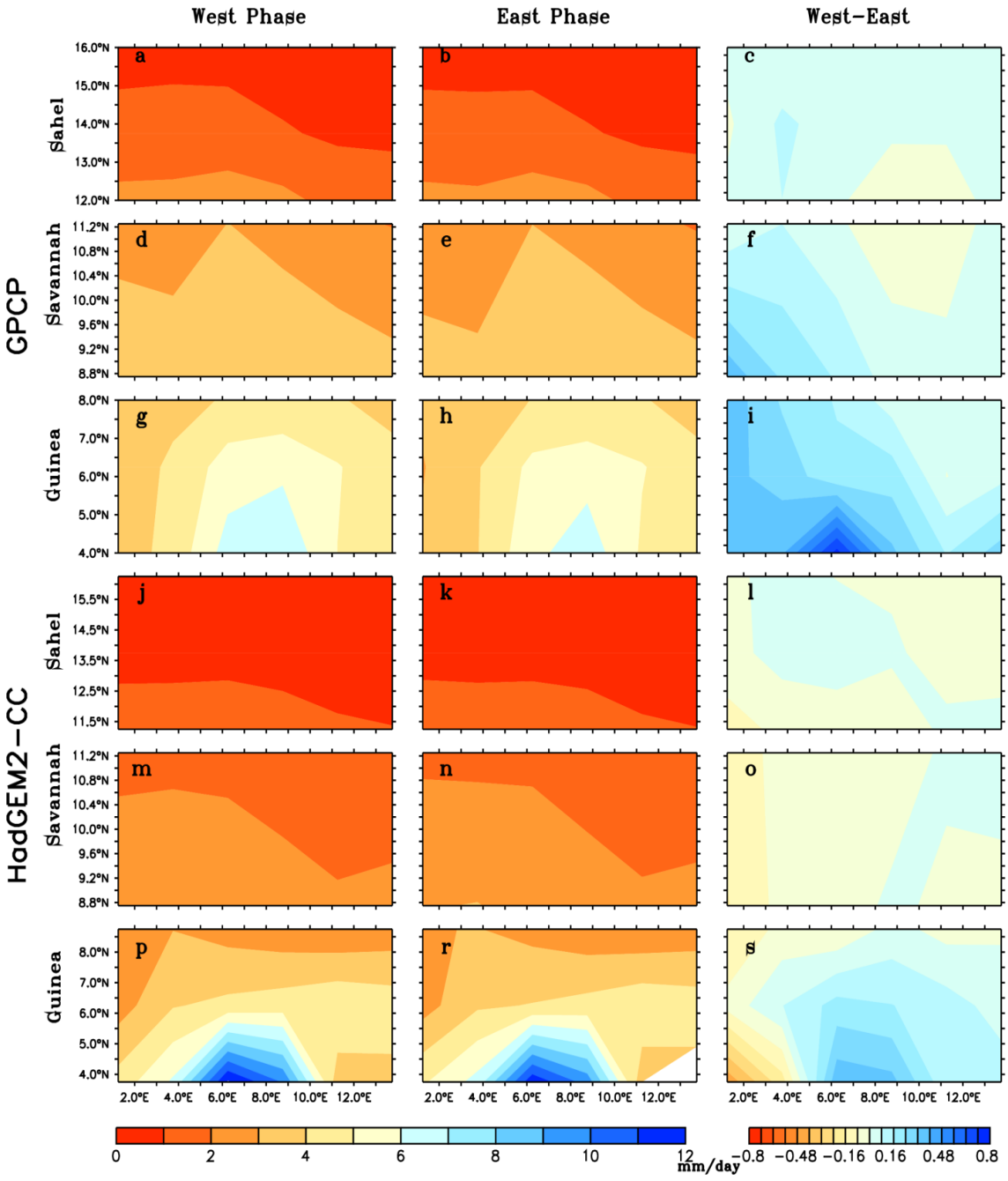

Figure 4.23: Same as in Figure 4.19 but for 50 hPa

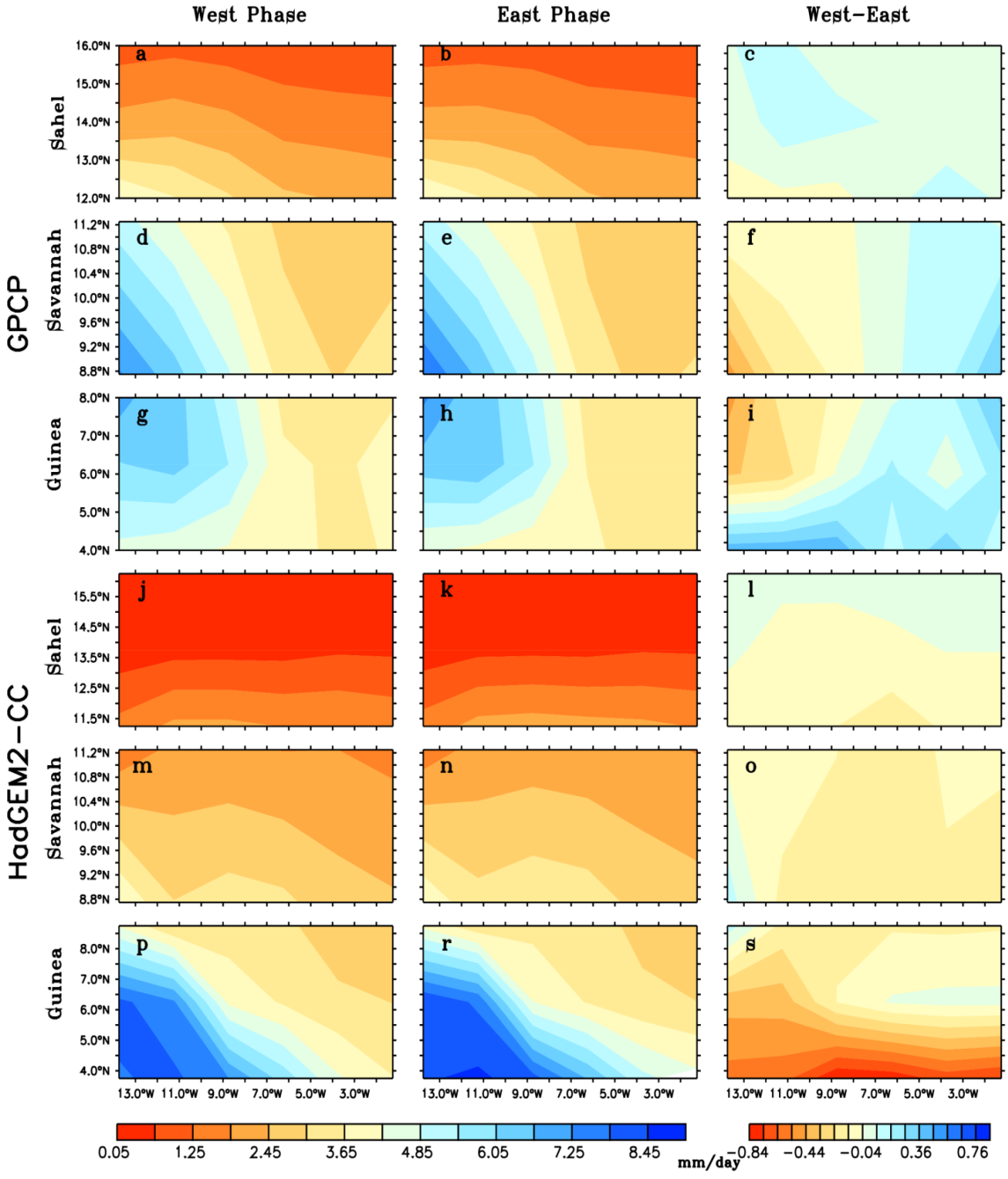

Figure 4.24: Composite evolution of rainfall at 50 hPa for 0-15W

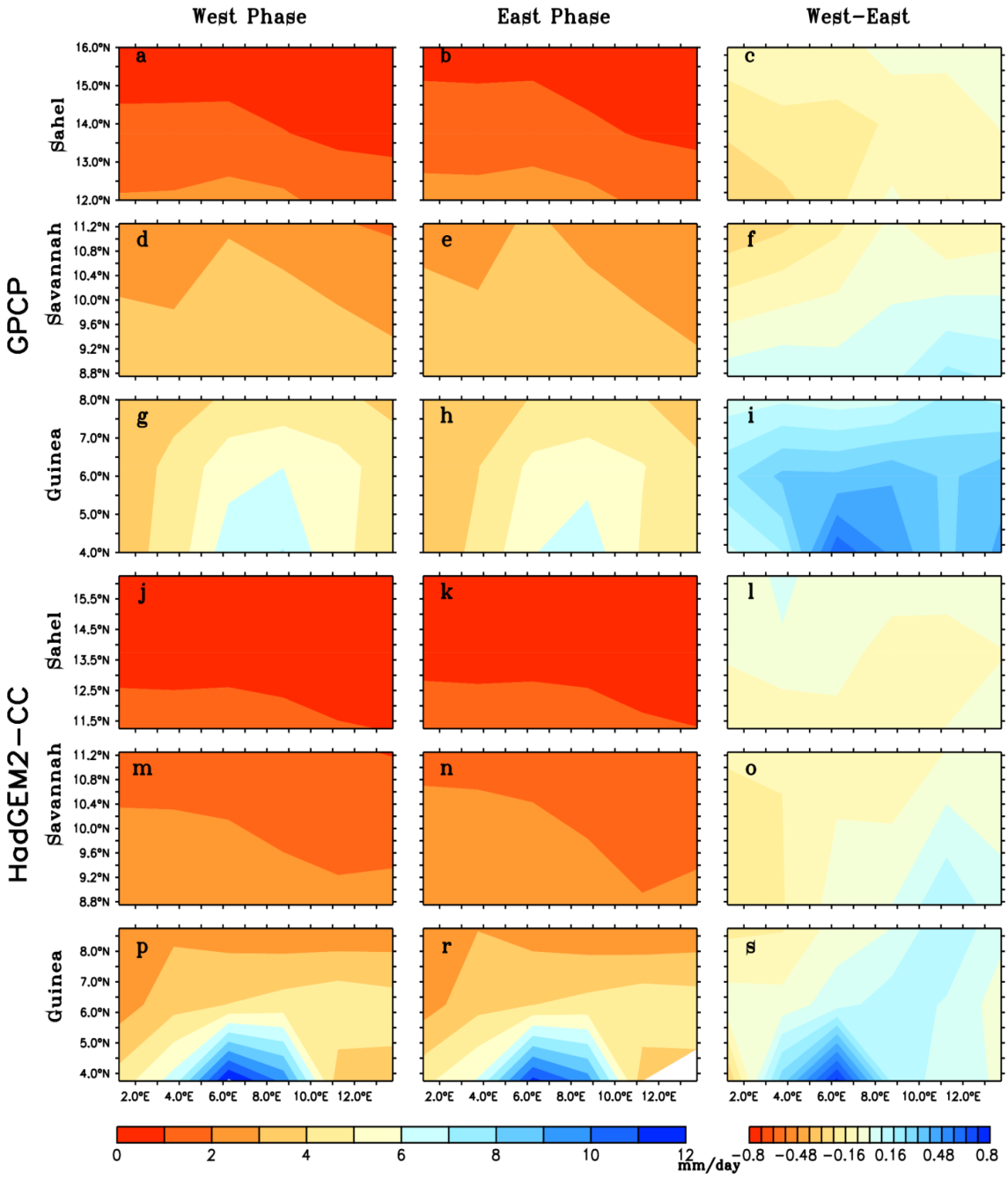

Figure 4.25: Composite evolution of rainfall at 30 hPa for 0-15E

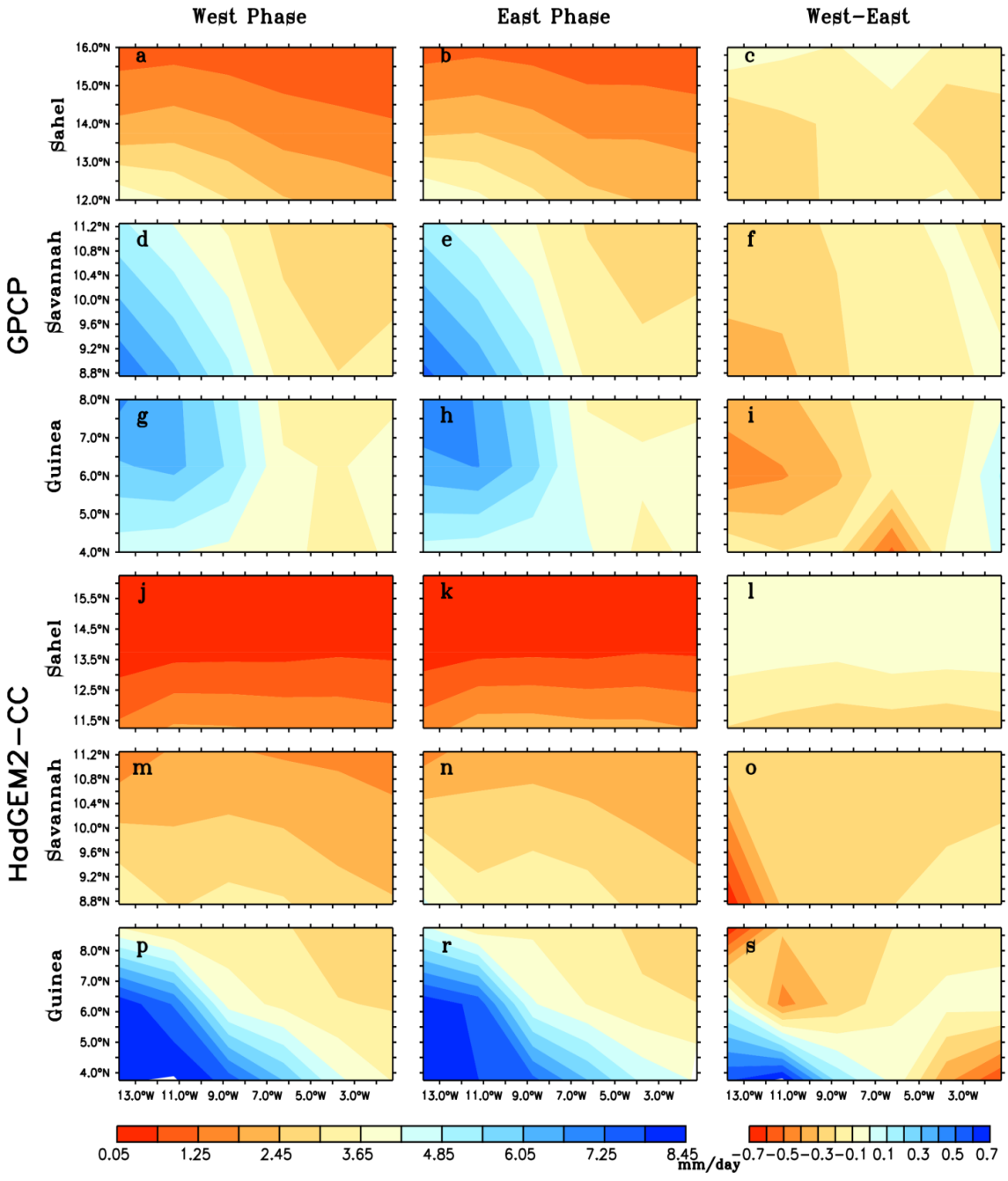

Figure 4.26: Composite evolution of rainfall at 30 hPa for 0-15W

4.2.5 Composite evolution of the specific humidity

4.2.5.1 QBO and non-QBO

In Figure 4.27-4.30, the composite at 50hPa (4.27 and 4.28) for longitude band 0-15E and 0-15W respectively are shown while those 30hPa are in Figure 4.29 and 4.30. It can be seen from Figure 4.27 and 4.28 that there is generally more humidity during the QBO than in non-QBO years, which is consistent to the founding in section 4.2.4.1. This general situation is also observed at 30hPa. However, while the observed (ERAINT) shows greater humidity during QBO years over all zone (Figure 4.27 – 4.28 and 4.30), the model overestimate these. Nevertheless, in Figure 4.28 while the ERAINT show greater moisture across whole West Africa, the model does not really produce these. From the observed (ERAINT) the influence of QBO is better observed over the Eastern half of West Africa, which is associated with high rainfall over the regions.

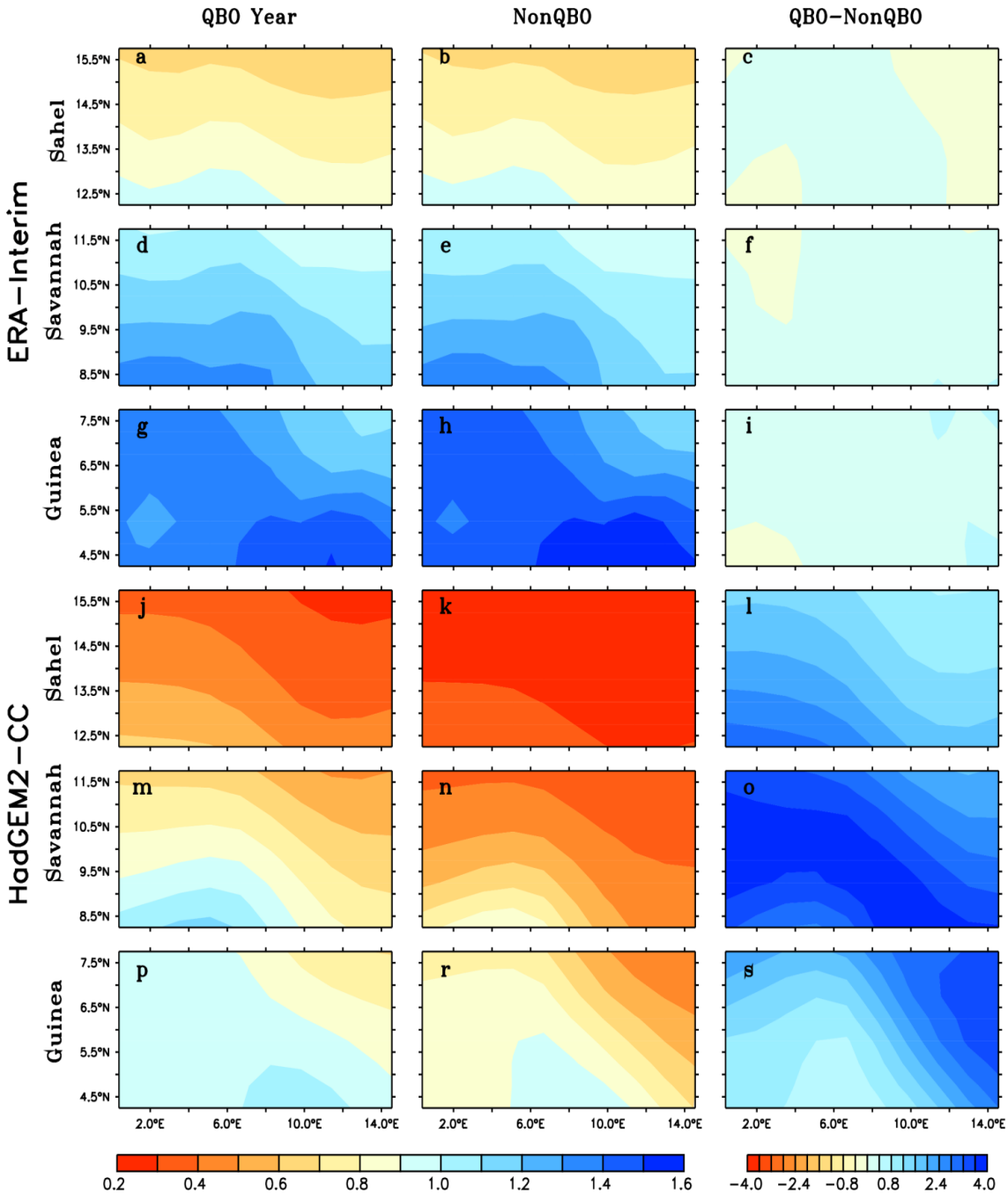

Figure 4.27: Composite of specific humidity at 0-15E for 50 hPa

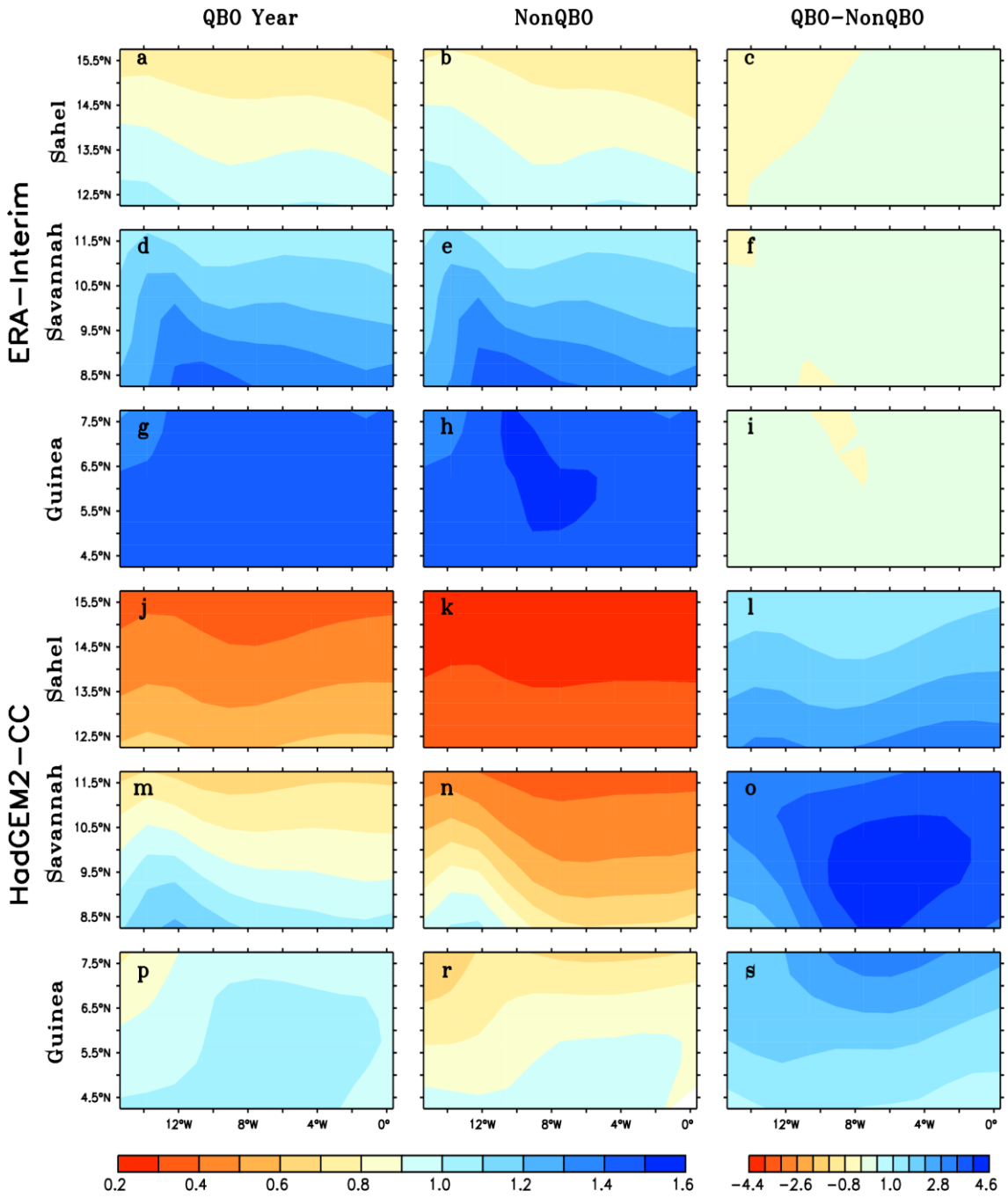

Figure 4.28: Composite of specific humidity at 0-15W for 50 hPa

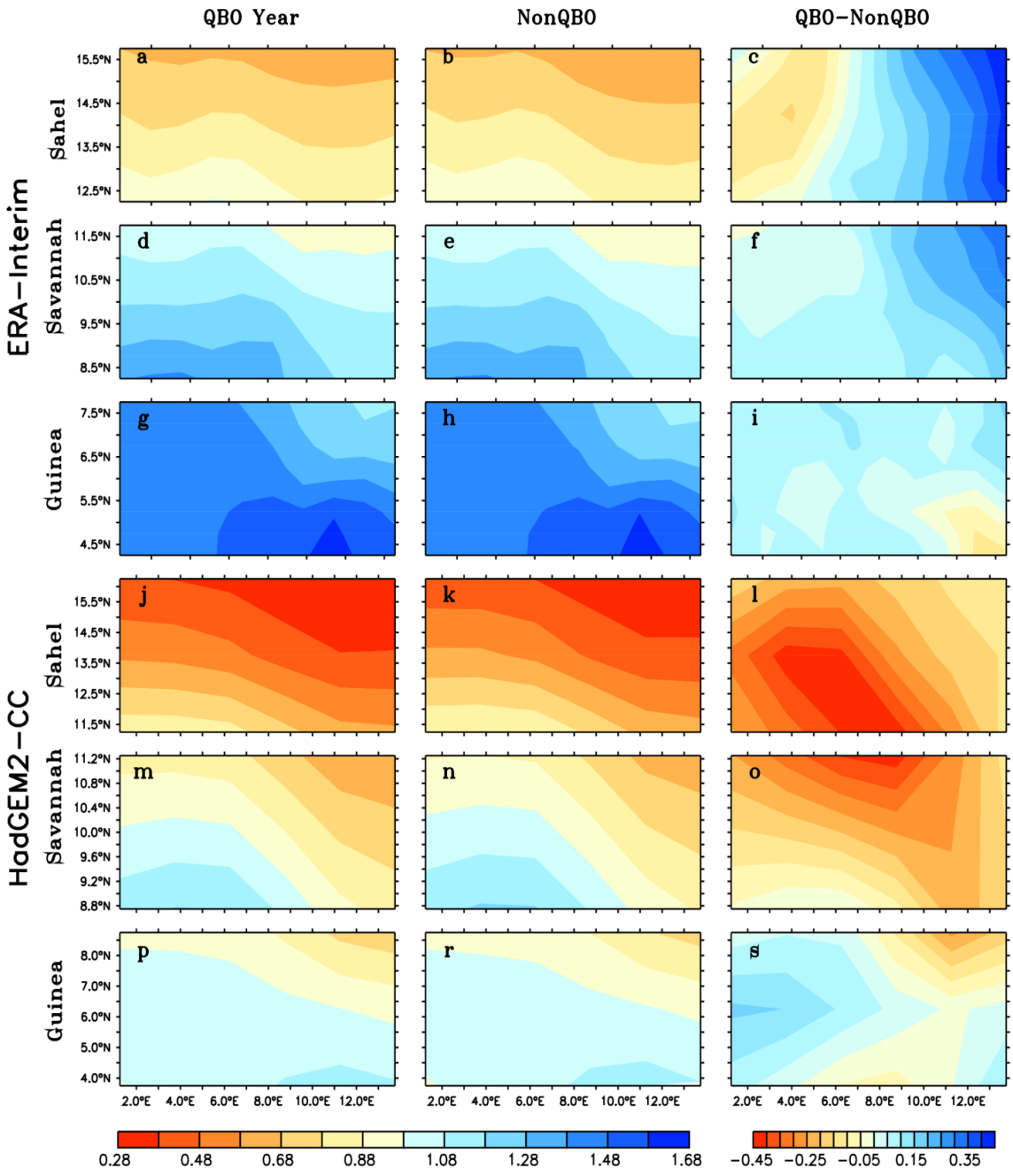

Figure 4.29: Composite of specific humidity at 0-15E for 30 hPa

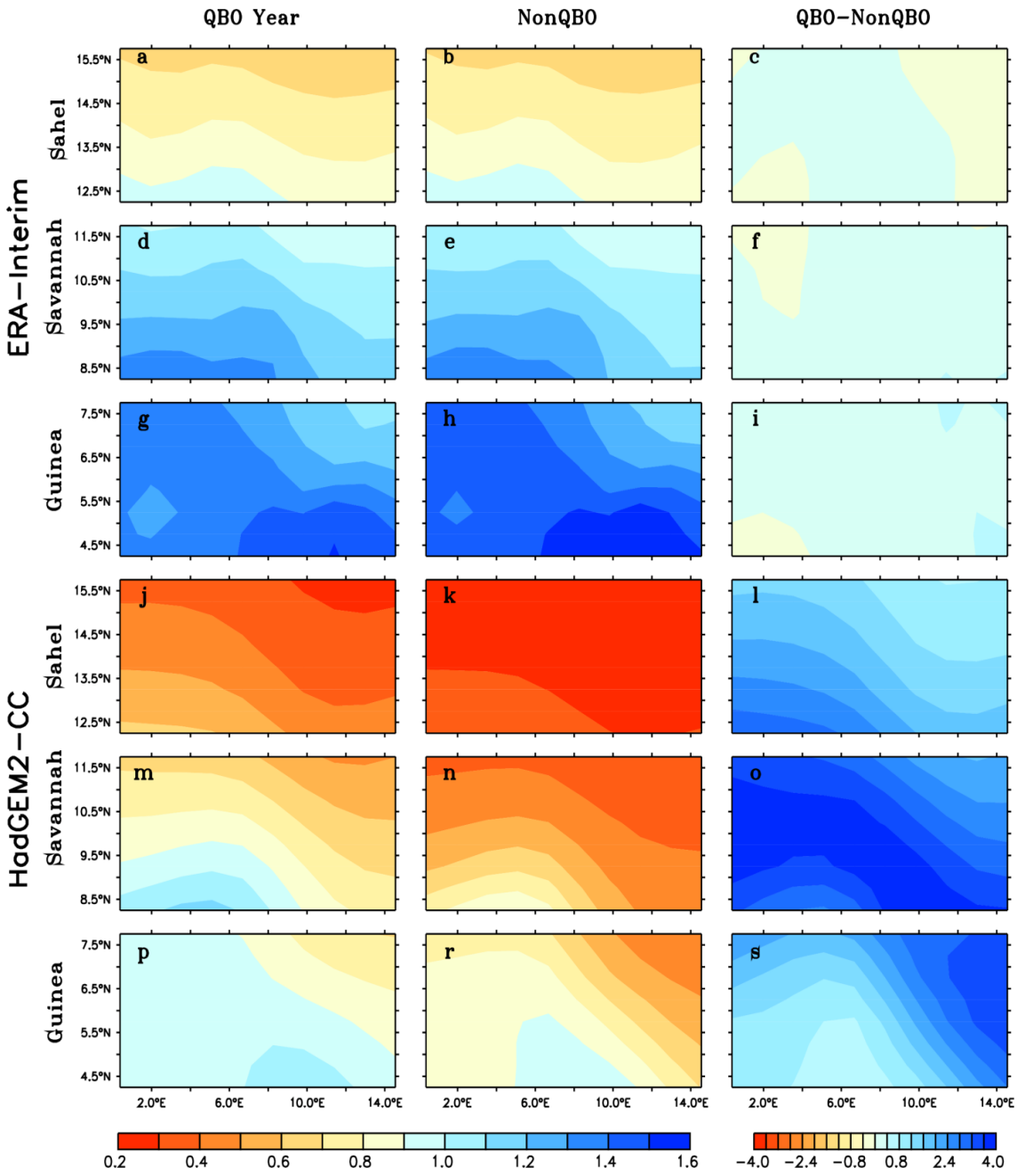

Figure 4.30: same as Figure 27

4.2.5.2 Composite for East and West Phases of QBO

The East and West phase of the QBO at 50hPa are given in Figures 4.31 and 4.32 while at 30hPa they are shown in Figure 4.33 and 4.34. At both the 50hPa level both model (HadGEM2-cc) and ERAINT show increased humidity across the three zones of entire West Africa except for the model at 0-15W. The excess of humidity is also greater over the Guinea and Savannah zone, but more so in HadGEM2-cc than in ERAINT. The observed ERAINT, Figure 4.34, it can be seen that there is little QBO effect west of 0^{o} long consistent with the rainfall in section 4.2.4.2.

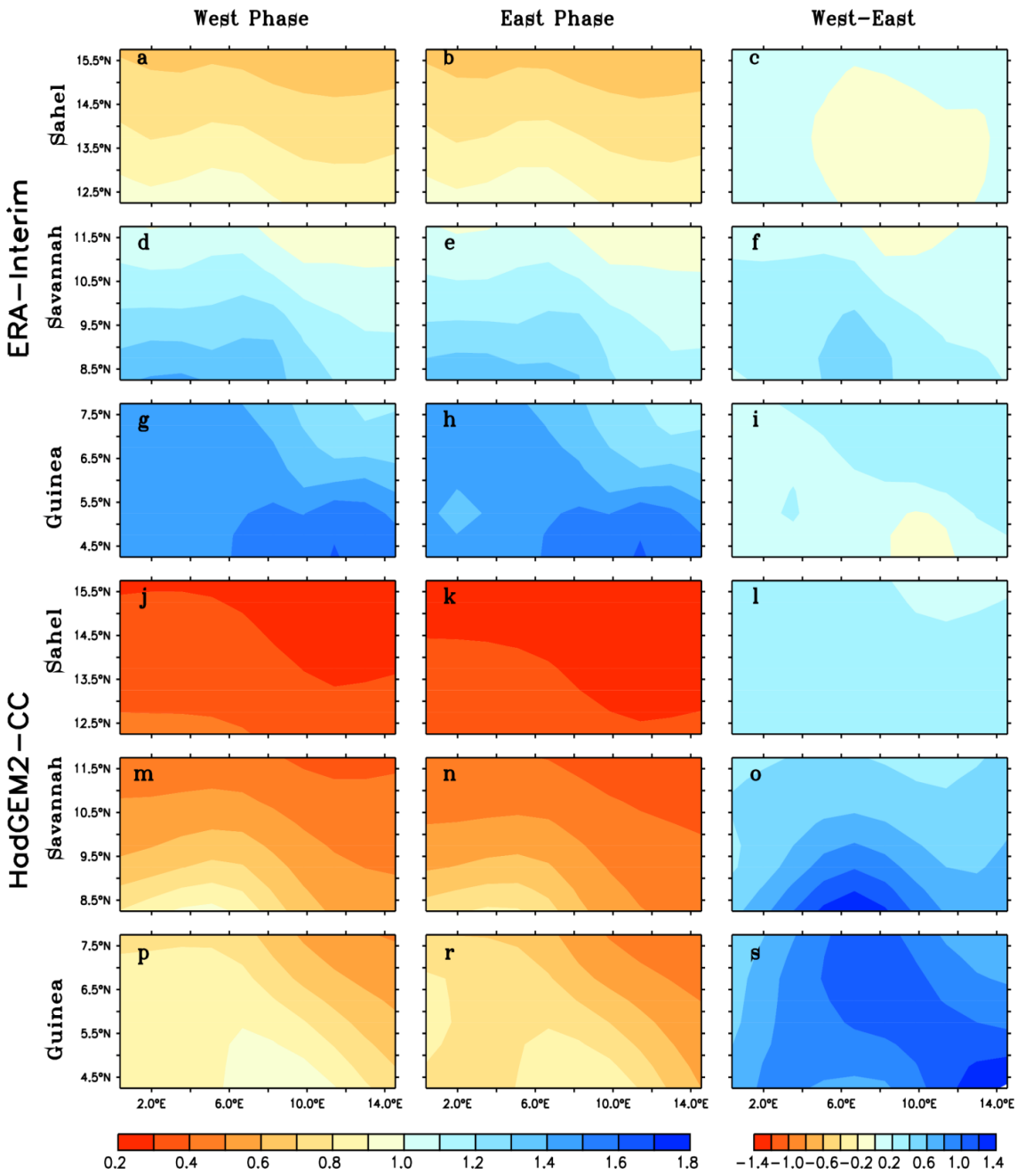

Figure 4.31: Composite of specific humidity at 50 hPa for longitude 0-15E

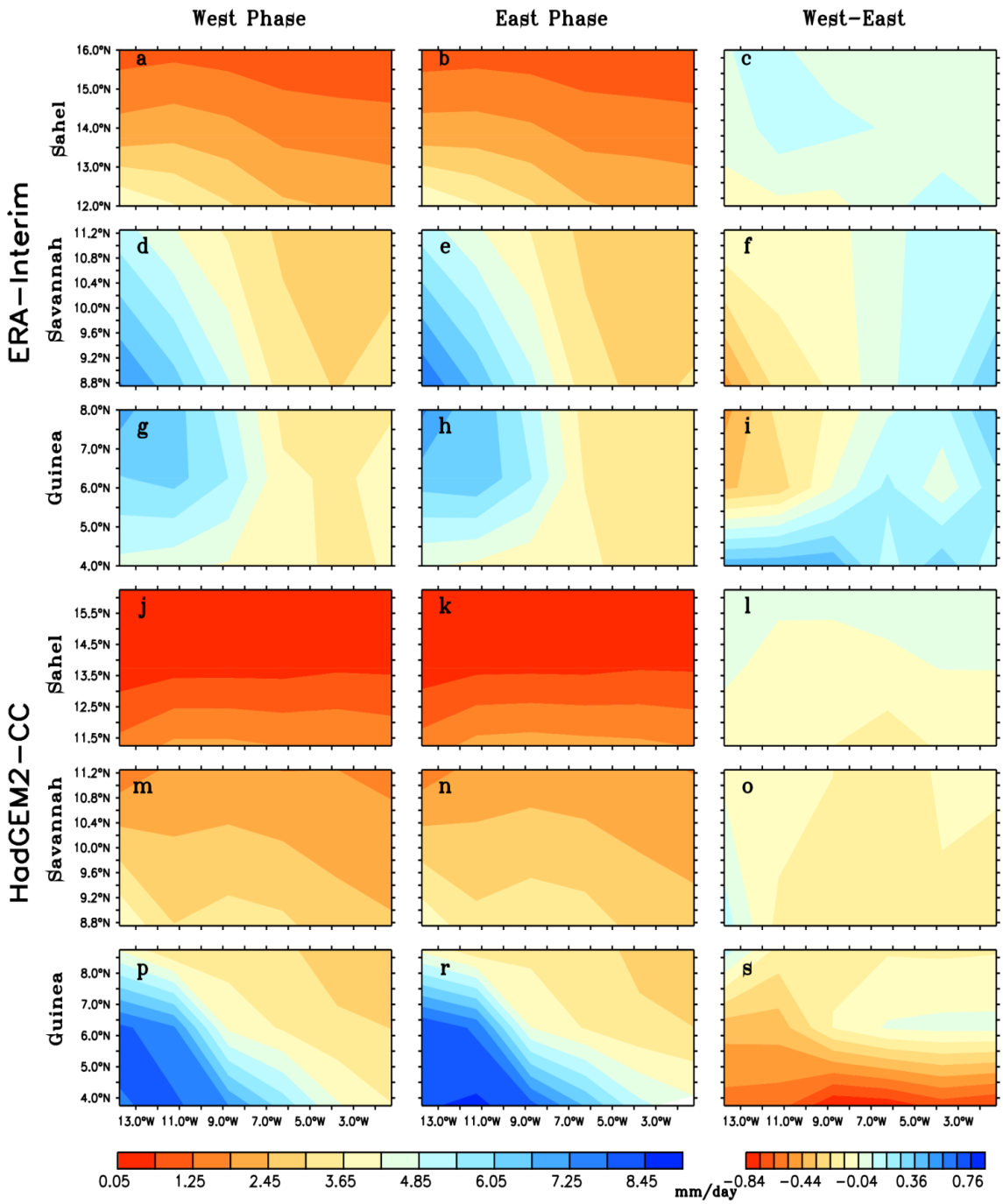

Figure 4.32: Composite of specific humidity at 50 hPa for longitude 0-15W

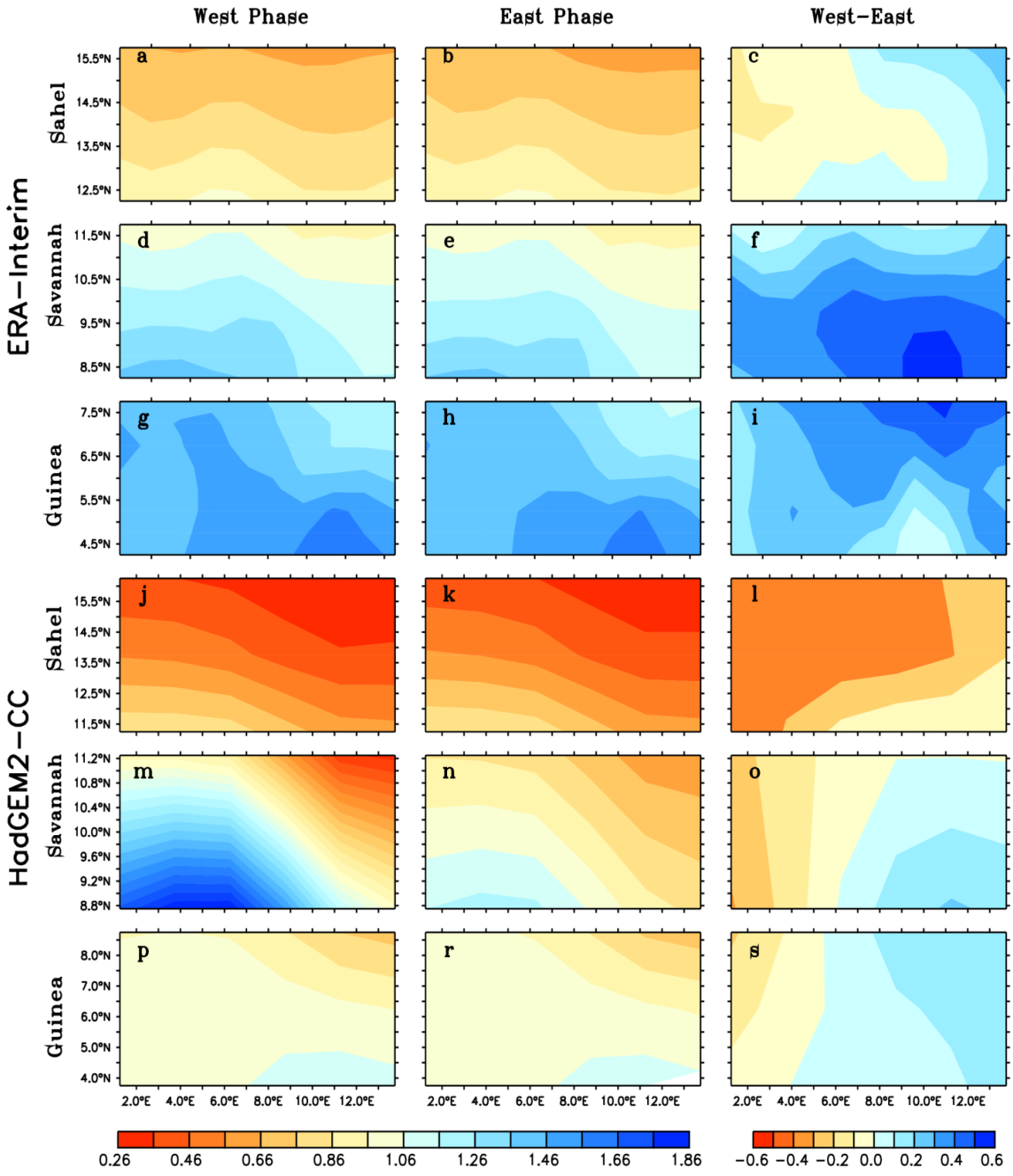

Figure 4.33: Composite evolution of specific humidity for 30 hPa at 0-15E

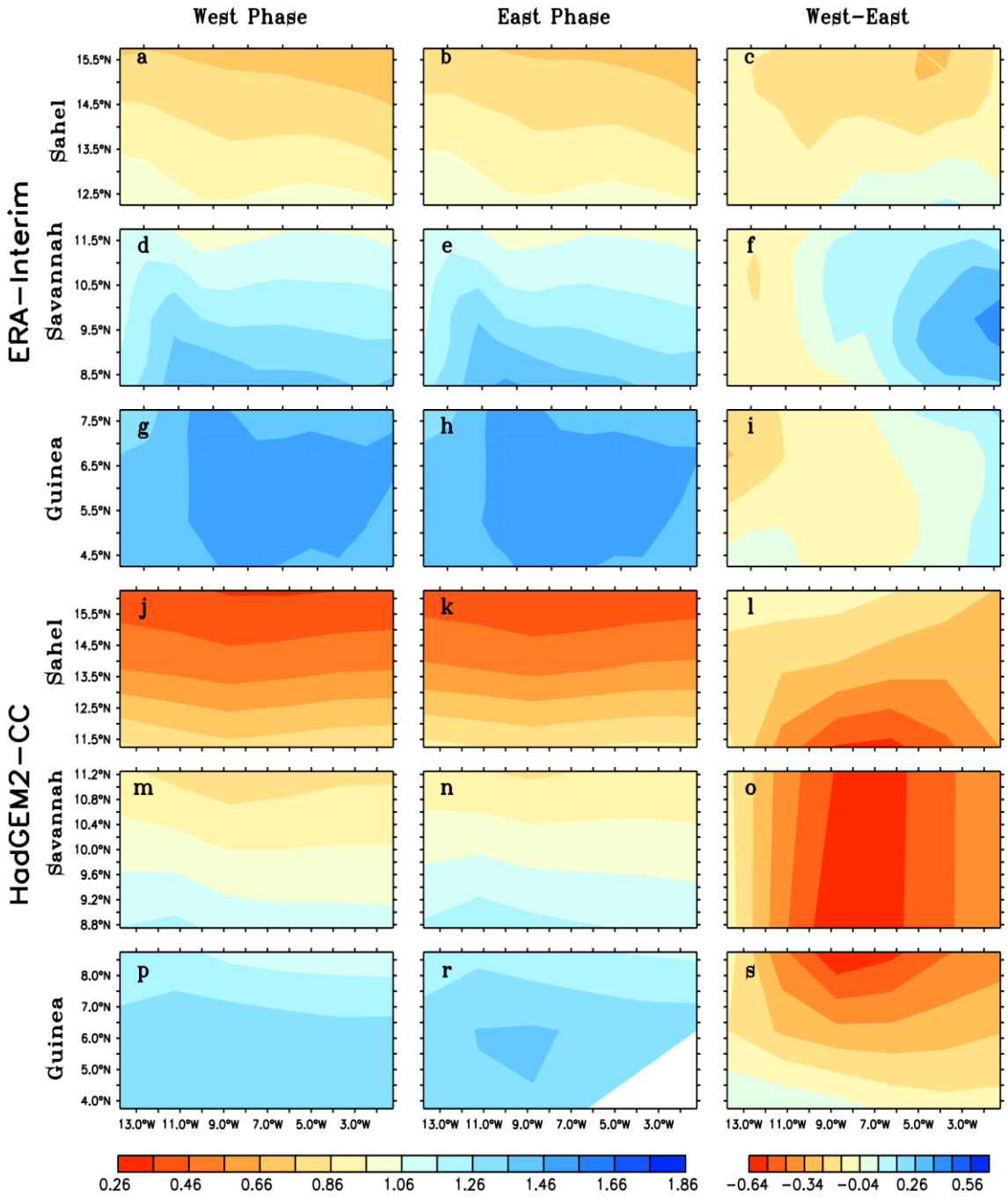

Figure 4.34: Composite evolution of specific humidity for 30 hPa at 0-15W

CHAPTER FIVE

CONCLUSION AND RECOMMENDATIONS

5.1 CONCLUSION

Firstly, in this study, we have analysed and examined the West African monsoon structure and its associated tropospheric jets together with the influencing sub-tropical westerly jet have been investigated. The association and relative influence of the jets (AEJ, TEJ and the West African Westerly Jet (WAWJ)) on the regions rainfall, including wet and dry periods are also investigated. The major findings can be summarized as follows:

- A crucial importance of West African monsoon structure is the deepening monsoon layer, the intensifying WAWJ and the AEJ, as well as the rapidly weakening but poleward retreating STJ, leading to the intensification of the AEJ and the sudden appearance of the TEJ in June.
- This sudden TEJ appearance (disappearance) is suggested to be linked to the equally sudden weakening (strengthening) and disappearance (appearance) of the stratospheric Quasi-biennial Oscillation (QBO), which begins to appear from October and weakens quickly thereafter to give way to TEJ appearance in June.
- The TEJ core does not arrive over West Africa until June/July, coinciding with a rapid poleward retreat of the sub-tropical westerly jet (STJ) between May and June. This was linked to the weakening of the stratospheric quasi-biennial oscillation (QBO).
- The relative influence of AEJ on rainfall is observed over West Africa through all months. The rainfall pattern follows behind and parallel to the AEJ core every month, suggesting a close relationship between the AEJ and rainfall distribution over West Africa.

- However, in contrast to the previous studies that suggest a strong link between TEJ and West African rainfall particularly in the Sahel, the present study shows clearly that the northward advance of the rainfall distribution shows little or no relationship with the TEJ movement as was the case with the AEJ. TEJ core always lags behind the rainfall maximum.
- The associated vertical motion shows stronger ascent during with higher rainfall amounts during wet than dry years through all months. The upward motion occurs both north and south of the AEJ core but strongest to the south, while it is always north of the TEJ core in both wet and dry cases.
- The poleward and height withdrawal of the STJ is found to be faster during wet years.

Secondly, the study therefore investigates the teleconnection between the stratospheric zonal wind and West African precipitation. Four historical experiments (CMCC-CMS, HadGEM2-CC, HadGEM3-A, MPI-ESM-MR and MIROC-ESM-MR) from Coupled Models Intercomparison Project Phase 5 (CMIP5) simulations were used for the study. The capability of the models to reproduce the QBO and the coherence between it and rainfall over the three zones (Sahel, Savannah and Guinea) of West Africa was also examined using wavelet analysis. Also, we applied the composite of the QBO to obtain the dominant impacts of its phases (west and east) over the region. The major findings can be summarised as follows:

- All four models considered produced realistic simulation of the general structure of the QBO and also capture all the essential features in the observed field. However, some of the model underestimate or overestimate the west and east phase compared to the ERAIN, that is, with some biases.

- Of all the models HadGEM2-CC has the least bias. HadGEM2-cc gives better representation of coherence over the three climatic zones (Sahel, Savannah and Guinea). It also produced more realistic spatial distribution of annual rainfall.
- The model reproduces the coupling between the stratospheric zonal winds and rainfall over West African, but the coupling varies with period as in ERAINT too. There is high coherence on timescales of between 0.7 and 1.0 year during 1991-2005 in ERA-Interim. In HadGEM2-CC this effect is strong between same period but for the years 1979-2002. This high coherence (0.6-0.8) is observed in both ERA-Interim and HadGEM2-CC for the intra-annual (i.e., 0.5-1.0 year) and inter-annual scales (2.0-4.0 years) in all climate zones at the two levels (30 and 50hPa) studied.
- These results all show that QBO has important influence on West African rainfall in both the model and the observed. An increase in precipitation is observed during the presence of QBO over the Guinea zone, but particularly over the eastern sector. The increase over Savannah and Sahel is minimal.
- During the West phase of a QBO year, rainfall rates were higher everywhere but more so over Savannah and Guinea region than during the east phase. The Sahel region is less influenced by the presence and phase of the QBO.

The results of this study also show that some GCM could be selected for further studies on the prediction of the influence of QBO on annual rainfall over West Africa. However, being the first study of QBO influence on West Africa precipitation, further investigations are needed to improve the ability of CMIP5 models to reliably capture the patterns of coherence; especially the use of the QBO year and its phases to improve the reliability of rainfall prediction over West Africa.

5.2 RECOMMENDATIONS

It is recommended that further work in the future can focus on the investigations of possible link between QBO disappearance, the STJ withdrawal and the monsoon jump to improve the mechanisms driving rainfall variability over West Africa. However, being the first study of QBO influence on West Africa precipitation, further investigations are also needed to improve the ability of CMIP5 models to reliably capture the patterns of coherence; especially the use of the QBO year and its phases to improve the reliability of rainfall prediction over West Africa. This will help climatologists to further understand the dynamics of rainfall and the winds vis-à-vis low and high yield.

REFERENCES

A. Giannini, R. Saravanan, P. C. (2003). Oceanic Forcing of Sahel Rainfall on Interannual to Interdecadal. *Science*, *302*(November), 1027–1031. https://doi.org/10.1016/S1364-8152(03)00114-2

Abdul Malik, Peer J. Nowack, Joanna D. Haigh, Long Cao, Luqman Atique, Y. P. (2019). Tropical Pacific Climate Variability under Solar Geoengineering: Impacts on ENSO Extremes. *Atmos. Chem. Phys.*, (January), 1–33.

Abiodun, B. J., Adeyewa, Z. D., & Ajayi, V. O. (2012). Modeling the impacts of reforestation on future climate in West Africa. *Theor Appl Climatol*, *110*, 77–96. https://doi.org/10.1007/s00704-012-0614-1

Abiodun, B. J., Pal, J. S., Afiesimama, E. A., Gutowski, W. J., & Adedoyin, A. (2008). Simulation of West African monsoon using RegCM3 Part II: Impacts of deforestation and desertification. *Theoretical and Applied Climatology*, *93*(3–4), 245–261. https://doi.org/10.1007/s00704-007-0333-1

Adepitan, J. O., & Falayi, E. O. (2019). Variability changes of some climatology parameters of Nigeria using wavelet analysis. *Scientific African*, *2*. https://doi.org/10.1016/j.sciaf.2018.e00017

Afiesimama, E. A., Pal, J. S., Abiodun, B. J., Jr, W. J. G., & Adedoyin, A. (2006). Simulation of West African monsoon using the RegCM3 . Part I : Model validation and interannual variability. *Theor. Appl. Climatol.*, *37*, 23–37. https://doi.org/10.1007/s00704-005-0202-8

Agus Santoso, Michael J. Mcphaden, and W. C. (2017). The Defining Characteristics of ENSO Extremes and the Strong 2015/2016 El Niño. *American Geophysical Union*, *55*, 1079–1129. https://doi.org/10.1002/2017RG000560

Alexander Lemburg, Jurgen Bader, M. C. (2019). Sahel Rainfall-Tropical Easterly Jet Relationship

on Synoptic to Interaseasonal Time Scales. *Amer Meteor. Soc*, *147*(20 February), 1733–1752. https://doi.org/10.1175/MWR-D-18-0254.1

Almazroui, M., Balkhair, K. S., Islam, M. N., & Sen, Z. (2017). Climate Change Impact on Monthly Precipitation Wet and Dry Spells in Arid Regions : Case Study over Wadi Al-Lith Basin. *Advances in Meteorology*, *2017*, 13.

Amekudzi, L., Yamba, E. I., Preko, K., Aryee, J., Baidu, M., & Codjoe, and S. N. A. (2015). Variabilities in Rainfall Onset, Cessation and Length of Rainy Season for the Various Agro-Ecological Zones of Ghana. *Climate*, *3*(15 June), 416–434. https://doi.org/10.3390/cli3020416

Anandhi, A., Srinivas, V. V, Nanjundiah, S., & Kumar, D. N. (2008). Downscaling precipitation to river basin in India for IPCC SRES scenarios using support vector machine. *International Journal of Climatology*, *28*(June), 401–420. https://doi.org/10.1002/joc

Augusto, C., Santos, G., Morais, B. S. De, Augusto, C., Santos, G., & Morais, B. S. De. (2013). Identification of precipitation zones within São Francisco River basin (Brazil) by global wavelet power spectra Identification of precipitation zones within São Francisco River basin (Brazil) by global wavelet power spectra. *Hydrological Sciences Journal*, *58*, 789–796. https://doi.org/10.1080/02626667.2013.778412

B. K. Mukherjee, K. Indira, R. S. R. and B. V. R. M. (1985). Quasi-Biennial Oscillation in Stratospheric Zonal Wind and Indian Summer Monsoon. *American Meteorological Society*, *113*(August).

Belen Rodrıguez-Fonseca, S. J., Mohino, E., Losada, T., Bader, J., Caminade, C., Gervois, S., … Voldoire, A. (2011). Interannual and decadal SST-forced responses of the West African monsoon. *Royal Meteorological Society*, *74*, 67–74. https://doi.org/10.1002/asl.308

BENJAMIN SULTAN and SERGE JANICOT. (2003). The West African Monsoon Dynamics . Part I : Documentation of Intraseasonal Variability, 3389–3406.

Berrisford, P., Kobayashi, S., Dee, D., Uppala, S., Simmons, A. J., Poli, P., & Sato, H. (2011). Atmospheric conservation properties in ERA-Interim 1382. *Q. J. R. Meteorol. Soc.*, *137*(July), 1381–1399. https://doi.org/10.1002/qj.864

Berrisford, Paul, Dee, D., Fielding, K., Fuentes, M., Kållberg, P., S, K., & S, U. (2009). The ERA-Interim archive. *ERA Report Series*, *1*, pp 16.

Byrne, M. P., Pendergrass, A. G., Rapp, A. D., & Wodzicki, K. R. (2018). Response of the Intertropical Convergence Zone to Climate Change : Location , Width , and Strength. *Curr Clim Change Rep*, (9 August), 355–370.

Chang, X., Wang, B., Yan, Y., Hao, Y., & Zhang, M. (2018). Characterizing effects of monsoons and climate teleconnections on precipitation in China using wavelet coherence and global coherence. *Climate Dynamics*, *0*(0), 0. https://doi.org/10.1007/s00382-018-4439-1

Charlton-perez, A. J., Baldwin, M. P., Birner, T., Black, R. X., Butler, A. H., Calvo, N., … Wilcox, L. (2013). On the lack of stratospheric dynamical variability in low-top versions of the CMIP5 models. *Journal of Geophysical Research*, *118*, 2494–2505. https://doi.org/10.1002/jgrd.50125

Chattopadhyay, J., & Bhatla, R. (2002). POSSIBLE INFLUENCE OF QBO ON TELECONNECTIONS RELATING INDIAN SUMMER MONSOON RAINFALL AND SEA-SURFACE. *Int. J. Climatol*, *127*(22), 121–127. https://doi.org/10.1002/joc.661

Christidis, N., Stott, P. A., Scaife, A. A., Arribas, A., Jones, G. S., Copsey, D., … Tennant, and W. J. (2012). A New HadGEM3-A-Based System for Attribution of Weather- and Climate-Related Extreme Events. *Journal of Climate*, *26*, 2756–2783. https://doi.org/10.1175/JCLI-D-12-00169.1

Cooper, P. J. M., Dimes, J., Rao, K. P. C., & Shapiro, B. (2008). Coping better with current climatic variability in the rain-fed farming systems of sub-Saharan Africa : An essential first step in adapting to future climate change ? *Agriculture, Ecosystems and Environment*, *126*, 24–35. https://doi.org/10.1016/j.agee.2008.01.007

Das, U., & Pan, C. J. (2013). Strong Kelvin wave activity observed during the westerly phase of. *Ann. Geophys.*, *31*, 581–590. https://doi.org/10.5194/angeo-31-581-2013

Dee, D. P., Uppala, S. M., Simmons, A. J., Berrisford, P., Poli, P., Kobayashi, S., … Dee, D. P. (2011). The ERA-Interim reanalysis : configuration and performance of the data assimilation system. *Q. J. R. Meteorol. Soc.*, *137*(April), 553–597. https://doi.org/10.1002/qj.828

Diallo, I., Bain, C. L., Gaye, A. T., Moufouma-Okia, W., Niang, C., Dieng, M. D. B., & Graham, R. (2014). Simulation of the West African monsoon onset using the HadGEM3-RA regional climate model. *Climate Dynamics*, *43*, 575–594. https://doi.org/10.1007/s00382-014-2219-0

Diallo, I., Sylla, M. B., Camara, M., & Gaye, A. T. (2013). Interannual variability of rainfall over the Sahel based on multiple regional climate models simulations. *Theoretical and Applied Climatology*, *113*, 351–362. https://doi.org/10.1007/s00704-012-0791-y

Diedhiou, A., Janicot, S., & Viltard, A. (2001). Composite patterns of easterly disturbances over West Africa and the tropical Atlantic : a climatology from the 1979 - 95 NCEP / NCAR reanalyses. *Climate Dynamics*, *18*, 241–253.

Dione, C., Lohou, F., Lothon, M., Adler, B., Babi, K., & Kalthoff, N. (2019). Low-level stratiform clouds and dynamical features observed within the southern West African monsoon. *Atmos. Chem. Phys.*, *19*, 8979–8997.

Douville, H. (2002). Influence of Soil Moisture on the Asian and African Monsoons . Part II : Interannual Variability. *Amer Meteor. Soc*, *15*(11 June), 701–720.

Dyn, C., Mohino, E., Janicot, S., & Bader, J. (2011). Sahel rainfall and decadal to multi-decadal sea surface temperature variability. *Clim Dyn*, (27 June). https://doi.org/10.1007/s00382-010-0867-2

Ern, M., & Preusse, P. (2009). Quantification of the contribution of equatorial Kelvin waves to the QBO wind reversal in the stratosphere. *Geophysical Research Letters*, *36*(November), 1–5.

https://doi.org/10.1029/2009GL040493

Fedorov, A V and Brown, J. N. (2009). Equatorial waves. *Elsevier*, (2005).

Felicitas Hansen, Katja Matthes, S. W. (2016). Tropospheric QBO – ENSO Interactions and Differences between the Atlantic and Pacific. *American Meteorological Society*, (15 February), 1353–1368. https://doi.org/10.1175/JCLI-D-15-0164.1

Folland, C. K., Office, M., & Palmer, T. (1986). Sahel rainfall and worldwide sea temperatures , 1901 – 85. *Nature*, *320*(April 1986). https://doi.org/10.1038/320602a0

Frédéric Hourdin, ionela Musat, Françoise GuicHard, Paolo MicHele ruti, Florence Favot, Marie-anGèle Filiberti,* Maï PHaM, Jean-yves GrandPeix, Jan PolcHer, Pascal Marquet, aaron boone, Jean-PHiliPPe laFore, Jean-luc redelsPerGer, alessandro dell'aquila, and H. G. (2010). AMMA-Model Intercomparison Project. *Amer Meteor. Soc*, (january), 95–104. https://doi.org/10.1175/2009BAMS2791.1

Furon, A. C., Wagner-riddle, C., Smith, C. R., & Warland, J. S. (2008). Wavelet analysis of wintertime and spring thaw CO 2 and N 2 O fluxes from agricultural fields. *Agricultural and Forest Meteorology*, *148*, 1305–1317. https://doi.org/10.1016/j.agrformet.2008.03.006

George J. Huffman, Robbert F. Adler, Mark M. Morrissey, David T. Bolvin, Scott Curtis, Robert Joyce, Brad McGavock, and J. S. (2001). Global Precipitation at One-Degree Daily Resolution from Multisatellite Observations. *Journal of Hydrometeorology*, *2*(9 October), 36–50.

Giorgetta, M. A., Manzini, E., Esch, E. R. and M., & Bengtsson, L. (2006). Climatology and Forcing of the Quasi-Biennial Oscillation in the MAECHAM5 Model. *Journal of Climate-Special Section*, *19*, 3882–3901.

Giorgetta, T. R. K. and M. A. (2014). Wave Forcing of the Quasi-Biennial Oscillation in the Max Planck Institute Earth System Model. *American Meteorology Society*, 1985–2006.

https://doi.org/10.1175/JAS-D-13-0310.1

Gong, E. A. B. E. and C. (1996). Dynamics of Wet and Dry Years in West Africa. *Journal of Climate*, *9*(October). https://doi.org/10.1175/1520-0442(1996)009<1030

Gray, W.M., C.W. Landsea, P.W. Mielke, Jr., and K. J. B. (1992). Predicting Atlantic seasonal hurricane activity 6-11 months in advance. *Weather and Forecasting*, *7*, 440–455.

Gray, S. M. O. and L. J., Hardiman, S. C., & Neal Butchart, and T. J. H. (2013). Stratospheric Variability in Twentieth-Century CMIP5 Simulations of the Met Office Climate Model : High Top versus Low Top. *American Meteorology Society*, *26*, 1595–1606. https://doi.org/10.1175/JCLI-D-12-00147.1

Grist, J. P. (2002). Easterly Waves over Africa . Part I : The Seasonal Cycle and Contrasts between Wet and Dry Years. *Monthly Westher Review*, *130*, 197–211.

Grist, S. E. N. and J. P. (2003). The Seasonal Evolution of the Atmospheric Circulation over West Africa and Equatorial Africa. *Journal of Climate*, *16*(1 April), 1013–1030.

Grodsky, S. A., Carton, J. A., & Murtugudde, R. (2001). Anomalous surface currents in the tropical Indian Ocean. *Geophysical Research Letters*, (25 June).

Grossmann, A., & Morlet, and J. (1984). Decomposition of Hardy Functions into Square Integrable Wavelets of Constant Shape. *Society for Industrial and Applied Mathematics*, *15*(August). https://doi.org/10.1137/0515056

Hagos, S. M., & Cook, K. H. (2007). Dynamics of the West African Monsoon Jump. *Journal of Climate*, *20*(September). https://doi.org/10.1175/2007JCLI1533.1

Huffman, G. J., Adler, R. F., Arkin, P., Chang, A., Ferraro, R., Gruber, A., … Schneider, U. (1997). The Global Precipitation Climatology Project (GPCP) Combined Precipitation Dataset. *Bull. Amer. Meteor. Soc.*, *0477*(February). https://doi.org/10.1175/1520-0477(1997)078<0005

Hulme, M., Doherty, R., Ngara, T., New, M., & Lister, D. (2001). African climate change : 1900 –

2100. *Climate Research*, *17*(17), 145–168.

Indeje, M., & Semazzi, F. H. M. (2000). Relationships Between QBO in the Lower Equatorial Stratospheric Zonal Winds and East African Seasonal Rainfall. *Meteorol. Atmos. Phys.*, *73*, 227–244.

Jalloh, A., Sarr, B., Kuiseu, J., Roy-Macauley, H., and S. P. (2011). *Review of climate in West and Central Africa to inform farming systems research and development in the sub-humid and semi-arid agroecologies of the region. Conseil Ouest et Centre Africain pour la Recherche et le Development Agricoles/West and Central Afr*.

Janicot, S., Harzallah, A., Fontaine, B., & Moron, V. (1998). West African Monsoon Dynamics and Eastern Equatorial Atlantic and Pacific SST Anomalies (1970 – 88). *Journal of Climate*, *11*, 1874–1882.

Janicot, S., & Sultan, B. (2001). Intra-seasonal modulation of convection in the West African Monsoon. *American Geophysical Union*, *28*(3), 523–526.

Jean-Luc Redelsperger, Chris D. Thorncroft, Arona Diedhiou, Thierry Lebel, Douglas J. Parker, and J. P. (2006). African Monsoon Multidisciplinary Analysis. *Amer Meteor. Soc*, (DECEMBER), 1739–1746.

Jenkins, G. S. (2005). Late 20th Century attribution of drying trends in the Sahel from the Regional Climate Model (RegCM3). *Geophysical Research Letters*, *32*(June), L22705. https://doi.org/10.1029/2005GL024225

Keener, V. W., Feyereisen, G. W., Lall, U., Jones, J. W., Bosch, D. D., & Lowrance, R. (2010). El-Niño / Southern Oscillation (ENSO) influences on monthly NO 3 load and concentration , stream flow and precipitation in the Little River Watershed , Tifton , Georgia (GA). *Journal of Hydrology*, *381*(3–4), 352–363. https://doi.org/10.1016/j.jhydrol.2009.12.008

Labat, D. (2010). Cross wavelet analyses of annual continental freshwater discharge and selected

climate indices. *Journal of Hydrology*, *385*(25 February), 269–278. https://doi.org/10.1016/j.jhydrol.2010.02.029

Laurent, V. M. and H. (2001). Life cycle of Sahelian mesoscale convective cloud systems. *Q. J. R. Meteorol. Soc.*, *127*, 377–406.

Lemaitre, B. and. (2014). Mesoscale Convective Systems in Relation to African and Tropical Easterly Jets, (2010), 3224–3242. https://doi.org/10.1175/MWR-D-13-00247.1

Lemburg, A., Bader, J., & Claussen, M. (2017). Is there a clear relationship between the Tropical Easterly Jet and Sahel rainfall ?, *19*, 8181.

Love, B. S., & Matthews, A. J. (2009). Real-time localised forecasting of the Madden – Julian Oscillation using neural network models. *Quarterly Journal of the Royal Meteorological Society*, *1483*(July), 1471–1483. https://doi.org/10.1002/qj

Lu, J., & Delworth, T. L. (2005). Oceanic forcing of the late 20th century Sahel drought. *Geophysical Research Letters*, *32*(May), 1–5. https://doi.org/10.1029/2005GL023316

M. P. Baldwin, L. J. Gray, Dunkerton, T. J. Hamilton, K. Haynes, P. H. Holton, J. R. Alexander, M. J. Hirota, I. Horinouchi, T. Jones, D. B. A. Marquardt, C. Sato, K. Takahashi, M. (2001). The Quasi-biennial Oscillation. *American Geophysical Union*, (1999), 179–229.

M. Paluš and Novotná, D. (2006). Quasi-biennial oscillations extracted from the monthly NAO index and temperature records are phase-synchronized. *Nonlin. Processes Geophys.*, *13*, 287–296.

Manzanas, R., Frías, M. D., Cofiño, A. S., & Gutiérrez, J. M. (2014). Validation of 40 year multimodel seasonal precipitation forecasts : The role of ENSO on the global skill. *Journal of Geophysical Research*, *119*, 1708–1719. https://doi.org/10.1002/2013JD020680.Received

Manzini, E., Giorgetta, M. A., Esch, M., Kornblueh, L., & Roeckner, and E. (2006). The Influence of Sea Surface Temperatures on the Northern Winter Stratosphere : Ensemble Simulations

with the MAECHAM5 Model. *American Meteorology Society*, *19*(August), 3863–3881.

Martin, G. M., Peyrille, P., Roehrig, R., Rio, C., Caian, M., Bellon, G., … Idelkadi, and A. (2016). Understanding the West Adrican Monsoon from the analysis of diabatic heating distribution as simulated by climate models. *Journal of Advances in Modeling Earth Systems*, 239–270. https://doi.org/10.1002/2016MS000697.Received

Mounier, F., Janicot, S., & Kiladis, G. N. (2008). The West African Monsoon Dynamics . Part III : The Quasi-Biweekly Zonal Dipole. *American Meteorology Society*, *21*, 1911–1928. https://doi.org/10.1175/2007JCLI1706.1

Ng'ongolo, H. K., & Smyshlyaev, S. P. (2010). The statistical prediction of East African rainfalls using quasi-biennial oscillation phases information. *Natural Science*, *Vol.2*, *No.*, 1407–1416. https://doi.org/10.4236/ns.2010.212172

Nicholson S. E. (1981). Rainfall and Atmospheric Circulation during Drought Periods and Wetter Years in West Africa. *American Meteorological Society*, *109*(October).

Nicholson, S E, & Grist, J. P. (2001). A CONCEPTUAL MODEL FOR UNDERSTANDING RAINFALL VARIABILITY IN THE WEST AFRICAN SAHEL ON INTERANNUAL AND INTERDECADAL TIMESCALES. *Int. J. Climatol*, *1757*(2 February), 1733–1757.

Nicholson, Sharon E. (2008). The intensity , location and structure of the tropical rainbelt over west Africa as factors in interannual variability. *International Journal of Climatology*, *1785*(March), 1775–1785. https://doi.org/10.1002/joc

Nicholson, Sharon E. (2013). The West African Sahel : A Review of Recent Studies on the Rainfall Regime and Its Interannual Variability. *ISRN Meteorology*, *2013*, 32.

Nicholson, Sharon E, & Webster, P. J. (2007). A physical basis for the interannual variability of rainfall in the Sahel, *2084*(November), 2065–2084. https://doi.org/10.1002/qj

Nur Zaman Fathullah, S. W. L. and S. S. (2017). Characteristics of Kelvin waves and Mixed

Rossby-Gravity waves in opposite QBO phases. *Earth and Environmental Science*, *54*. https://doi.org/10.1088/1742-6596/755/1/011001

Okonkwo, C., Demoz, B., & Tesfai, S. (2014). Characterization of West African jet streams and their association to ENSO events and rainfall in ERA-Interim 1979-2011. *Advances in Meteorology*, *2014*, 14–17. https://doi.org/10.1155/2014/405617

Omotosho, J. B. (1990a). Onset of thunderstorms and precipitation over northern nigeria. *Int. J. Climatol*, *10*, 849–860.

Omotosho, J. B. (1990b). Onset of Thunderstorms and precipitation over northern Nigeria. *International Journal of Climatology*.

Omotosho, J. B. (2008). Pre-rainy season moisture build-up and storm precipitation delivery in the West African Sahel. *International Journal of Climatology*, *946*(August 2007), 937–946. https://doi.org/10.1002/joc

Omotosho, J. B., & Abiodun, B. J. (2007a). A numerical study of moisture build-up and rainfall over West Africa. *Royal Meteorological Society*, *225*(July), 209–225. https://doi.org/10.1002/met

Omotosho, J. B., & Abiodun, B. J. (2007b). A numerical study of moisture build-up and rainfall over West Africa. *Meteorol Appl*, *225*(July), 209–225. https://doi.org/10.1002/met

Pante, G., & Knippertz, P. (2019). Resolving Sahelian thunderstorms improves mid-latitude weather forecasts. *Nature Communications*, 1–9. https://doi.org/10.1038/s41467-019-11081-4

Peyrille, N. M. J. H. and P. (2006). Dynamics of the West African monsoon Dynamics of the West African Monsoon. *Journal de Physique*, (December 2006). https://doi.org/10.1051/jp4

Richard S. Lindzen and James R. Holton. (1968). A Theory of the Quasi_Biennial Oscillation. *Atmospheric Sciences*, *25*.

Robert A. Houze, J. (1977). Structure and Dynamics of a Tropical Squall-Line System. *Monthly*

Westher Review, *105*(September).

Rufus, E., Yixuan, S., & Shaowen, S. (2013). Tropospheric Circulation Features During Wet and Dry Years over. *J. Meteorol. Rel. Sci*, *7*, 2–16. https://doi.org/http://dx.doi.org/10.20987/jmrs.05.2013

Sanogo, S., Fink, A. H., Omotosho, J. A., & Ba, A. (2015). Spatio-temporal characteristics of the recent rainfall recovery in West Africa. *International Journal of Climatology*, *4605*(March), 4589–4605. https://doi.org/10.1002/joc.4309

Santos, C. A. G., Galvao, C. D. O., Suzuki, K., & Trigo, R. M. (2001). Matsuyama City rainfall data analysis using wavelet transform. *Annual Journal of Hydraulic Engineering*, *45*(January). https://doi.org/10.2208/prohe.45.211

Schmidt, H., Rast, S., Bunzel, F., Esch, M., Giorgetta, M., Kinne, S., … Walz, M. (2013). Response of the middle atmosphere to anthropogenic and natural forcings in the CMIP5 simulations with the Max Planck Institute Earth system model. *Journal of Advances in Modeling Earth Systems*, *5*, 1–19. https://doi.org/10.1002/jame.20014

Stefan Hastenrath, L. G. (1991). The Monsoonal Current Regimes of the Tropical Indian Ocean ' Observed Surface Flow Fields and Their Geostrophic and Wind-Driven Components. *Journal of Geophysical Research*, *96*(15 July), 619–633.

Steinig, S., Harlaß, J., Park, W., & Latif, M. (2018). Sahel rainfall strength and onset improvements due to more realistic Atlantic cold tongue development in a climate model. *Scientific Reports*, *8*(1), 1–9. https://doi.org/10.1038/s41598-018-20904-1

Suhas P Wani, Johan Rockstrom, and T. O. (2009). *Rainfed Agriculture : Unlocking the Potential*.

Sylla, Mouhamadou Bamba., Coppola, E., Mariotti, F., Giorgi, F., Ruti, P. M., Dell'Aquila, A. and Bi, X. (2010). Multiyear simulation of the African climate using a regional climate model (RegCM3) with the high resolution ERA-interim reanalysis. *Climate Dynamics*, *Volume*

35(Issue 1), 231–247. https://doi.org/10.1007/s00382-009-0613-9

Sylla, M B, Giorgi, F., Ruti, P. M., Calmanti, S., & Aquila, A. D. (2011). The impact of deep convection on the West African summer monsoon climate : a regional climate model sensitivity study The role of the representation of deep convection on key elements of the West RegCM3 . Two simulations in which a scheme of deep convecti. *Q. J. R. Meteorol. Soc.*, *137*(July), 1417–1430. https://doi.org/10.1002/qj.853

Sylla, Mouhamadou Bamba, Giorgi, F., Pal, J. S., Gibba, P., Kebe, I., & Nikiema, M. (2015). Projected Changes in the Annual Cycle of High-Intensity Precipitation Events over West Africa for the Late Twenty-First Century *. *American Meteorological Society*, *28*, 6475–6488. https://doi.org/10.1175/JCLI-D-14-00854.1

Taylor, K. E., Ronald, S., & Meehl, and G. A. (2012). An Overview of CMIP5 and the experiment Design. *American Meteorological Society*, (April). https://doi.org/10.1175/BAMS-D-11-00094.1

Tompkins, A. M., Diongue-Niang, A., Parker, D. J., & Thorncroft, and C. D. (2005). The African easterly jet in the ECMWF Integrated Forecast System : 4D-Var analysis. *Q. J. R. Meteorol. Soc.*, *131*, 2861–2885. https://doi.org/10.1256/qj.04.136

Torrence, C., & Compo, G. P. (1998). A Practical Guide to Wavelet Analysis. *American Meteorological Society*, *79*(1 January).

Vautard, R., Christidis, N., Ciavarella, A., Carmen, M., Bellprat, O., Christiansen, B., … Bellprat, O. (2018). *Evaluation of the HadGEM3-A simulations in view of detection and attribution of human influence on extreme 2 events in Europe To cite this version : HAL Id : hal-01759412 Evaluation of the HadGEM3-A simulations in view of detection and attribution of huma*.

Wang, S., & Gillies, R. R. (2011). Dynamic Linkage between the Sahel Greening and Intense Atlantic Hurricanes, (October), 3–6.

Watanabe, S., Hajima, T., Sudo, K., & Nagashima, T. (2011). MIROC-ESM 2010 : model description and basic results of CMIP5-20c3m experiments. *Geoscientific Model Development*, (October). https://doi.org/10.5194/gmd-4-845-2011

Webster, C. T. and P. J. (1999). Interdecadal Changes in the ENSO – Monsoon System. *American Meteorological Society*, 2679–2690.

World Bank. (2017). *Republic of Niger priorities for ending poverty and boosting shared prosperity*.

Wu, M.-L. C., Reale, O., & Schubert, S. D. (2013). A Characterization of African Easterly Waves on 2 . 5 – 6-Day and 6 – 9-Day Time Scales. *Journal of Climate*, *26*, 6750–6774. https://doi.org/10.1175/JCLI-D-12-00336.1

Yoden, S., Bui, H.-H., & Nishimoto, E. (2017). *Stratosphere-Troposphere Two-Way Dynamical Coupling in the Tropics through Organizations of Moist Convective Systems*.

Yoo, C., & Son, S. (2016). Modulation of the boreal wintertime Madden-Julian oscillation by the stratospheric quasi-biennial oscillation. *Geophysical Research Letters*, *43*, 1392–1398. https://doi.org/10.1002/2016GL067762.Received

Zaroug, M. A. H., Giorgi, F., Coppola, E., Abdo, G. M., & Eltahir, E. A. B. (2014). Simulating the connections of ENSO and the rainfall regime of East Africa and the upper Blue Nile region using a climate model of the Tropics. *Hydrology and Earth System Sciences*, *18*, 4311–4323. https://doi.org/10.5194/hess-18-4311-2014

Zipser, E. J. (1969). The Role of Organized Unsaturated Convective Downdrafts in the Structure and Rapid Decay of an Equatorial Disturbance. *Journal of Applied Meteorology*, *8*(October).

National Weather Service Weather glossary Cited: 2012, [Available online at http://forecast.weather.gov/glossary.php?word=MCS].

APPENDICES

Appendix 1

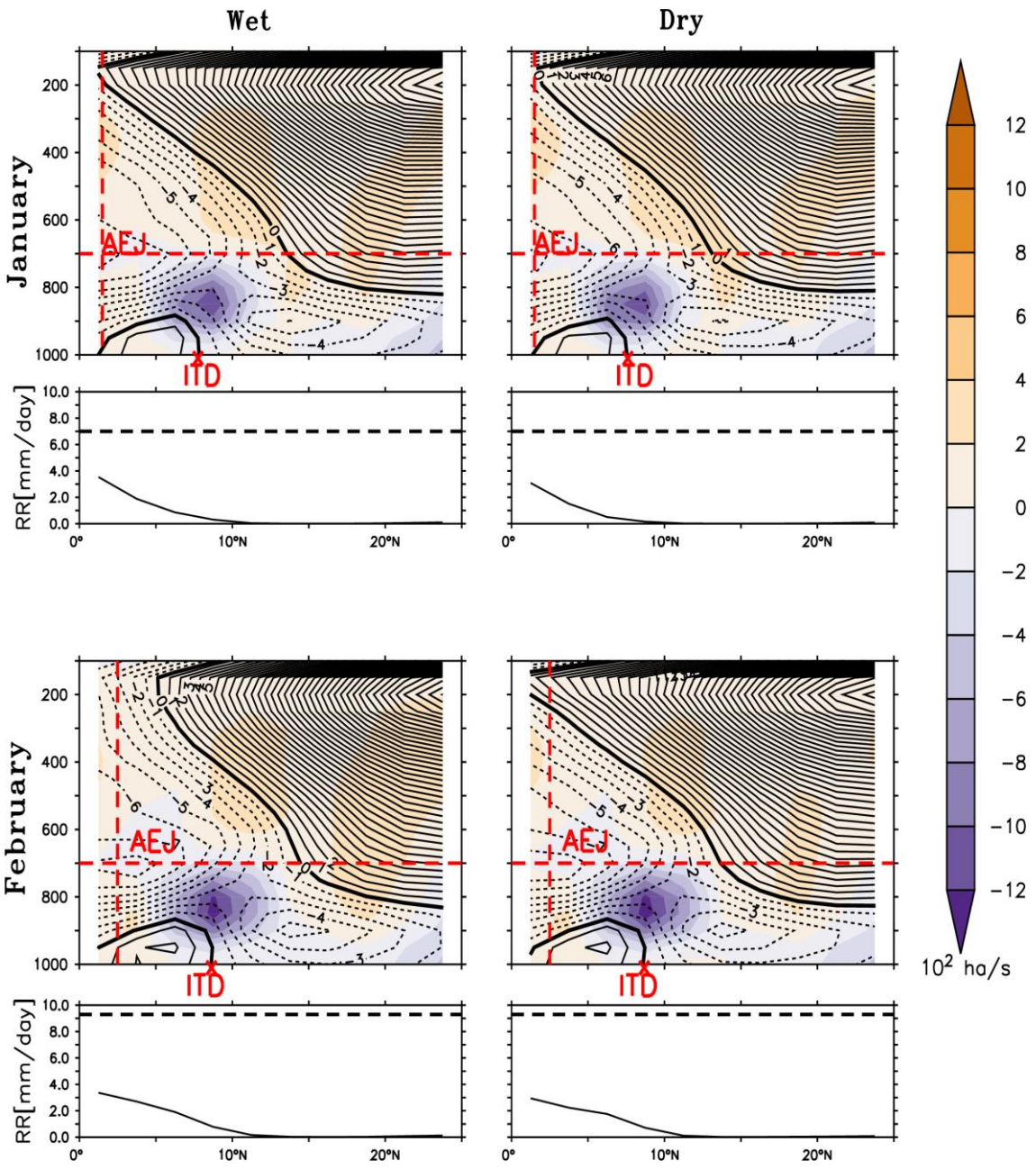

Figure 4.35: Cross section of composite evolution of wet and dry years cross section averaged at longitude 10W-10E. Wind speeds are in isotach. Latitudinal and vertical positions of jet cores in tick dash lines.

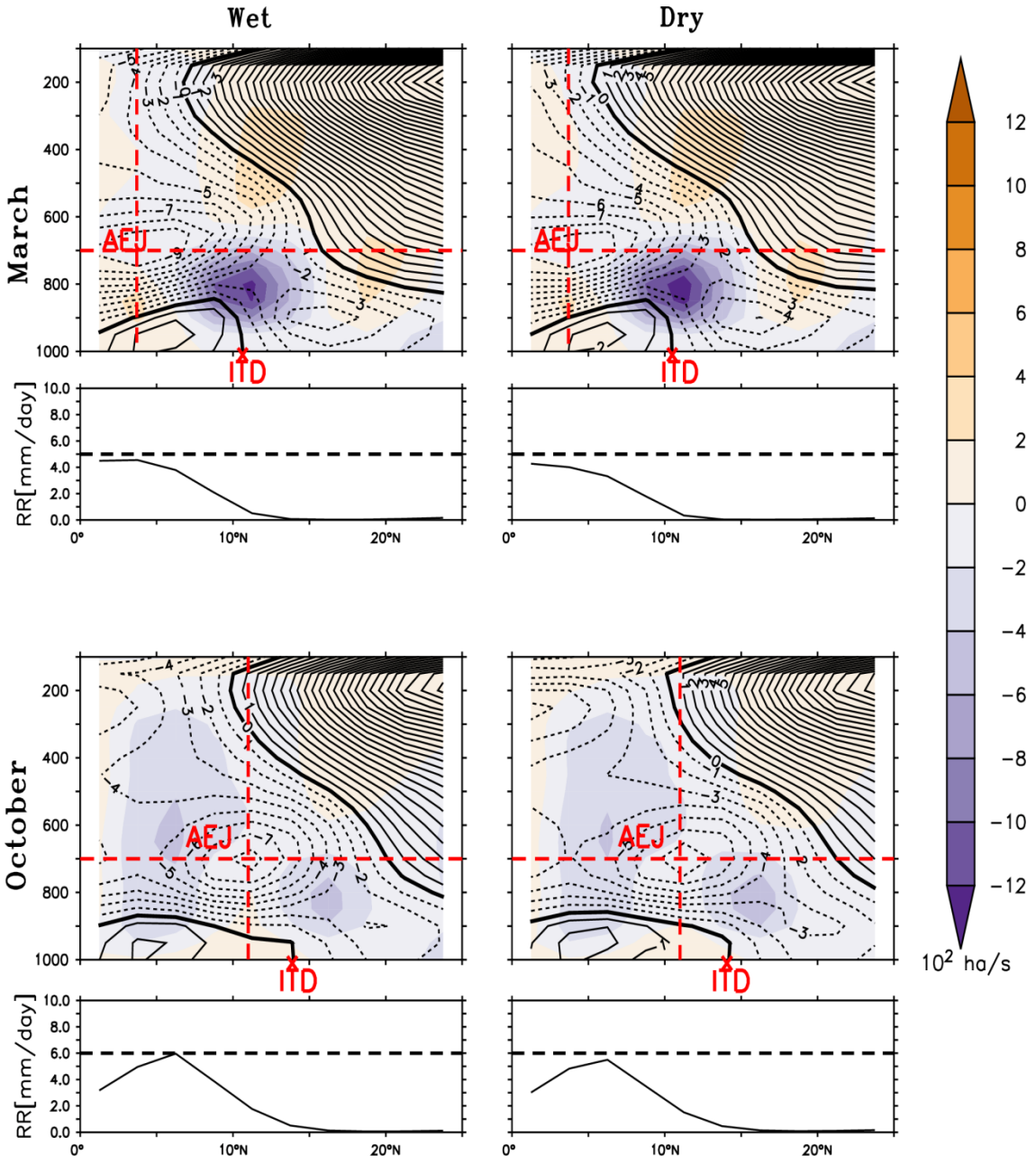

Figure 4.36: same as Figure 4.35 but for March and October

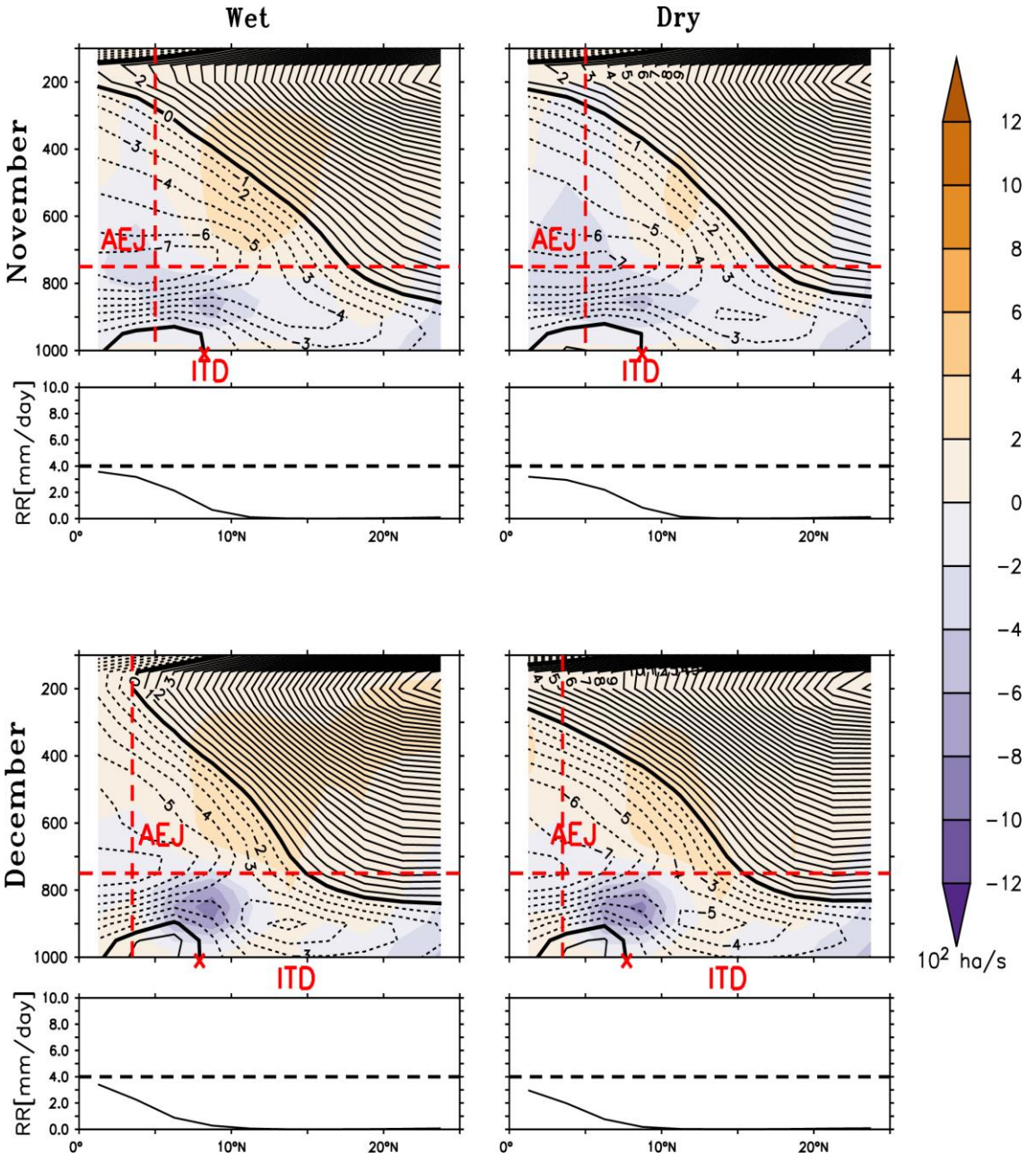

Figure 4.37: same as Figure 4.35 but for November and December

APPENDIX 2

A. PUBLICATIONS FROM THE THESIS

1. Submitted, Abdoulaye Ballo, J. Bayo Omotosho, Nana Ama Browne Klutse, Babatunde J. Abiodun and Amadou Coulibaly (2019): Investigation of the influence of Quasi-biennial Oscillation on West African Rainfall. Climate Dynamics Journal with manuscript number of CLDY-D-19-00659.

2. Submitted, Abdoulaye Ballo, J. Bayo Omotosho, Nana Ama Browne Klutse and Babatunde J. Abiodun (2019): The Relative Influence of the West African Monsoon Components over the Region. International Journal of Climatology with manuscript ID: JOC-19-0694